VTT PUBLICATIONS 301

Perpendicular-to-grain creep of Finnish softwoods in high temperature drying conditions

Experiments and modelling in temperature range 95–125 °C

Antti Hanhijärvi

VTT Building Technology

TECHNICAL RESEARCH CENTRE OF FINLAND
ESPOO 1997

ISBN 951–38–5041–2 (soft back ed.)
ISSN 1235–0621 (soft back ed.)

ISBN 951–38–5042–0 (URL: http://www.inf.vtt.fi/pdf/)
ISSN 1455–0849 (URL: http://www.inf.vtt.fi/pdf/)

JULKAISIJA – UTGIVARE – PUBLISHER

Valtion teknillinen tutkimuskeskus (VTT), Vuorimiehentie 5, PL 2000, 02044 VTT
puh. vaihde (09) 4561, faksi (09) 456 4374

Statens tekniska forskningscentral (VTT), Bergsmansvägen 5, PB 2000, 02044 VTT
tel. växel (09) 4561, fax (09) 456 4374

Technical Research Centre of Finland (VTT), Vuorimiehentie 5, P.O.Box 2000, FIN–02044 VTT, Finland
phone internat. + 358 9 4561, fax + 358 9 456 4374

VTT Rakennustekniikka, Rakennusmateriaalit ja -tuotteet sekä puutekniikka,
Puumiehenkuja 2 A, PL 1806, 02044 VTT
puh. vaihde (09) 4561, faksi (09) 456 7027

VTT Byggnadsteknik, Byggnadsmaterial och -produkter, träteknik,
Träkarlsgränden 2 A, PB 1806, 02044 VTT
tel. växel (09) 4561, fax (09) 456 7027

VTT Building Technology, Building Materials and Products, Wood Technology,
Puumiehenkuja 2 A, P.O.Box 1806, FIN–02044 VTT, Finland
phone internat. + 358 9 4561, fax + 358 9 456 7027

Technical editing Leena Ukskoski

VTT OFFSETPAINO, ESPOO 1997

Hanhijärvi, Antti. Perpendicular-to-grain creep of Finnish softwoods in high temperature drying conditions. Experiments and modelling in temperature range 95 – 125 °C. Espoo 1997, Technical Research Centre of Finland, VTT Publications 301. 94 p. + app. 176 p.

UDC 674.032:674.04:539.376
Keywords softwoods, spruce wood, pine wood, creep properties, high temperature tests, drying tests

ABSTRACT

This publication reports the results obtained in a project to clarify the perpendicular-to-grain mechanical properties of spruce (*Picea abies*) and pine (*Pinus sylvestris*) in high temperature drying conditions. The work consisted of a literature review, an extensive experimental programme and development of a new constitutive model for the description of the creep behaviour in the high temperature conditions. All these tasks are documented in this publication.

The experimental work consisted of tension creep experiments at constant saturated (green) condition at constant temperatures 95, 110 and 125°C and in drying conditions of maximum reached temperature 95, 110 or 125°C. From these experiments a large amount of data was obtained about shrinkage, hygrothermal deformation, modulus of elasticity, viscoelastic creep and mechano-sorptive creep. A limited strength test series was also carried out on spruce at 95 and 125°C.

For the use of the obtained knowledge in computational simulation of drying stresses a constitutive model of the creep behaviour was developed for the high temperature conditions. The new model is based on linear shrinkage and on using the time–temperature–moisture-content superposition principle for modelling elastic and viscoelastic strain. For mechano-sorptive creep a new type of model is introduced, where the developing strain is partly recoverable and partly not.

PREFACE

This publication is a report of results obtained in the project ‘High temperature creep of wood’ conducted at VTT Building Technology in 1994–1995. The project was financed by the Technology Development Centre (TEKES) and VTT, which is gratefully acknowledged. The project was Finnish contribution to the COST 508 Wood Mechanics action.

The project was lead by a directing board, whose members were Managing Director Aarni Metsä (Finnish Wood Research Ltd.), Prof. Mauri Määttänen (Helsinki University of Technology), Research Manager Olli-Pekka Nordlund (Technology Development Centre), Prof. Tero Paajanen (Helsinki University of Technology), Prof. Alpo Ranta-Maunus (VTT) and Prof. Pertti Viitaniemi (VTT). The members are thanked for fruitful co-operation. In the actual research work, Prof. Ranta-Maunus acted as the responsible director of the project and Dr. Antti Hanhijärvi as the project manager who conducted the main research work.

The author would also like to thank Mr. Erkki Järvinen for the indispensable help in building the regulation system for the drying condition test chamber. Mr. Rauno Vinttala and Mr. Mats Rundt are thanked for the careful and painstaking work in building of the drying condition test set-up and the preparation of specimens as well as the performing the lengthy experiments. Mr. Pentti Kankaanpää is thanked for careful execution of the saturated condition experiments.

Thanks are also due to Casco Nobel company for providing the polyurethane glue needed for the specimen preparation.

Antti Hanhijärvi

CONTENTS

APPENDICES

Appendices of this publication are not included in the PDFversion. Please order the printed version to get the complete publication (http://www.inf.vtt.fi/pdf/publications/1998/)

LIST OF SYMBOLS

Latin

a	shift factor
a_{ir}, $a^{ir}{}_{,i}$	parameters
b_{ir}, $b^{ir}{}_{,i}$	parameters
J	compliance
J_0, J_i	parameters
$J^{ve}{}_{,0}$, $J^{ve}{}_{,i}$	limit compliances of Kelvin units
J_{ir}, $J^{ir}{}_{,i}$	parameters
J_M	master curve compliance
J_{ms}, $J^{ms}{}_{,i}$	parameters
k_T, k_u	parameters
m	mass
m_0	mass in the absolute dry condition
T	temperature
T_{ref}	reference temperature
t	time
u	moisture content (dry weight basis)
u_{FS}	value of moisture content at the fiber saturation point
u_{ref}	reference moisture content
$\hat{u}$	effective moisture content $\hat{u} = \min(u, u_{FS})$

Greek

α	hygroexpansion coefficient
β	hygrothermal coefficient
β_{FS}	value of β at fiber saturation point
ε	strain
ε_{ht}	hygrothermal strain
ε_{ir}, $\varepsilon^{ir}{}_{,i}$	internal variables
ε_{max}, $\varepsilon^{max}{}_{,i}$	internal variables
ε_{min}, $\varepsilon^{min}{}_{,i}$	internal variables
ε_{ms}	mechano-sorptive strain
$\varepsilon^{ms}{}_{,i}$	strain of a mechano-sorptive creep model unit
ε_s	shrinkage strain
ε_{ve}	viscoelastic strain
$\varepsilon^{ve}{}_{,0}$, $\varepsilon^{ve}{}_{,i}$	strains of Kelvin units
σ	stress
τ	time variable
τ_i	parameters
$\tau^{ve}{}_{,i}$	retardation times of Kelvin units
τ_{ms}, $\tau^{ms}{}_{,i}$	parameters
ξ	material time

Abbreviations

FSP	fiber saturation point
HT	high temperature
HTD	high temperature drying
MOE	modulus of elasticity
ms	mechano-sorptive
ve	viscoelastic

1 INTRODUCTION

During the last c. five years a good competence in the computational simulation of kiln drying of wood has been obtained at VTT Building Technology (Ranta-Maunus et al. 1995, Hukka 1996). Two computer programs for the simulation of the moisture content and stress development in a drying piece of sawn timber have been developed: LAATUKAMARI, which simulates the drying process one-dimensionally for optimisation purposes in industrial kilns, and PEO, which can simulate the cross-section of a drying piece of timber two-dimensionally for more research related purposes. The two programs have been developed for temperatures used conventionally in Finnish saw mills, up to about 80°C. The work introduced in this publication is a part of an attempt to widen the capability of the simulations to higher temperatures, up to 125°C. Fig. 1 presents the overall plan for the development of high temperature drying technology at VTT Building Technology and the connection of this study to the other projects.

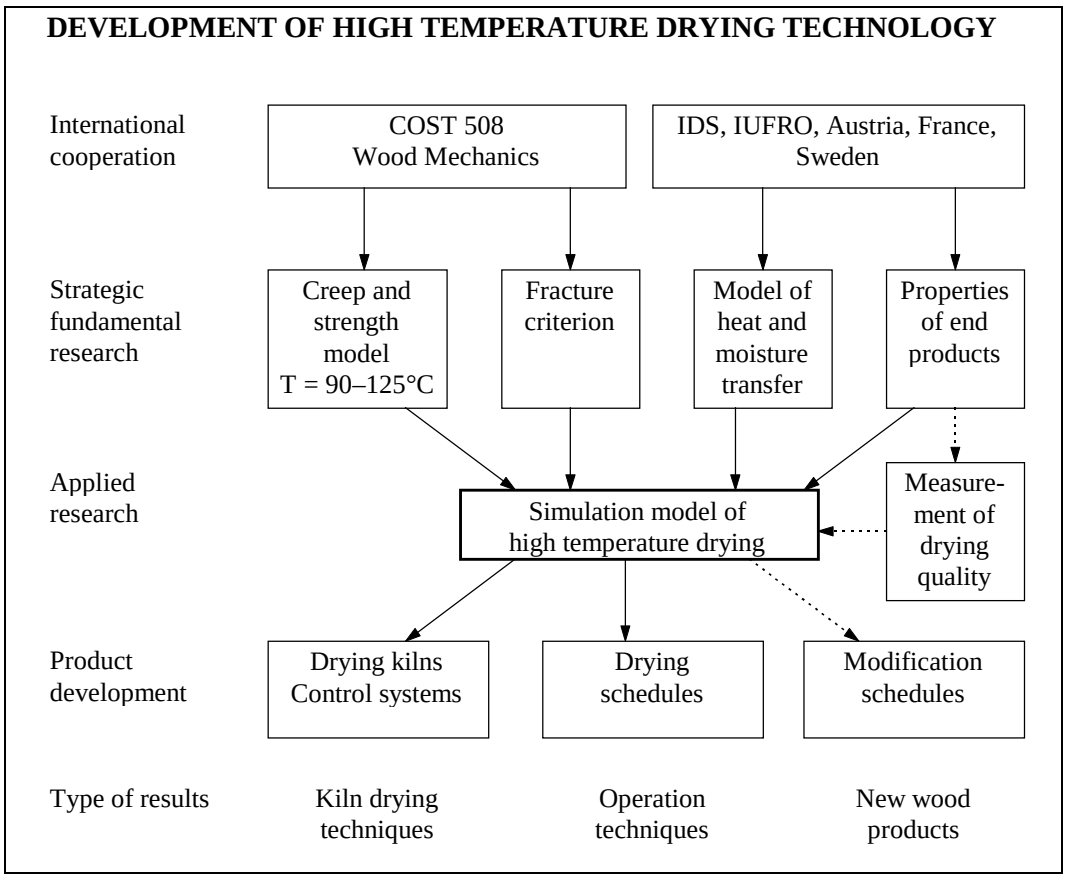

Fig. 1. The overall plan for development of high-temperature drying technology at VTT.

The plan for the present work consisted of two main efforts:

1. An experimental part, which included a literature review of earlier experiment results and an extensive programme of novel experiments, in which the mechanical properties of the two main

Finnish softwoods would be investigated in directions perpendicular to the grain.

2. Analysis of the obtained experimental data and conveyance of it into a suitable mathematical model for application in the drying simulation programs.

The documentation of the work and results of these tasks are presented in this publication in detail and in the order: 1) literature review 2) experimental work 3) analysis and 4) model.

2 REVIEW OF SOME PREVIOUS EXPERIMENTS ON PERPENDICULAR-TO-GRAIN PROPERTIES

The mechanical properties of wood are not very well known at temperatures relevant in the high-temperature drying (HTD) process, viz. around 90–120°C. This applies especially to the time dependent phenomena, creep and long-term strength (reduction of strength in prolonged loading); although there are some publications concerning the instantaneous elastic and strength properties as well as dynamic properties at these temperatures, hardly anything is available in the published literature touching the static long-term behaviour. And although the HTD process itself has caught attention among researches, this has not lead to detailed studies of the basic material properties of wood in these conditions. The lack of research on the long-term material properties in HTD conditions can also be interpreted as an indication that experiments on these properties are still going on in the conventional drying temperature range, say 50–80°C, in which a certain increase in research activity can be seen to have taken place during recent years. So, the review presented here will contain sources mainly on short term properties in the conventional and HT conditions and long-term properties in conventional drying conditions. The review is not exhaustive, but rather contains a list of sources that were found most useful during this project.

2.1 EXPERIMENTS AT VTT

The short term mechanical properties in the tangential direction of the three most important Finnish wood species, *Pinus sylvestris*, *Picea abies* and *Betula verrucosa*, were investigated at VTT already in the 60's (Siimes 1967) in connection with the spread of kiln drying in Finland. The study made under Siimes' direction contains a comprehensive experimental clarification of the tangential modulus of elasticity (MOE) and strength both in tension and compression for a temperature range relevant in conventional kiln drying. Experiments were made in compression and tension, at temperatures 20, 40, 60 and 80°C, moisture contents 4, 8, 12, 16 and 20% plus green (saturation) condition. Moreover, the specimens represented a wide density range and results have been given for three density categories. Altogether, there are thus 144 cases for one species and one property (strength or MOE), which tells about the large extent of the work.

Due to the exhaustive quality of Siimes' study it provides a good basis for further studies on the mechanical properties in the perpendicular-to-grain directions. The results of Siimes are used in this work as a main source of reference and the relationships found by him between the mechanical properties and different conditions can be utilised as giving more confidence to results that exceed his range of conditions and that are made with fewer specimens.

The research of the perpendicular-to-grain material properties in relation to drying was started again at VTT in 1980's under the management of Prof. Alpo Ranta-Maunus. The newer research has concentrated on long-

term properties, foremost on creep. Before the present project, the work has focused on exploring the creep properties at conventional drying temperatures. Results of the newer research have been documented in references Kangas and Ranta-Maunus (1989), Kangas (1990), Ranta-Maunus (1992) and summarised by Ranta-Maunus (1993). A great deal of experience obtained in these preceding projects has been applied in the present project.

Kangas and Ranta-Maunus (1989) dealt with creep in constant moisture content and changing moisture content as well as undertook some effort in regard to long-term strength. The foremost outcome of the work is the grasp of the relative importance of the moisture change induced creep, the mechano-sorptive effect in the perpendicular-to-grain directions in the conditions of drying. In the work of Kangas (1990) the creep of drying wood is studied at temperatures 40, 60 and 80°C under tensile load. The work masters in developing new experimental techniques and shows especially the need for the reliable evaluation of the zero-load shrinkage during a creep experiment. The work confirms the importance of the mechano-sorptive effect and gives experimental data for its quantification in conventional drying conditions. As mentioned, both the above studies are summarised in Ranta-Maunus (1993).

2.2 OTHER EXPERIMENTS IN THE LITERATURE

2.2.1 Modulus of elasticity

Of the different basic deformation properties the modulus of elasticity (MOE) along with shrinkage are the most studied ones. Even so, not many reports have been published on the MOE of wood in directions perpendicular to grain in the high temperature range, above 90°C.

The review of Gerhards (1982) on “Effect of moisture content and temperature on the mechanical properties of wood: an analysis of immediate effects” is a good overview of literature published on the moisture content and temperature influence on both strength and MOE until the late 1970’s. It concerns all material directions of wood; and the test results by different authors on different species are gathered comprehensively and compared in regard to the effect of moisture content and temperature (the actual values of the results are not compared). Of the works on perpendicular-to-grain MOE that Gerhards mentions, only two contain results that are above 85°C (Byvshykh 1959, Okuyama et al. 1977). For temperature range 20–80°C there are more publications.

Okuyama et al. (1977) measured bending MOE for two Southeast Asian hardwoods. The results are interesting in that the measurements were done in the tangential and radial directions and in various angles between them. Also, the temperature range is wide: 20–97°C.

Of other studies, the works of Salmén (1984) and Iida (1986) are of interest. Salmén measured the dynamic properties of spruce (*Picea abies*) in wet condition over temperature range 20–140°C. The dynamic

measurements are not directly comparable to the static results, but the storage modulus provides a good reference value for the static MOE – the better the lower the frequency used in tests is. The lowest frequency in Salmén's tests is 0.05 Hz corresponding half period length of 10 seconds, which is well comparable to the loading times in static tests.

Iida (1986) measured the perpendicular-to-grain MOE in bending in water saturated condition for several species. The temperature range was 10–95°C.

2.2.2 Short term strength

Gerhards' (1982) review mentions three studies on perpendicular-to-grain strength that reach above 85°C: Byvshykh (1959), Goulet (1960) and Okuyama et al. (1977). Studies below 80°C are again more numerous. The work of Okuyama et al. is again interesting because strength has been measured in different angles to the material directions.

The work of Koran (1979) on perpendicular-to-grain tension strength of spruce is interesting as the temperature range is very wide, reaching up to 250°C. Tests were made with saturated wood, saturated either in water or glycerine. Both tangential and radial directions are treated.

2.2.3 Viscoelastic creep

Not many references were found on the perpendicular-to-grain viscoelastic properties of wood. Of the ones found the only static creep results that extend to the high temperature range are the test results of Sawabe (1974) who describes an experiment on the creep of dry hinoki (*Chamaecyparis obtusa Sieb.*) in the temperature range 20–180°C. Also some experiments on dynamic viscoelastic properties touch the high temperature range: Salmén and Fellers (1982) and Salmén (1984) report dynamic measurements between 20 and 140°C.

Results of viscoelastic creep in the conventional drying temperature range are given in the works of Svensson (1995 and 1996) at two temperatures (60 and 80°C) and two moisture contents. The work of Joyet (1992) is also interesting as it contains measurements at many moisture contents, even if testing temperatures are near room temperature. Both radial and tangential directions are treated.

2.2.4 Mechano-sorptive creep

No references could be found on the mechano-sorptive behaviour in the high temperature conditions. However, in the conventional drying conditions results of quite a few recent studies are available.

Hisada (1986) performed on extensive study on the deformation behaviour of makanba (*Betula maximowicziana Reg.*) and hinoki (*Chamaecyparis obtusa Sieb.*) specimens (tangential) during drying under variable loads, including zero load. Drying conditions included constant temperatures 20, 30, 50, 70 and 80°C. The experiments included different

loading schemes, in which the load was applied in the beginning of drying and removed in the late part of it, or was applied only at different stages of drying. Measurements were also made on volumetric shrinkage, which allows inference to be made on the interaction between the material directions in creep (Poisson effect type behaviour in creep).

Svensson's (1995) results contain both drying strain measurement results and restrained shrinkage force results, giving considerably better picture of the deformation behaviour than creep results alone. Temperatures include 60 and 80°C.

The work of Joyet (1992) is directed to investigating creep in service conditions (~ room temperature) but provides very useful fundamental information about the mechano-sorptive creep, especially concerning the effect of many repeated moisture cycles.

3 EXPERIMENTS

In order to quantify the mechanical properties of wood for the simulation of the stress development during a high temperature drying process, a series of experiments was arranged in conditions that resemble the real drying situation as well as possible. Tests were made in tension both in constant wet condition and in drying condition, and for specimens of spruce (*Picea abies*) and pine (*Pinus sylvestris*) wood.

3.1 ACQUIRING AND PREPARATION OF SPECIMENS

All the specimens were manufactured from three tree trunks, two spruce ones and one pine trunk. The three trees had been grown at a location in Nurmijärvi, near Helsinki, and were felled in autumn (October). After felling the trunks, they were cut into logs, whose length was about 0.5–0.7m (Fig. 2). The two spruce trunks were labelled by the letters K and S and the pine trunk by the letter M. The logs cut out of them were numbered beginning from the root. Altogether eighteen spruce logs – labelled K1–K12 and S0–S5 – and nine pine logs – labelled M0–M8 – were acquired as raw material for test specimens. The transportation of the logs to the laboratory facilities was done inside a plastic cover to avoid any drying. They were stored to wait for preparation of test specimens inside large closed containers, in which there was some water on the bottom to ensure moist conditions to prevent any drying.

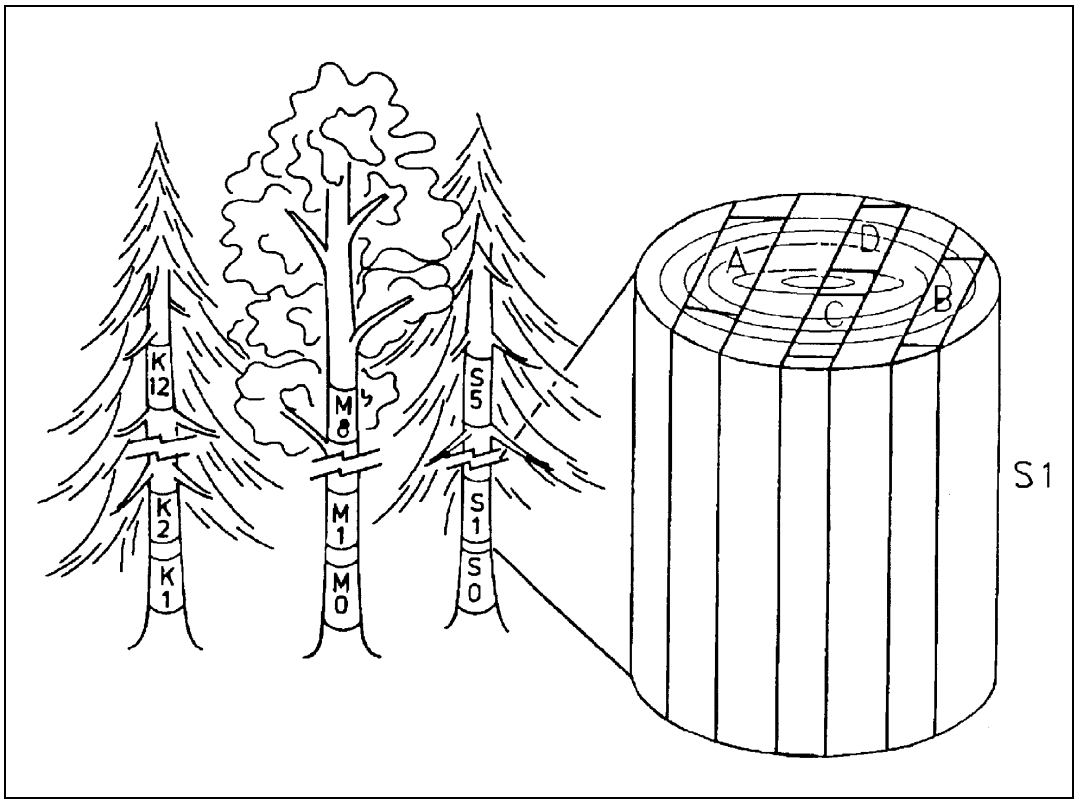

Fig. 2. Cutting of 0.5–0.7 m long logs to be used as raw material for test specimens. Two spruce trunks (K and S) and one pine trunk (M) were felled and cut into altogether 27 logs. In preparing the specimens, four narrow slices were cut out of the logs. Slices labelled A and B were cut from opposite sides of the log to be further produced into tangential test specimens whereas slices labelled C and D were cut across the middle of the log to be produced into radial specimens.

Specimens were prepared from the logs by cutting them first to four narrow parallel-to-grain slices (Fig. 2). Two of them, which were cut tangentially to the growth rings at two opposite sides of the log, were further produced into tangential specimens. The other two, which were cut across the middle of the log, were further produced into radial specimens. The tangential slices were marked by the letters A and B and the radial ones by the letters C and D.

These slices were glued along their long edges to auxiliary slices of equal thickness but whose grain direction was at 90° angle (Fig. 3). This was done in order to enable force transmission to the test specimens by longitudinal parts in the ends of the ready-made specimens. The slices containing the actual test material were cut to be defect-free, i.e. knots and other defects were avoided as well as possible. The auxiliary slices were obtained from the same logs from the left-over parts. The gluing was done by a finger joint type assembly using one component polyurethane adhesive (which was supplied by Casco-Nobel company), which is hardened by contact with moisture. The needed moisture for the adhesive to harden was provided by the natural water contained in the wood as it was in an undried state. During the preparation process the specimens were not allowed to dry

at any stage (they were kept inside plastic cover and in a refrigerator), but remained wet until they were taken to the test chamber. The only time they were dried just slightly was before the gluing, when the finger jointed surfaces were dried by a hot-air-blower. This was done cautiously so that only the very surface was affected to allow the adhesive to attach. Thus the drying that the specimens suffered during the creep experiments was the first one. The method of preparing perpendicular-to-grain tension specimen for tension in this manner has originally been developed by Kangas (1990) in an earlier study of the transverse creep of at conventional drying temperatures.

The preliminary plates obtained by the gluing were cut into four creep specimens (Fig. 3). Each of them was denoted by a four character label, in which the first two characters signify the log, from which it is taken, and the third character the slice and the forth character is for numbering of the specimens. In some cases, viz. logs from the trunk S, even more than four creep specimens were obtained from the preliminary plates.

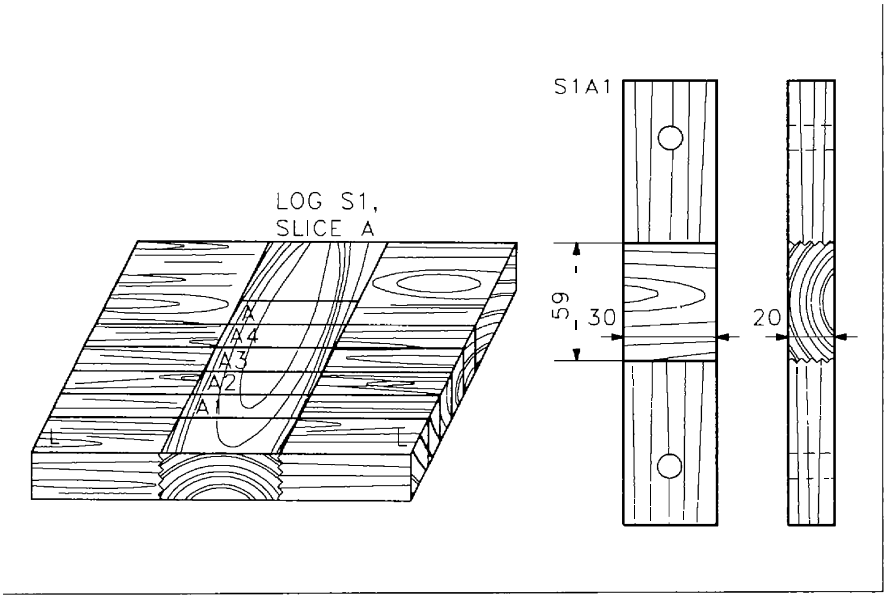

Fig. 3. Preparation of the test specimens. Each preliminary slice was glued along the two long edges unto two auxiliary slices (L) by a finger joint type assembly using one component polyurethane adhesive. The thus obtained plate was sawn into four creep test specimens, which were denoted by a four character label. The first two characters signify the log, where it is taken from, the third character the preliminary slice label and the four character is for the numbering of the individual specimens. Also, an additional specimen to be used as a weighing specimen was sawn beside the creep specimens. It was denoted simply by a three character label, which was the same as the three first characters of the creep specimens. In some cases even more than four creep specimens were sawn from the preliminary plates.

Also, an additional specimen to be used as a moisture content monitoring specimen (by continuous measurement of its weight changes) was sawn beside the creep specimens. It was denoted simply by a three character label, which was the same as the three first characters of the creep specimens. Its ends were sealed by moisture penetration blocking substance to make its moisture transfer properties to resemble those of the creep specimens.

The dimensions of the final specimens were (Fig. 3): cross-section 20mm × 30mm, where the shorter dimension is along the R- (tangential specimens) or T-direction (radial specimens) and the longer one along the longitudinal direction; measurement length (i.e. the length of the T- or R-direction middle part) 59mm. Displacement transducers were attached on two sides of the specimens onto the longitudinal end-piece, Fig 4.

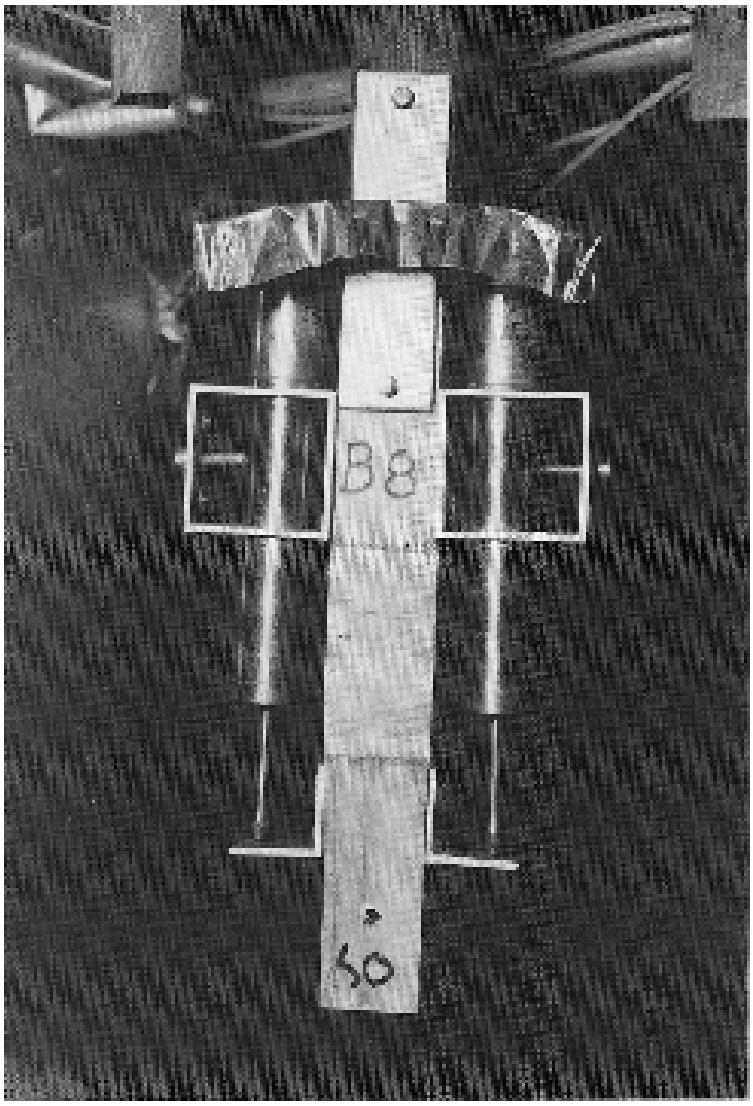

Fig. 4. Displacement transducers were attached on two sides of the specimen, because uneven shrinkage causes the specimen to warp during the test.

3.2 EXPERIMENTAL PROGRAMME

Creep experiments at conventional drying temperatures have shown that the mechano-sorptive creep – creep induced by simultaneous mechanical loading and moisture content changes – has a strong effect on the total amount of perpendicular-to-grain deformation during drying (Kangas and Ranta-Maunus 1989, Ranta-Maunus 1993, Svensson 1996). Thus main emphasis in this work was laid on the effect of moisture content changes and different temperature levels.

The experimental programme consisted of two main creep experiment series. 1) Creep experiments of wet (green condition) wood in water saturated condition in a hot water/steam bath inside a pressurised cylinder at temperatures 95°C, 110°C and 125°C. And 2) creep experiments of drying wood in a test chamber, where the humidity and temperature were controlled to simulate real drying conditions. Although the main purpose of these experiments was to measure the amount of creep deformation during different conditions, a great deal of additional information was also gathered concerning shrinkage, hygrothermal deformation, elastic properties and strength.

3.3 CREEP EXPERIMENTS IN CONSTANT CLIMATE

Almost all constant climate creep experiments were made for specimens in green condition, i.e. the specimens were not allowed to dry below fiber saturation at any state before or during the experiment. The decision to use the saturated condition was made primarily because viscoelastic creep is the most substantial for wet wood and because saturated conditions are easy to maintain by a water/steam bath.

There was also a small amount of constant climate creep tests for specimens, whose moisture content was taken below fiber saturation before loading. These experiments were made using the test chamber and set-up built for tests in drying conditions, which is to be introduced later.

3.3.1 Test apparatus

The creep experiments for saturated wood were made using a material testing machine to produce the desired loading, and a water/steam circulation system combined with a pressurised test cylinder to produce the desired temperature and saturation conditions. During the experiment the tested specimen was in a hot water/steam bath inside the test cylinder. The capacity for pressure development in the system permits testing at temperatures above 100°C. The apparatus is originally developed by Viitaniemi and Pennanen (1993) and is illustrated schematically in Fig. 5.

In this apparatus, water is heated in the pressure vessel, whose temperature is regulated by a control unit, that uses a temperature sensor inside the vessel. Steam/hot water is circulated between the pressure vessel and the test cylinder by an electric pump. Due to heat loss in the circulation, the temperature in the pressure vessel must be kept a few degrees higher

than the required temperature in the test cylinder. The temperature inside the test cylinder can be checked by a manually operated thermometer, whose sensor is inside the cylinder. The cylinder can be put temporarily out of circulation by directing the flow through a short-cut circuit in order to put in the specimen. After being mounted in the cylinder, the specimen is heated by the circulating steam/water.

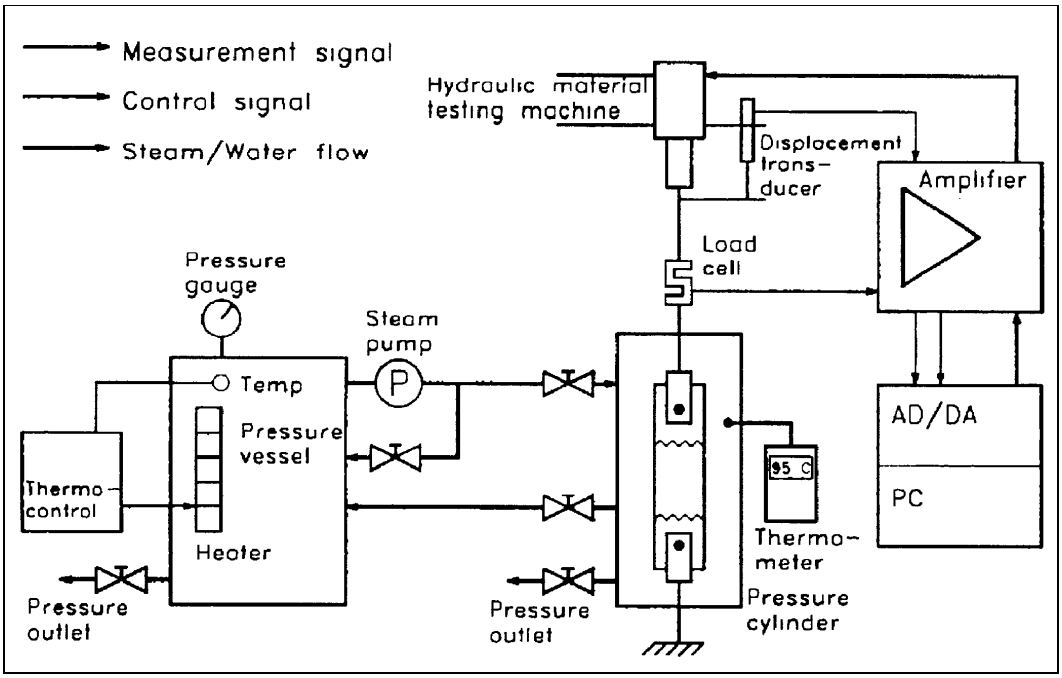

Fig. 5. Schematic illustration of the experimental set-up for creep tests in the saturated condition. Steam/water is circulated between a pressure vessel and a pressurised test cylinder, in which the specimen is kept during the test. Water/steam is heated in the pressure vessel, in which the temperature is controlled by a control unit. Due to heat loss in the circulation, the temperature in the pressure vessel must be kept a few degrees higher than the desired temperature in the test cylinder, which can be checked by a manually operated thermometer, whose sensor is inside the cylinder. The cylinder can be put temporarily out of circuit by directing the flow through a short-cut circuit in order to enable mounting of a new specimen.

The load is measured using a load cell that is mounted as a part of the force transmitting mechanism. The deformation is measured by a displacement transducer, which is attached to the main body of the material testing machine and whose measurement tip to the piston.

The fact that the measurement of displacements was not done directly from the specimen but outside the pressure cylinder from the piston causes error to the displacement measurements. The error is induced by the compliance of the force transmitting system and the yielding of the dowel joint used in the attachment of the specimen. The error induced by the compliance of the force transmission is by nature instantaneous but partly irrecoverable, whereas the error caused by the yielding of the joint is also time-dependent (the joint may creep). These errors were compensated by a

time-dependent correction, which was determined by performing some tests in conditions similar to the actual tests for a few specimens that were otherwise similar to the actual test specimens but which were wholly longitudinal.

3.3.2 Loading

The test set-up allows testing of only one specimen at a time. The tested specimen was first allowed to heat up in the hot bath for at least 20 min. After that, in order to remove any free motion, the test was started by raising the load slowly to a small value, which corresponds to 0.015 MPa stress. Then, the actual loading to the desired full load was done. In many cases, the full load was first kept on for c. 10 min but then lowered down to a value of 1/10 of the full load to be kept there for c. 10 min and then raised again to the full load. But in about as many tests, this early recovery period was omitted. The length of the actual long loading period ranged from few hours to c. 24 hours. In many cases, there was also a final recovery period with 1/10 load lasting for a few hours. All load raises and drops (except the starting slow removal of the free motion) were done in c. 10 s.

3.4 CREEP EXPERIMENTS IN DRYING CONDITIONS

The creep experiment series in drying conditions was considered as the most important part in the experimental programme of this project, because of the significance of the mechano-sorptive effect. It was also given the most effort. For the purpose of performing creep experiments for drying wood in conditions that resemble the conditions inside a drying kiln, a laboratory scale drying test chamber was built. In fact the constructed apparatus allows laboratory scale simulation of kiln drying conditions for small creep specimens under tensile load.

3.4.1 Test apparatus

The base of the apparatus is an aluminium frame box, the test chamber (inside dimensions roughly: height 0.5m, width 1.5m, depth 1m), which is insulated by rock wool. Photographs of the chamber are provided in Figs. 6 and 7. The front wall of the chamber is removable and it serves as the access panel for the mounting of specimens, etc. The chamber is equipped with a temperature and humidity regulating system. The function of the system is illustrated in the schematic diagram given in Fig 8 and the placement of the different components in Fig. 9. The regulated variables inside the chamber are the dry bulb temperature (i.e. the air temperature) and the wet bulb temperature (which is equivalent to regulating the humidity). The basic idea of the temperature and humidity control is the same as in the experiments of Kangas (1990), but numerous modifications have been incorporated.

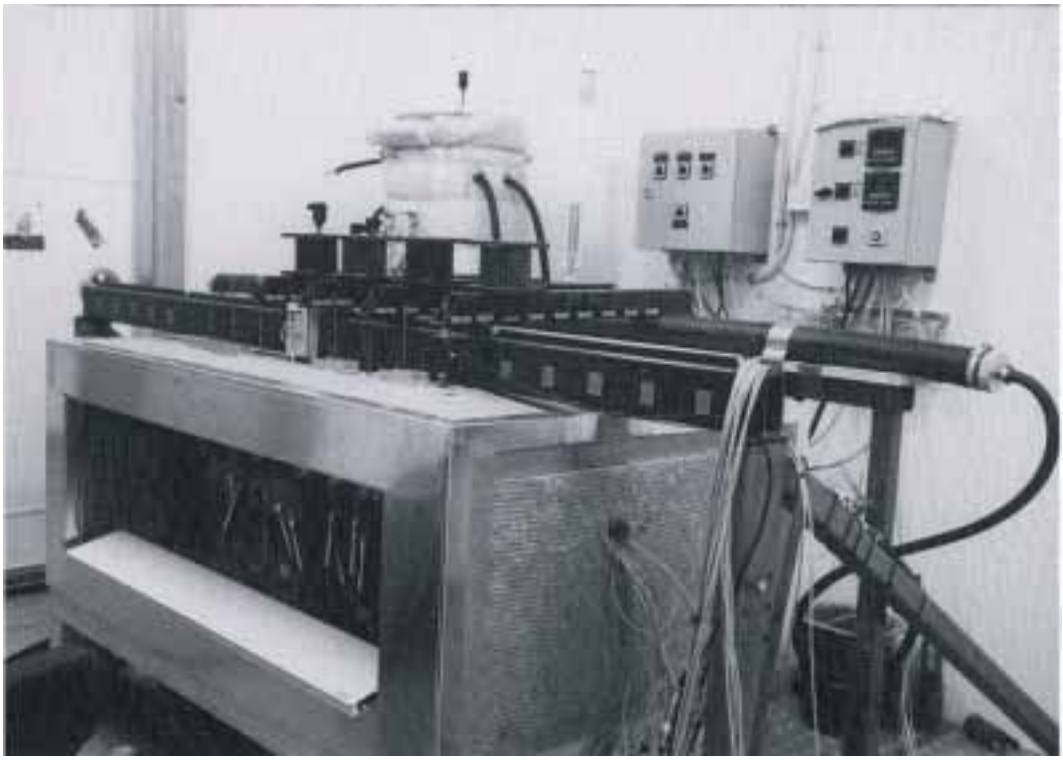

Fig. 6. Test chamber for conducting creep experiments in drying conditions.

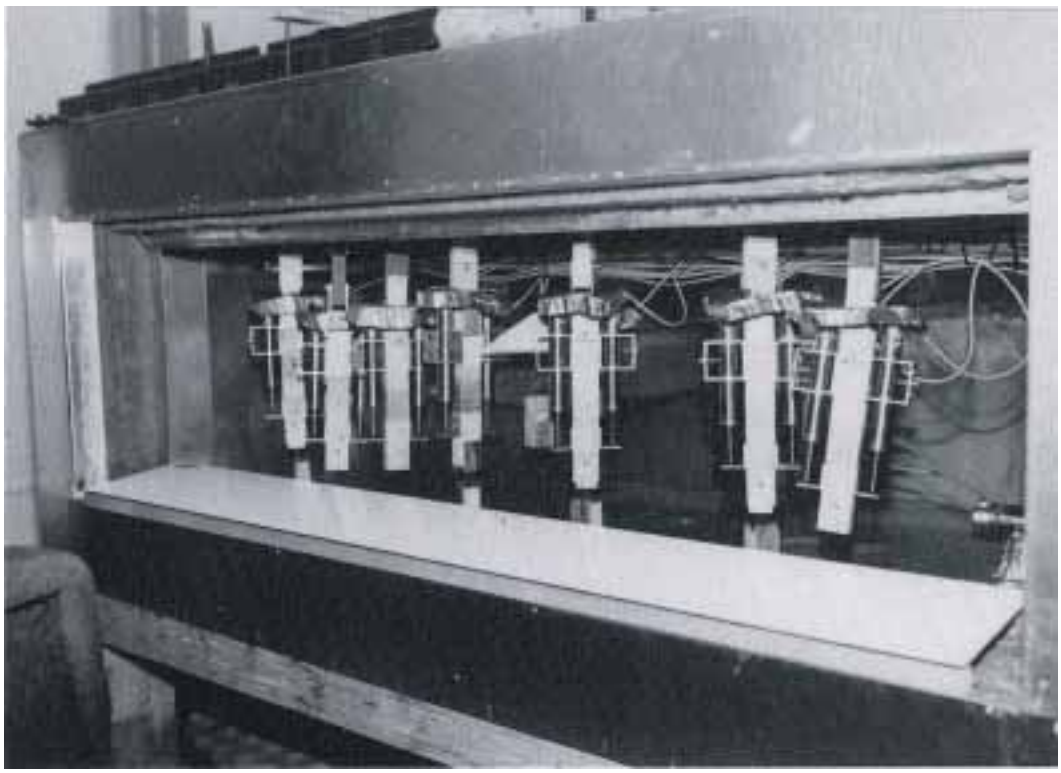

Fig. 7. A detail of the inside of the test chamber.

The temperature inside the chamber is regulated by switching on or off an electric heater when necessary; the control is implemented by an electronic temperature controller, which obtains the measurement signal from a temperature sensor inside the chamber. The regulation of the humidity (i.e. the wet bulb temperature) is basically achieved by heating or cooling water in an open basin inside the chamber. The temperature of the water controls the amount of evaporation on the water surface, which in turn controls the humidity of the air. The water is heated, when necessary, by an electric heater inside the basin and cooled, when necessary, by letting cold water in from the water supply. The regulation is again done using an electronic temperature controller, which obtains the measurement signal from a wet bulb temperature sensor. The water level in the basin is controlled by level controllers, which either drain water out through the bottom of the basin or let pre-heated water in the basin.

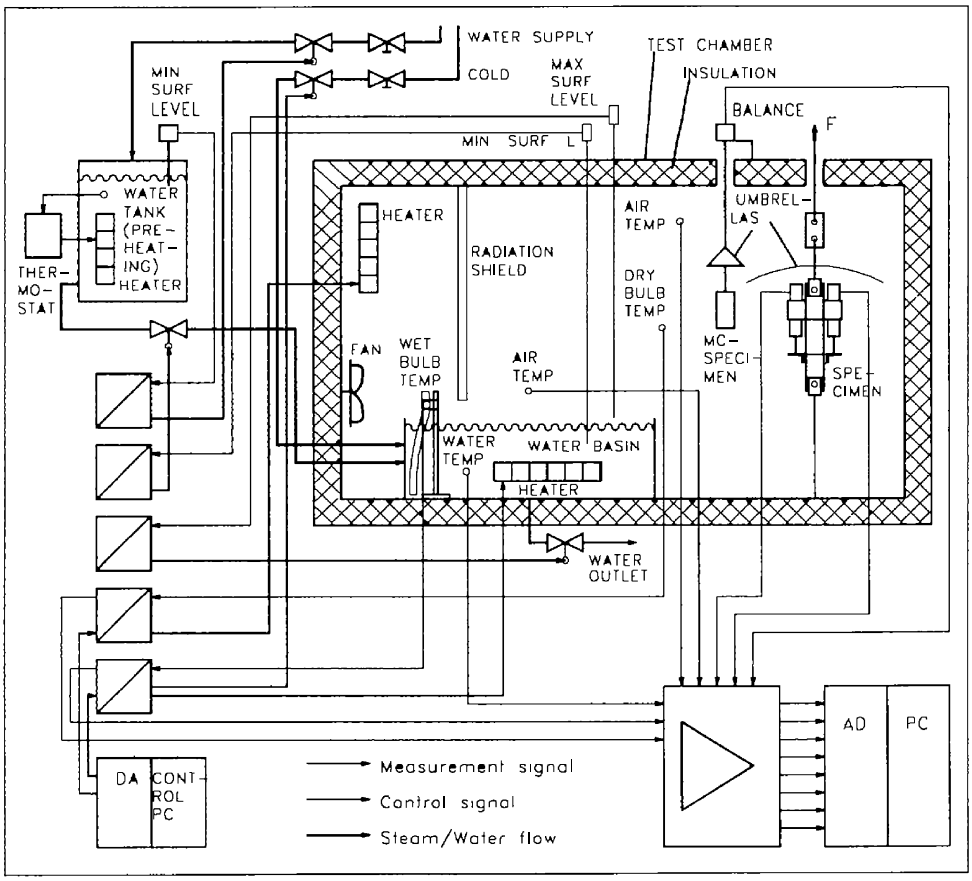

Fig. 8. Schematic view of the function of the experimental set-up for creep tests in drying conditions.

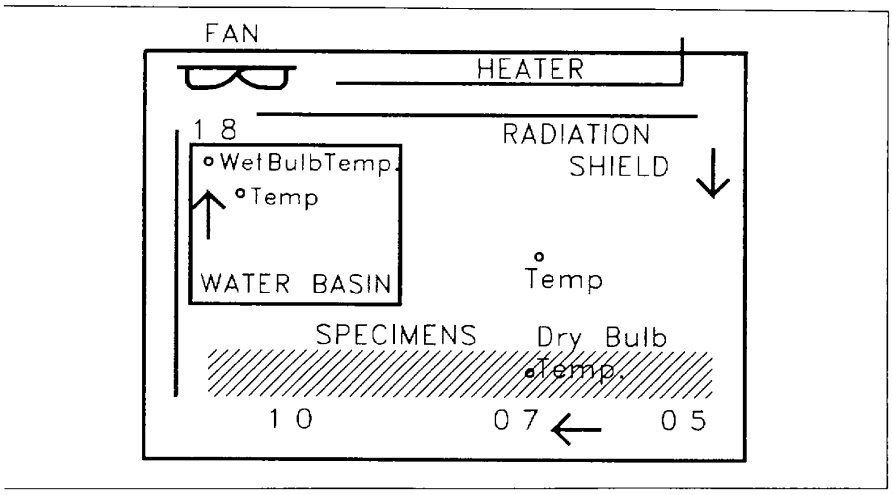

Fig. 9. Schematic view of the test chamber seen from the top and placing of the specimens and temperature sensors. The fan is of centrifugal type, which is used for example in convection ovens. The radiation shield and the additional partitioning plate near the left side of the chamber extend in height from the floor of the chamber up to its ceiling and they are used to direct the air flow in order to enable the centrifugal fan idea to work better. The arrows show air flow and the figures show the measured air velocities (m/s) inside the test chamber.

3.4.2 Loading system and mounting of specimens

The loading of tension specimens is implemented by weights and lever arms located outside the chamber. The force is transmitted by pull rods that go through small holes in the ceiling of the chamber. The chamber can at a time take four tension specimens for creep measurement and four zero-load 'dummy' specimens for measurement of free shrinkage. In addition, it can employ two balance specimens for continuous weighing for the purpose of moisture content monitoring. One test series thus contains four creep-specimen–dummy pairs and two moisture content specimens.

The drying condition tests were arranged so that all specimens used in any one test were taken from a single log, from the two slices that were of the same material direction. The specimens to each loaded position and the dummy position next to it were always selected to be adjacently cut ones. The sustaining to this arrangement of adjacent creep and zero-load specimen pairs was chosen, because it was judged to give the best reliability in measurement of the difference between the loaded and zero-load behaviour.

3.4.3 Drying schedule and loading scheme

The regulation of the conditions (wet and dry bulb temperature) varied between tests, but followed a certain basic scheme. In most experiments the drying schedule was according to the pattern described in the following and shown examplewise in Fig. 10.

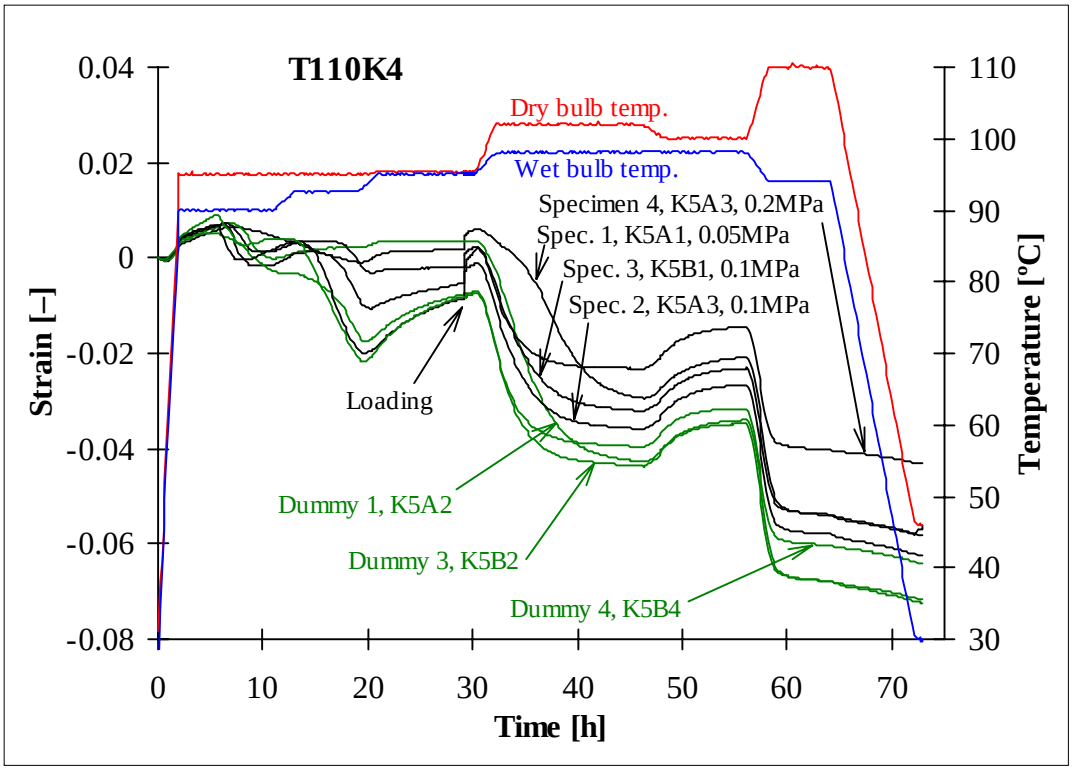

Fig. 10. Example of the evolution of a creep test in drying conditions. The drying schedule consists of a heating period (0–2h), an initial drying period (2–30h), during which the specimens are brought to a moisture content level close to FSP, loading at c. 28h, the actual drying period below FSP (30–64h) and final cooling (64–72h). Note the deformation behaviour of the specimens during the heating and few hours after, which shows the hygrothermal phenomenon. 'Dummy' means a zero-load specimen to control free shrinkage.

Each test started with a heating period of 2 hours, during which the temperature was raised from room temperature to 95°C. The schedule continued then with an initial drying period of c. 28 h, during which the drying power (difference of the dry and wet temperature) was first high but was diminished gradually, so that during the last 8 h of this period the wet bulb temperature was kept as close to the dry bulb temperature as the equipment was able to perform. The intention for this initial drying period was that the specimens, whose moisture content is initially high above the fibre saturation point (FSP), are brought to moisture content level close to FSP for loading. The purpose of the moist period is that the moisture content distribution in the specimens has time to even up. About 2 h before

the end of this period (i.e. c. 28 h after start of the experiment) the specimens are loaded.

After the initial drying period the actual drying below FSP is started and shrinkage is assumed to begin. In most tests, drying was done first to an intermediate level, followed by some re-moistening before a final drying period down to a moisture content of 2–5%. But in order to investigate the effect of different moisture-change patterns there were also some tests in which the drying was completely monotonous and some tests in which there were many drying-moistening cycles before the final drying.

In all tests the initial drying period was done at 95°C, but drying below FSP varied between tests so that the maximum temperature reached during the test was either 95, 110 or 125°C. For tests at 95° the temperature could be kept constant and the humidity control done merely by the wet bulb temperature value, whereas in tests with maximum temperature 110 or 125°C the humidity regulation had to be realised partly by the dry bulb temperature and thus the test temperature was not constant. In most tests there was also a final cooling period, during which the temperature was taken down to near room temperature in a controlled manner. After the test the final moisture content and density of the specimens were measured by weighing and oven-drying method.

Loading was done simultaneously for all specimens by letting pressure air out of a tube, which when inflated supports the lever arms that produce the load. The period of load increase from zero to full load took c. 10 s. Constant load was used, i.e. the load was kept on unchanged until the end, but in many tests the load was temporarily removed for a few minutes in order to study the value of the modulus of elasticity at given conditions during the test. Also, to study the creep recovery properties, load was in some tests removed for a longer period of time.

3.5 ACHIEVEMENT OF MEASUREMENTS AND PROCESSING OF DATA

The experiments yielded a large amount of raw data, which required much processing before being easily comprehensible. The achievement of the test conditions, quality of the obtained measurement data and the way the data was processed are cursorily described before going on into the final results.

3.5.1 Experiments in constant conditions

A list of all successful experiments in the constant wet condition set-up is given as part of Appendix A (altogether 34 specimens). In these tests the temperature inside the test cylinder varied a little and the achieved accuracy is estimated to be c. ±2°C, which is based on sample measurements made by a manually operated temperature sensor inside the cylinder. The accuracy was probably somewhat better for most of the time.

As was mentioned in the introduction of the experimental set-up, the displacement measurements were not made directly from the specimen, which was inside the pressurised test cylinder, but from the testing machine

piston. Thus the measured displacements contain error that is induced by the compliance of the test machine and the yielding of the dowel joint by which the specimen is attached. These errors were compensated by a time-dependent correction, which was based on similar tests on specimens that were purely longitudinal. The compliance curve obtained from these subsidiary experiments was subtracted from the actual measured compliance of the perpendicular-to-grain specimens to obtain the 'true' compliance. However, as it turned out that the correction compliance to be subtracted comprised a fairly large proportion of total measured displacement (c. 50% for radial specimens, c. 30% for tangential specimens) and the measured correction compliances also showed scatter, it is assumed that some error (scatter) may be left in the final results despite the correction.

The specimens were allowed to heat for 20 min before loading, which should be enough to reach equilibrium with the temperature of the water/steam bath. However, as the hygrothermal deformation may occur as delayed, it is not known whether it has had some effect on the measured strains. The results have not been corrected for the possible effect of hygrothermal deformation.

The modulus of elasticity was determined for each specimen from the compliance value at 1 min after loading.

3.5.2 Experiments in drying conditions

Altogether 45 tests were made in the drying condition chamber. They were identified by a letter–number combination, such as T110K3, where the number after T denotes the maximum temperature reached during the test and K plus the second number is a sequential label. A list of all test series and specimens is given in Appendix A. Because of simultaneous test method development and starting troubles with the moisture control system, the specimens in the first tests did not dry as was intended but remained wet for long. Thus, in fact, the very first tests did not yield drying condition results but instead constant wet condition creep curves, which are valuable results, too. Also, some later experiments yielded constant wet condition results, because of deficiencies in the drying of specimens due to variable reasons. In some tests the fan did not work and in many 'successful' tests the period from loading to the beginning shrinkage is long enough to give an idea of the constant condition response. Some tests were also intentionally made in moist conditions to yield wet condition results.

Overall, after the starting hardships the climate control system worked well. The regulation of both the dry bulb temperature and the wet bulb temperature functioned with good accuracy most of the time. In some tests there are departures, peaks or oscillation, from the control curve, the cause of which is not known, possibly an interference from outside source.

Also the measurement of displacements functioned well. This type of measurement requires that there are two transducers measuring one specimen, because in practise there is always some uneven shrinkage causing warping, so that the employment of the average of the displacements measured on two sides is necessary. Unfortunately, two displacement transducers broke down during the experimental programme

and the number of specimens had to be reduced. This was done by removing one dummy position from service. However, the principle of having adjacently cut creep-specimen–dummy pairs needed not to be violated, because one dummy could serve as the zero-load control for the two creep specimens cut along its sides.

Moisture content measurements were not quite as successful. The weight drop measurement itself functioned well: although the swinging motion of the hanging specimens due to air circulation causes oscillations, the weight changes are detectable. However, the initial moisture content values calculated backwards based on the final dry weight and the measured weight drop are too high. The cause for this is that other constituents than water are extracted from wood in the high temperature conditions. Another potential cause for inaccuracy is that water, which possibly condenses on the specimen and on the suspension wire, may alter the result. Nevertheless, the weight drop measurements do give good qualitative information of the moisture content changes, although moisture content values based on them should not be taken as absolutely exact.

The displacement measurements of each creep and zero-load specimen were processed by taking the average of the transducer readings measuring on the two sides and transforming it to strain and compliance values.

Initial MOE values were determined based on compliance values at 1 min after first loading. Similarly, the MOE values at the subsequent unloading-loading sequences later during the course of the experiment were determined based on the compliance change at 1 min after unloading.

The time-dependent compliances of loaded specimens were calculated by determining an estimate for their zero-load behaviours and subtracting those from the measured strains under load. For each creep specimen, the estimated zero-load behaviour was based on its matched dummy pair, whose origin had been adjacent to the creep specimen. The basic idea in the estimation was that the shrinkage behaviour of the loaded specimen and its dummy is the same, so that if there is enough time for them to dry and the moisture content to reach equilibrium, their shrinkages will be equal. The estimated zero-load behaviour was determined as a new curve which before loading moment follows the measured strain of the creep specimen but after loading gradually begins to approach the measured strain curve of the dummy and reaches it at the first equilibrium moisture level during drying. An example of the estimation procedure is shown in Fig. 11. In some rare cases, when it was clearly seen that the above procedure would not give the best result, the estimated zero-load behaviour after loading was assumed to follow directly the length changes of the dummy.

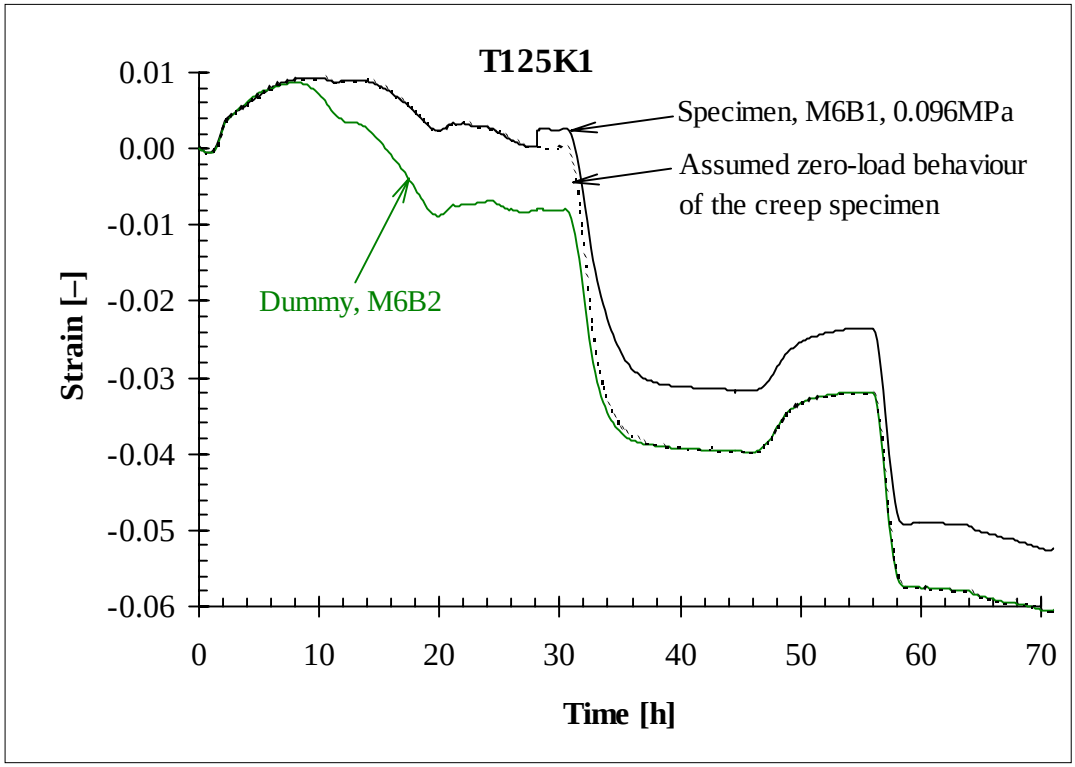

Fig. 11. An example of the estimation of the zero-load shrinkage behaviour for a loaded creep specimen based on the measurement of the shrinkage of a dummy specimen, which has been cut adjacent to the creep specimen. The estimation is based on the idea that if there is enough time for both specimens to dry and their moisture contents to reach equilibrium, their shrinkages will be equal.

The laborious procedure of producing matched creep-specimen–dummy pairs and of estimating the zero-load shrinkage in the rather complicated manner was made as an attempt to ensure best possible accuracy in final compliance results. The fundamental cause for the need of careful matching is of course that the zero-load and non-zero-load behaviour cannot be measured on the same specimen (any drying from green permanently changes the properties). However, even if the specimens and their dummies were well matched, their shrinkages may have been different due to the inevitable variability of wood material. This causes scatter of the final compliance curves, which seems to not be completely avoidable; but with results from a sufficient number of pairs the average result should be reliable.

Besides the errors caused by the difference of the final shrinkage values of the specimen and its dummy, there can be errors caused by differences in their drying speeds and consequent shrinkage rates. Contrary to the above, these effects can be corrected in the final compliance curves. The shrinkage rate difference, which could also be described as a ‘phase shift’ between the shrinkages, induces a ‘mountain’ or a ‘valley’ onto the compliance curve during a rapid shrinkage period. These errors can be easily detected and corrected as is shown in Fig. 12.

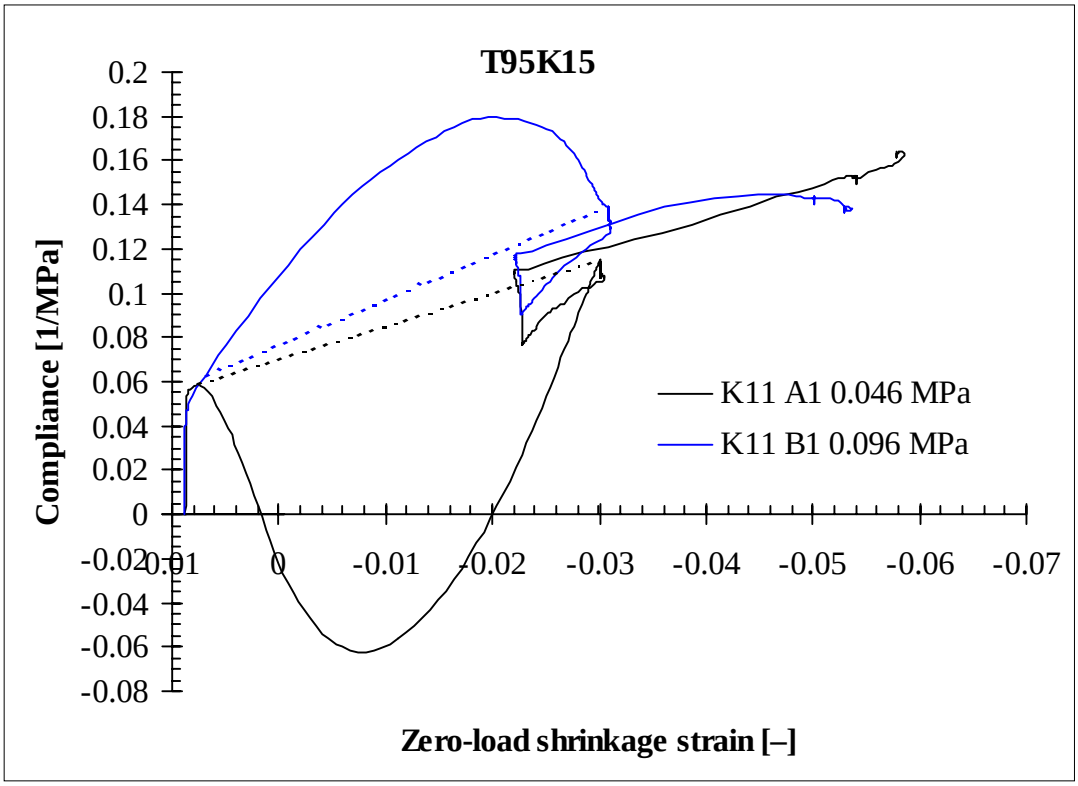

Fig. 12. Example of the error in the compliance caused by the difference between the shrinkage rates of the creep specimen and its dummy. This difference induces a 'mountain' or a 'valley' onto the compliance curve depending on whether the dummy or the specimen shrinks faster. The error can be easily corrected (dotted lines).

3.6 RESULTS

All results are given in Appendices B and C in such a form that the behaviour of each specimen is distinguishable. In the following, the results are gathered for better evaluation.

3.6.1 Hygrothermal deformation

As can be seen in Fig. 10 and in the figures of Appendix C, an interesting feature in the results of drying condition tests is the behaviour of the specimens during the heating period and few hours after it. Namely, tangential specimens swell during the heating but radial specimens shrink (the specimens in Fig. 10 are tangential). This is a manifestation of the hygrothermal deformation phenomenon, which occurs when wet wood is heated (e.g. Kubler 1973). It seems that for most radial specimens the hygrothermal shrinkage occurs until the heating period is finished and does not continue much afterwards, whereas for tangential specimens swelling may continue few hours after the heating is finished. It is possible to

estimate the magnitude of the hygrothermal strain based on the experiments, but it should be noted that since the heating is made in air true shrinkage may affect the results. According to the measurements, on heating to 95°C the hygrothermal strain is c. 0.8% (swelling) in tangential direction and –0.3% (shrinkage) in radial direction. These results are in good agreement with earlier findings (Kubler 1973).

3.6.2 Shrinkage

Shrinkage was studied using the measurements on the dummy specimens in the drying condition tests. Based on shrinkage at the end of the final drying period (before cooling), an estimated shrinkage value on drying from green condition at room temperature to 0% MC at the final temperature was calculated. This value, which includes the effect of hygrothermal deformation is plotted against density in Figs. 13 and 14. The dependence of shrinkage on density is clearly seen for the radial shrinkage but is not as clear for tangential shrinkage. This may be caused by the fact that perfectly tangentially directed specimens are much more difficult to manufacture than radially directed ones, and consequently tangential results contain more scatter.

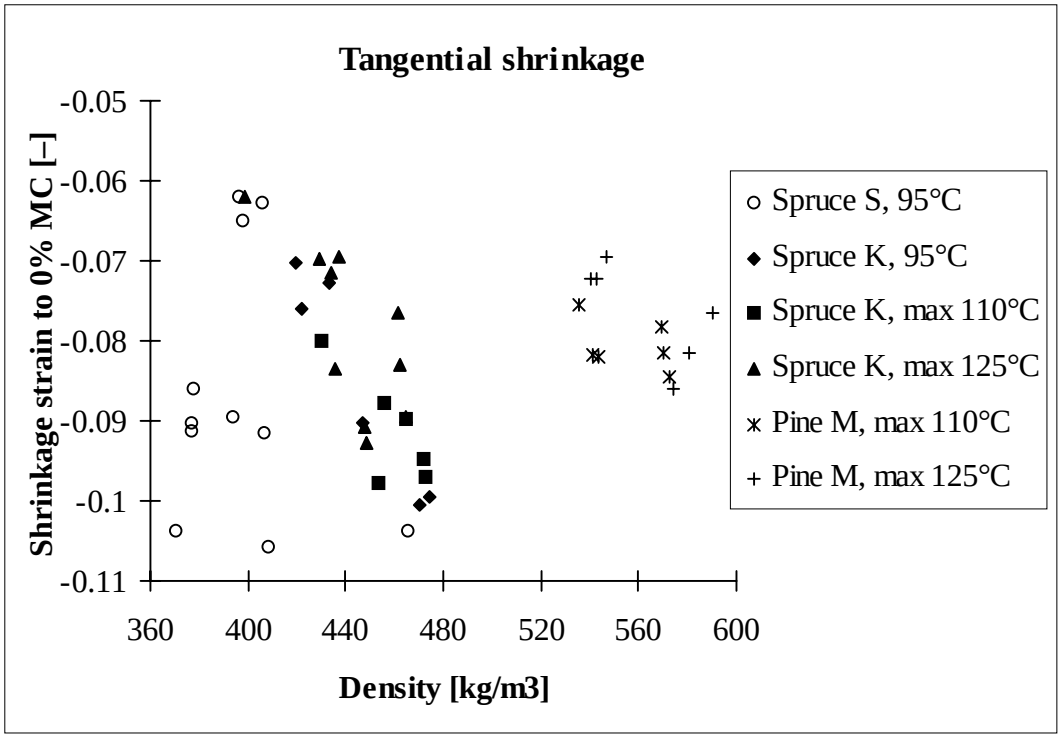

Fig. 13. Dependence of tangential shrinkage on density. Shrinkage (which includes the hygrothermal effect) to 0% MC has been calculated based on shrinkage after the final drying but before cooling. The temperature values 110 and 125°C indicate the maximum temperature during the experiment and thus a substantial part of the shrinkage has actually occurred at lower temperature.

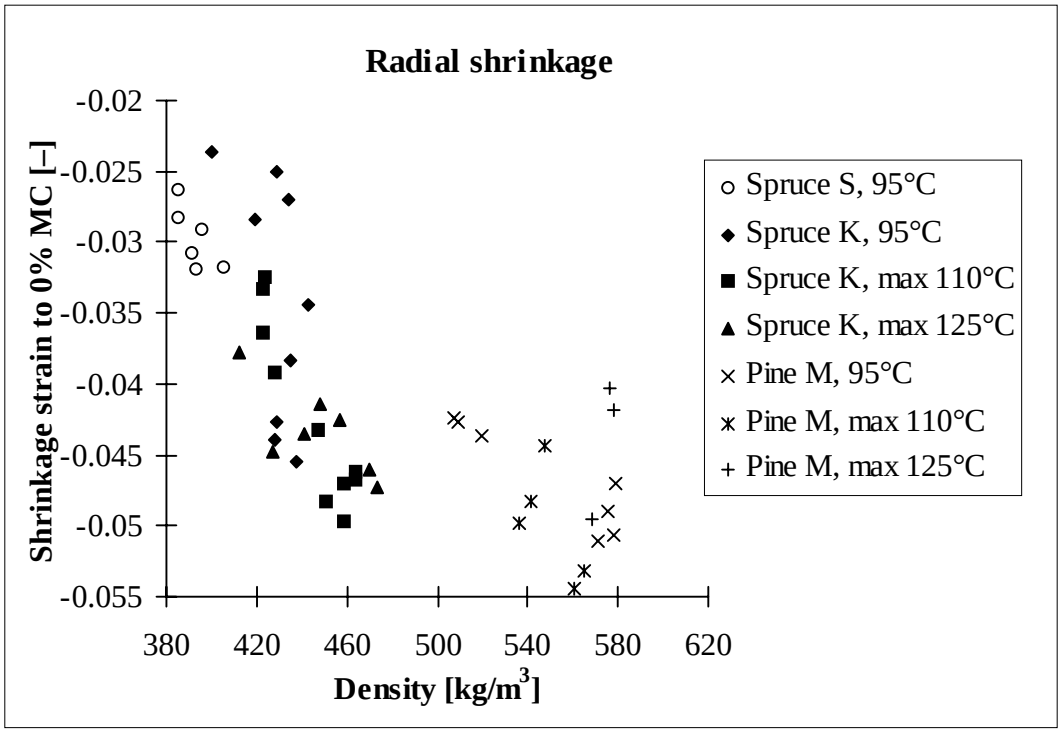

Fig. 14. Dependence of radial shrinkage on density. Shrinkage (which includes the hygrothermal effect) to 0% MC has been calculated based on shrinkage after the final drying but before cooling. The temperature values 110 and 125°C indicate the maximum temperature during the experiment and thus a substantial part of the shrinkage has actually occurred at lower temperature.

3.6.3 Modulus of elasticity

The results from both drying condition and wet condition tests were used to study the modulus of elasticity (MOE). The dependence of the MOE on moisture content and temperature are the most interesting aspects.

Based on the drying condition tests, the modulus of elasticity is plotted against moisture content for tangential and radial specimens of Spruce K at 95°C in Figs. 15 and 16, respectively. Each point represents one measurement and points joined with lines represent measurements on a single specimen. The many measurements on a single specimen are based on the first loading (~ saturated condition) and subsequent unloading–loading sequences in different conditions during the course of the drying condition test. Similar graphs for Pine M are given in Figs 17 and 18. The results show the huge effect of moisture content on the MOE.

In Figs. 19 and 20 the effect of temperature on the tangential MOE in wet condition is shown for spruce and pine, respectively. For comparison, the measurements of static MOE over the temperature range 20–80°C by Siimes (1967, *Picea abies* and *Pinus sylvestris*) are shown as well as the measurement of dynamic MOE at 20–140°C by Salmén (1984, *Picea abies*). The new results show a very consistent continuation to the earlier results.

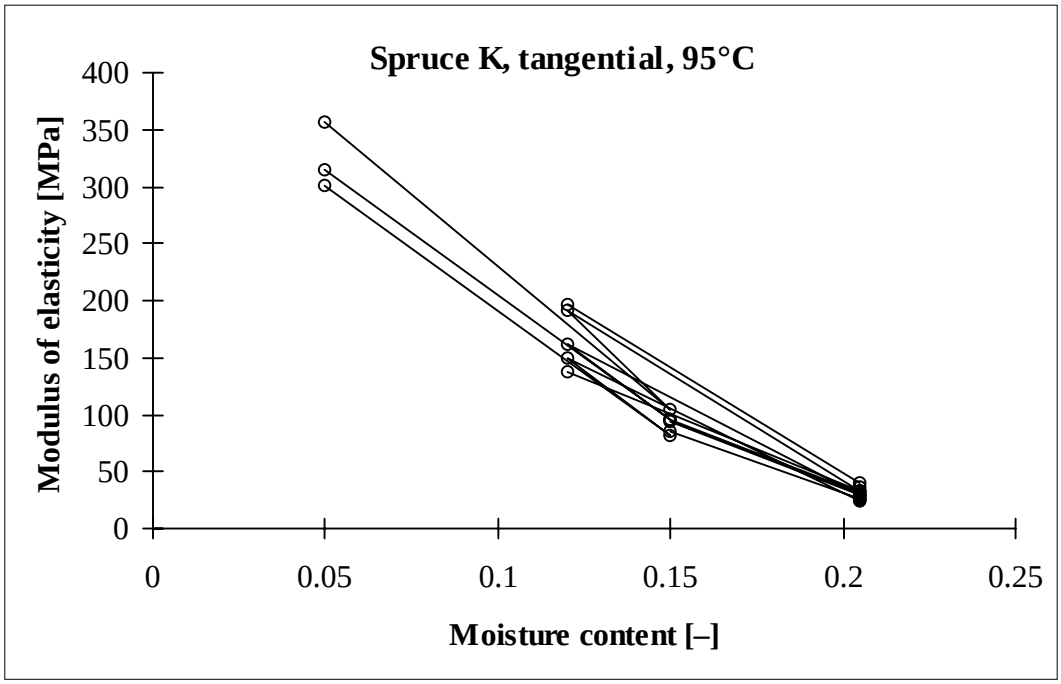

Fig. 15. Modulus of elasticity against moisture content for tangential specimens of Spruce K at 95°C. Each point represents one measurement; points joined with lines represent measurements on a single specimen at first loading and subsequent unloading-reloading sequences during the course of the experiments. Values have been determined corresponding to compliance change at 1 min after load change.

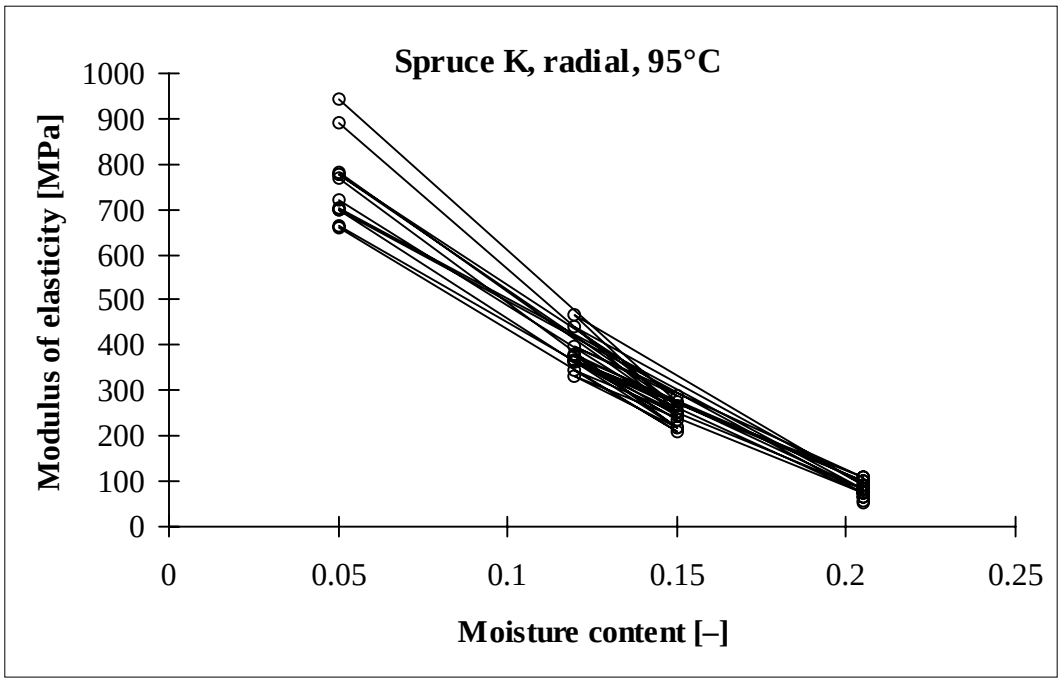

Fig. 16. Modulus of elasticity against moisture content for radial specimens of Spruce K at 95°C. See note in the caption of Fig. 15.

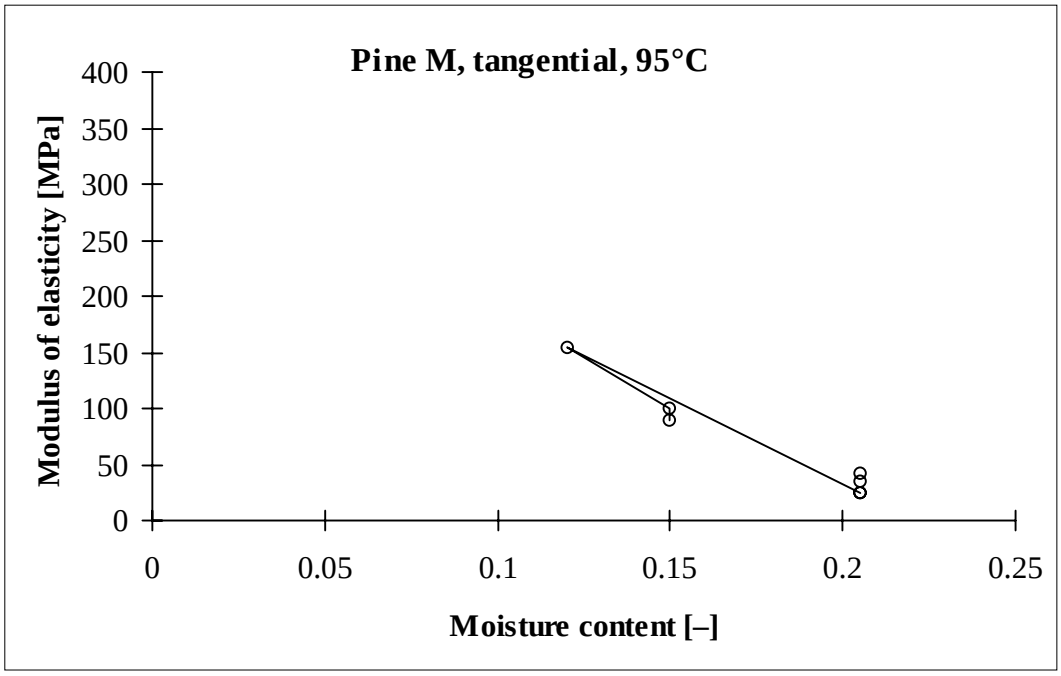

Fig. 17. Modulus of elasticity against moisture content for tangential specimens of Pine M at 95°C. See note in the caption of Fig. 15.

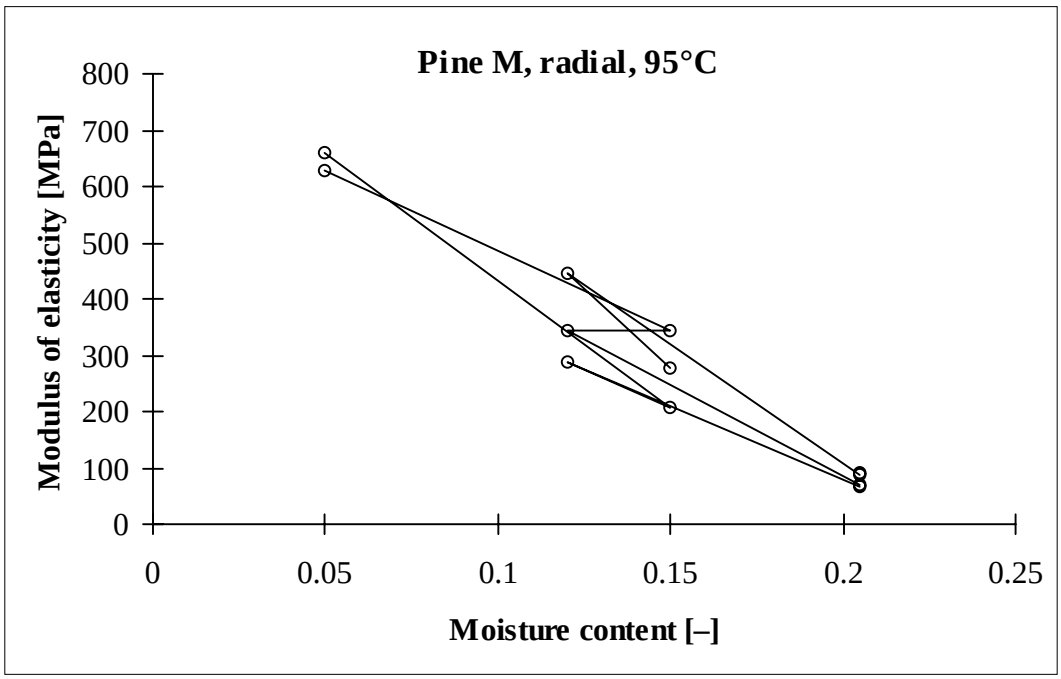

Fig. 18. Modulus of elasticity against moisture content for radial specimens of Pine M at 95°C. See note in the caption of Fig. 15.

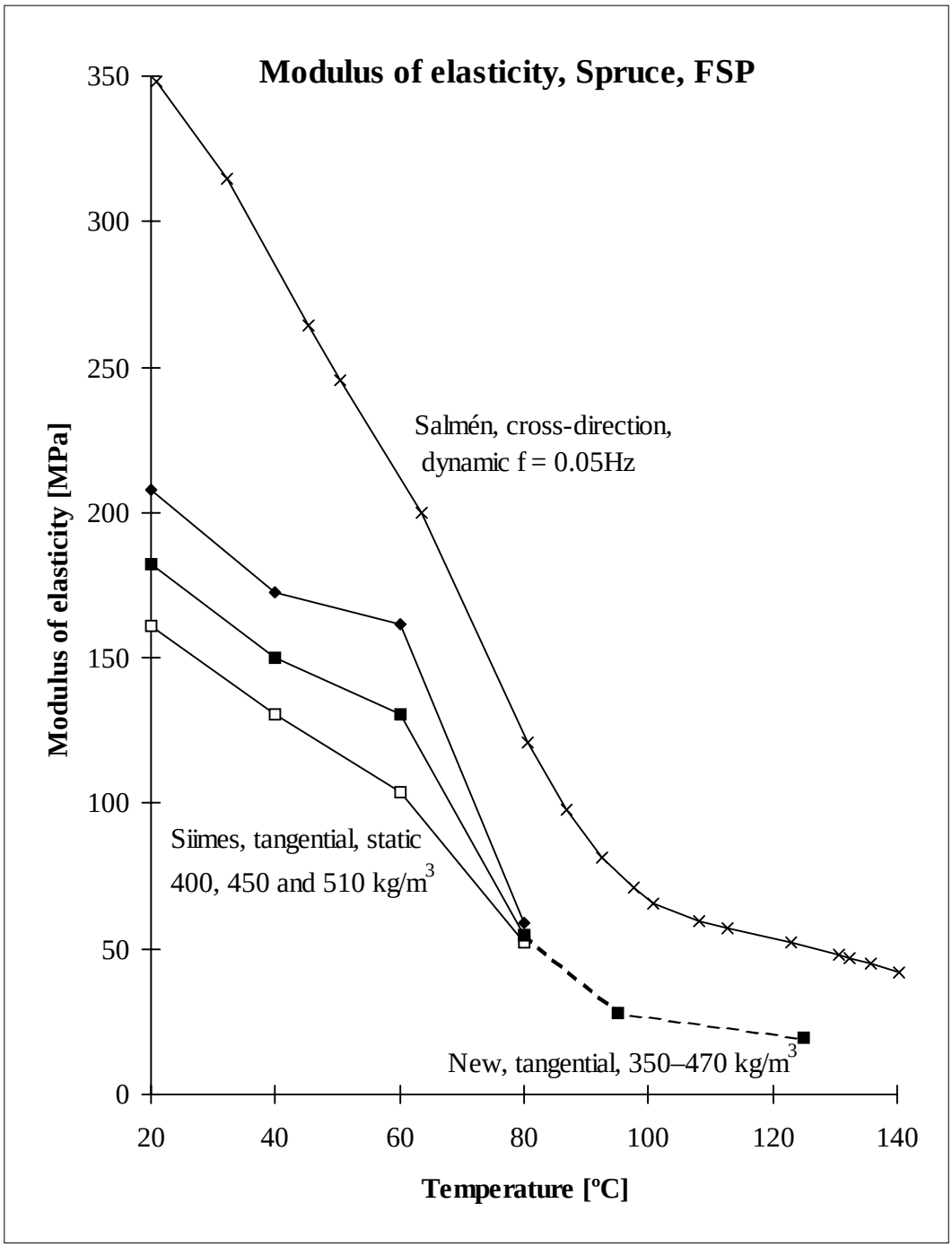

Fig. 19. The effect of temperature on tangential MOE in wet condition for spruce (New, Picea abies). For comparison, the measurements done earlier at VTT on static MOE in temperature range 20–80°C (Siimes 1967, Picea abies) are shown as well as the measurements on dynamic MOE at 20–140°C by Salmén (1984, Picea abies).

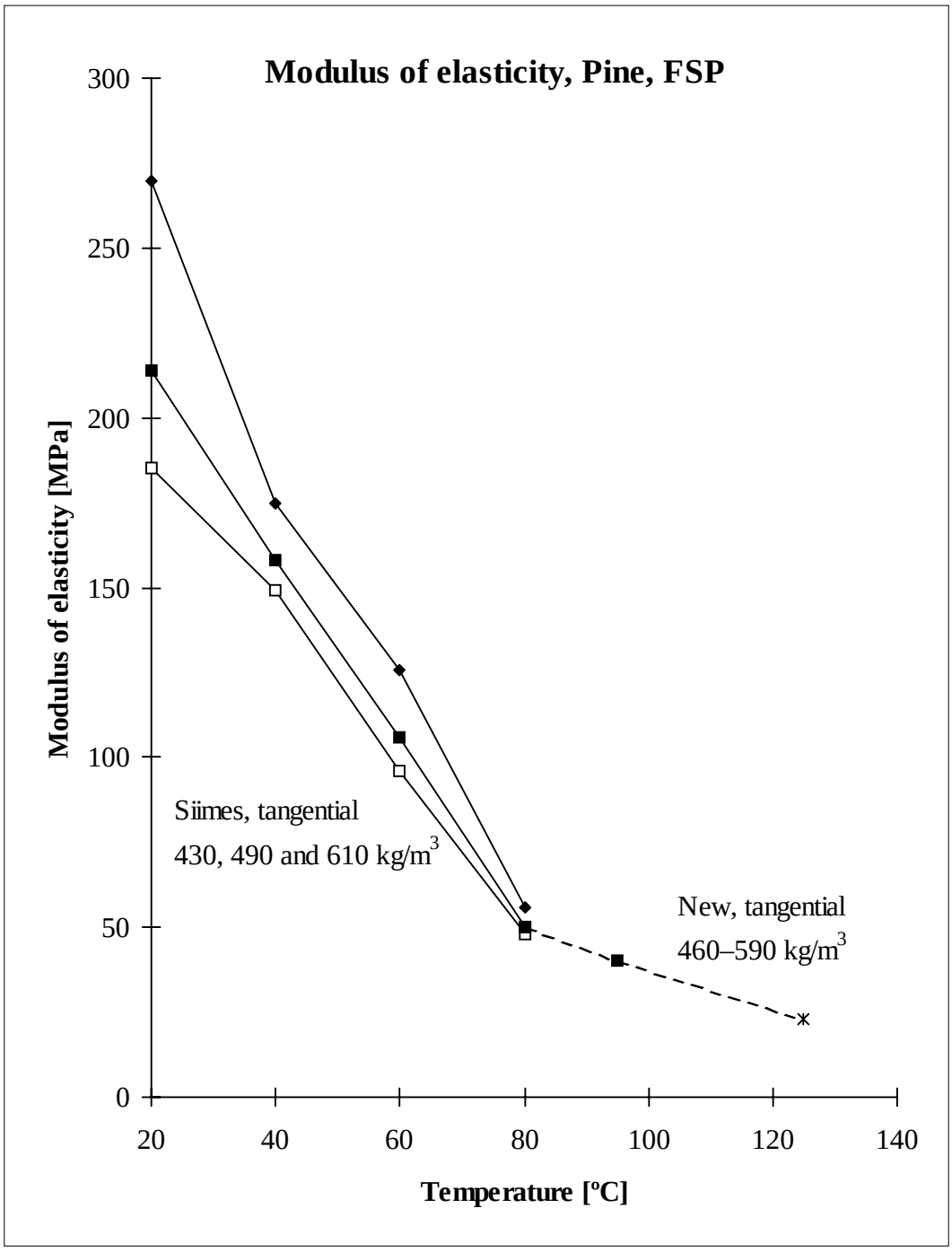

Fig. 20. The effect of temperature on tangential MOE in wet condition for pine (New, Pinus sylvestris). For comparison, the measurements done earlier at VTT on static MOE in temperature range 20–80°C (Siimes 1967, Pinus sylvestris) are shown. Experimental point denoted by the asterisk (∗) is based on only two specimens.

3.6.4 Viscoelastic creep

Of the constant wet condition viscoelastic creep tests, the ones of Spruce S specimens were the most successful. Their compliances in wet condition at 95 and 125°C are shown in Figs. 21 and 22. The 95°C curves have been extracted from tests both in the hot water/steam bath condition and in moist condition in the drying test chamber. The latter ones have been corrected against possible effect of hygrothermal strain based on zero load dummy specimens in the same tests, but no correction was possible to do for the test made in the hot bath as there were no comparison specimens. The curves show clearly the increase of the creep rate due to temperature raise.

For the two other trunks there were fewer results and they showed more scatter, but the appearance is quite similar to the Spruce S results. The compliances for Spruce K are shown in Figs. 23 and 24 and for Pine M in Figs. 25 and 26. The greater scatter of the results is assumed to be due to error, which remains in the results after correction for the machine and dowel joint compliances. Apparently, for some reason, there has been more variability in the compliance of the dowel joints in Spruce K and Pine M specimens than Spruce S specimens, which causes more scatter in the results (the correction was the same for all specimens). However, if enough results are available, the average is assumed to be quite reliable even for Spruce K and Pine M. Mathematical creep curves were determined for the wet condition in the different cases by graphical estimation; and they are also shown in Figs. 21–26.

There was also one test made in the drying test chamber, in which constant condition below FSP, viz. about 18% moisture content, was maintained after loading. This test was made with Spruce S and the results are shown in Fig. 27.

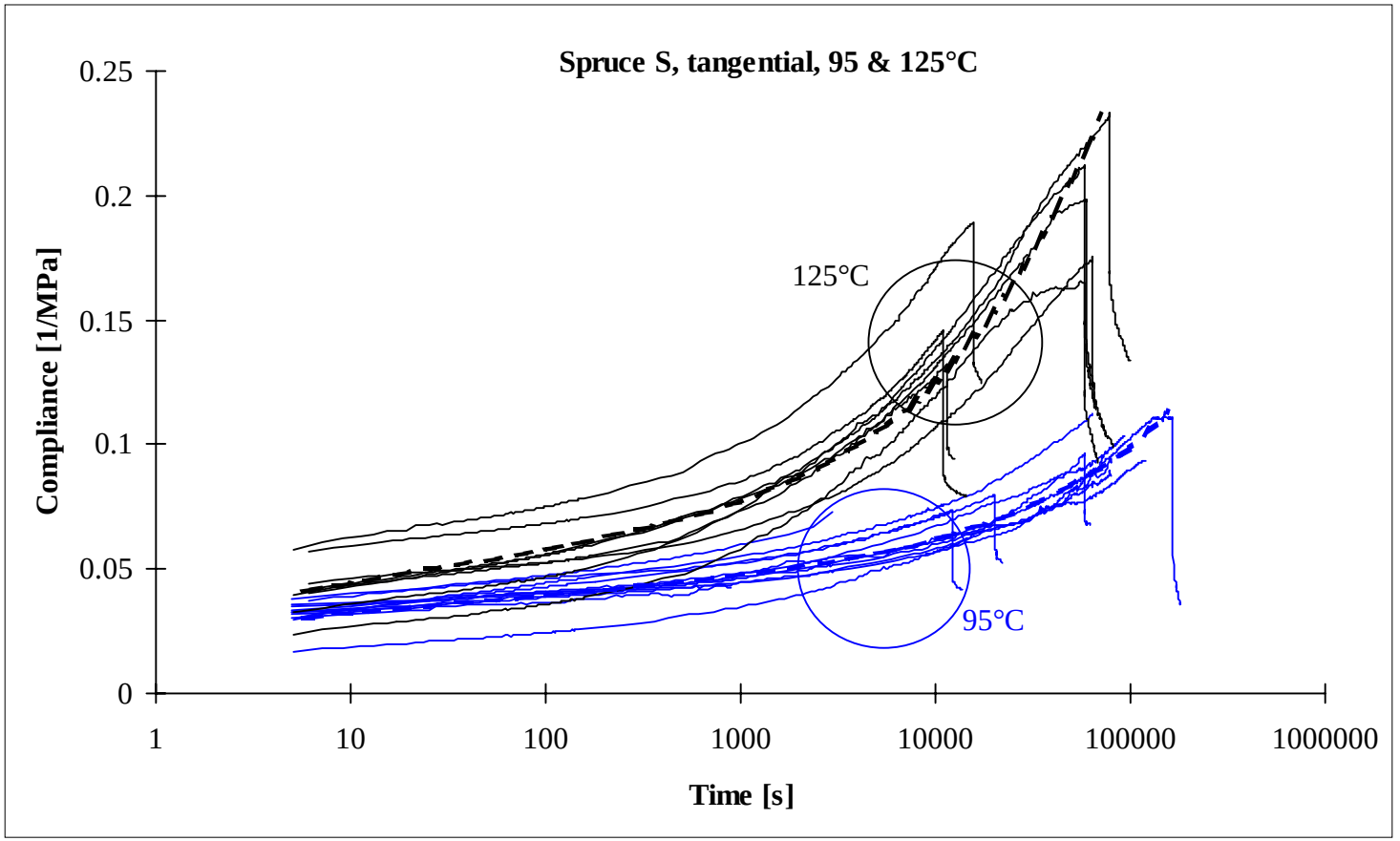

Fig. 21. Compliance in wet condition creep tests drawn against log_{10}-time for tangential Spruce S specimens at temperatures 95 and 125°C, stress 0.046–0.2 MPa. In most tests the load was removed for few hours before the end of the experiment to investigate recovery.

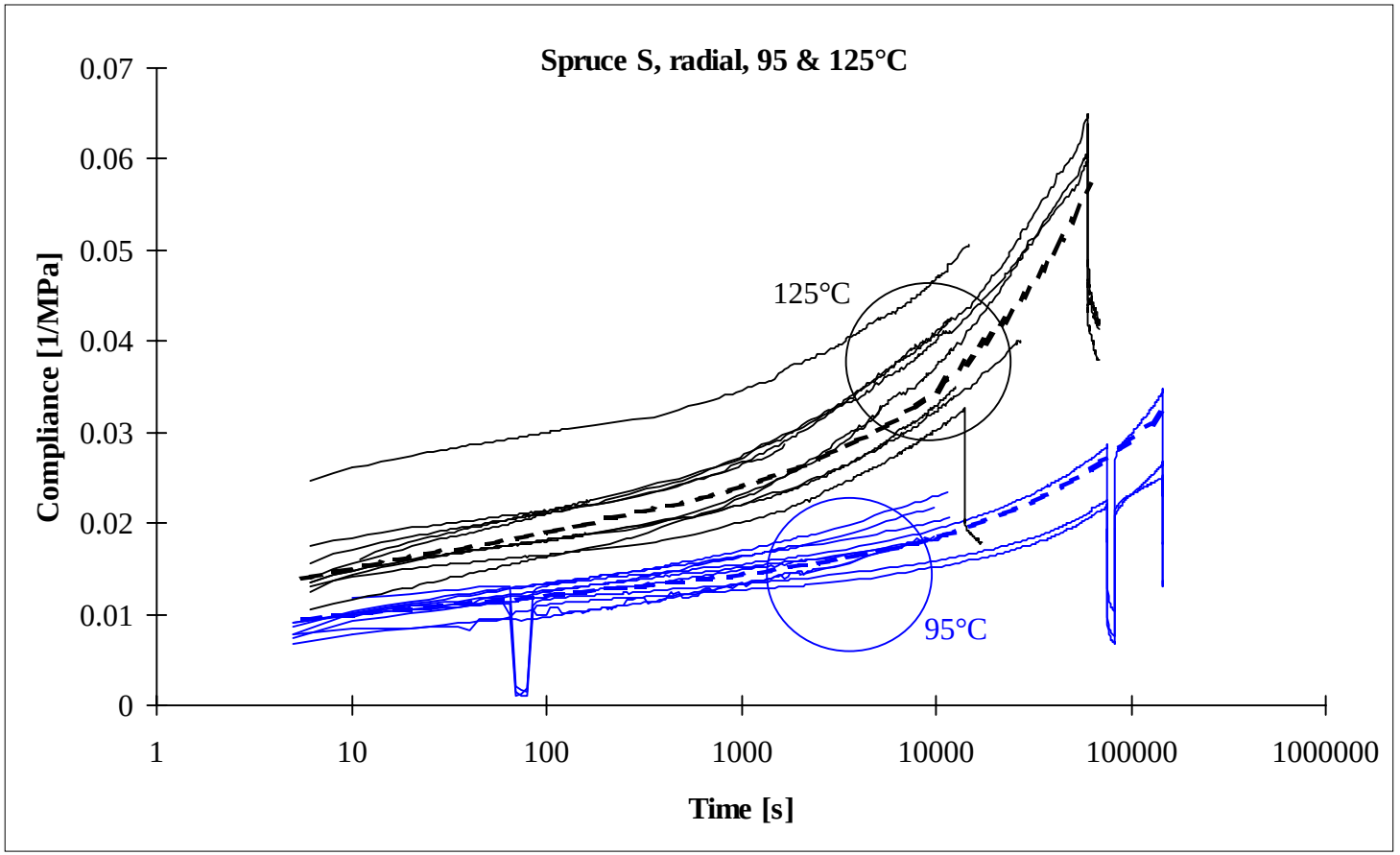

Fig. 22. Compliance in wet condition creep tests drawn against log_{10}-time for radial Spruce S specimens at temperatures 95 and 125°C, stress 0.096–0.4 MPa. In most tests the load was removed for few hours before the end of the experiment to investigate recovery. In some cases there was a short recovery period even earlier during the experiment.

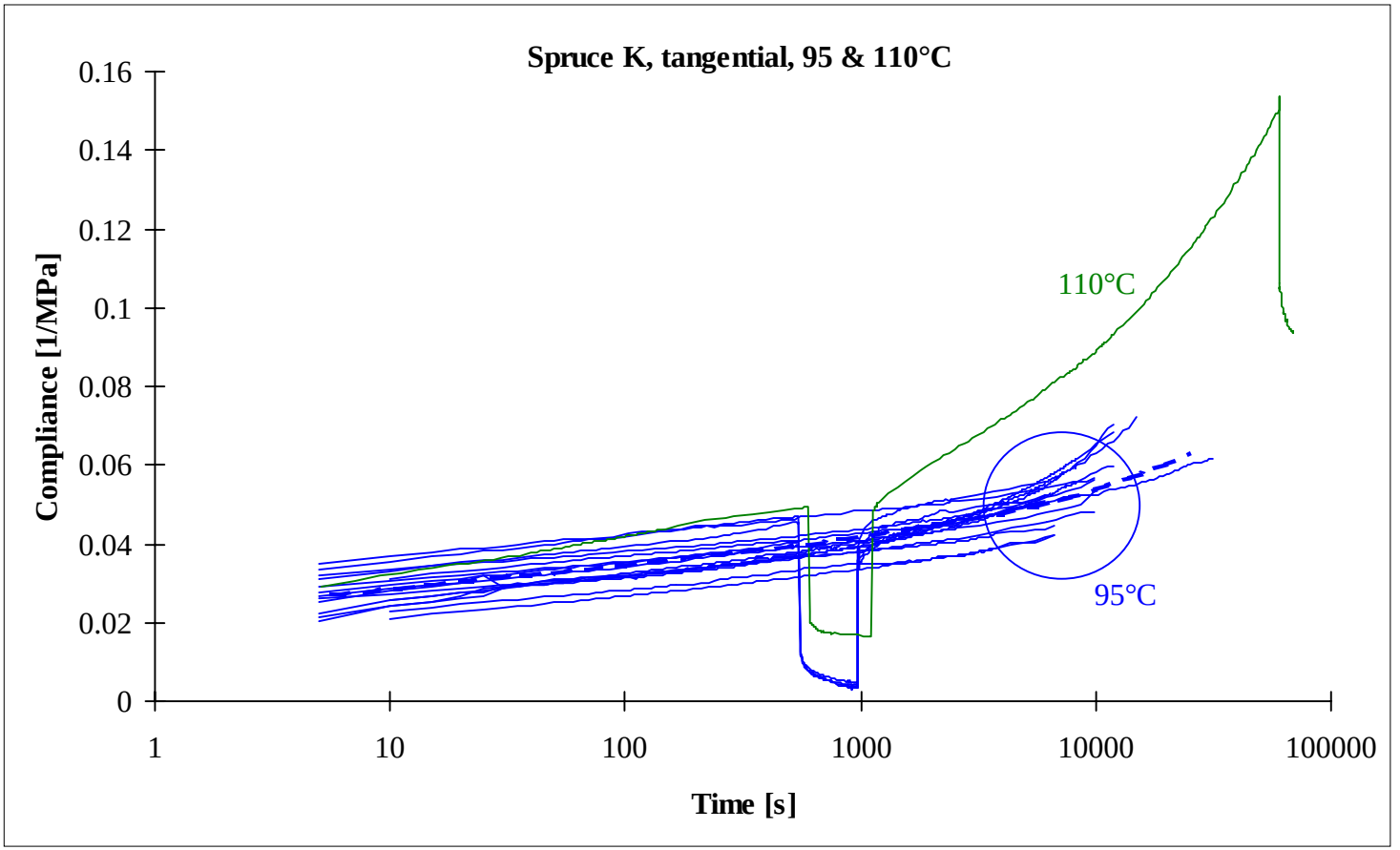

Fig. 23. Compliance in wet condition creep tests drawn against log_{10}-time for tangential Spruce K specimens at temperatures 95 and 110°C, stress 0.046–0.296 MPa. In most tests the load was removed for few hours before the end of the experiment to investigate recovery. In some cases there was a short recovery period even earlier during the experiment.

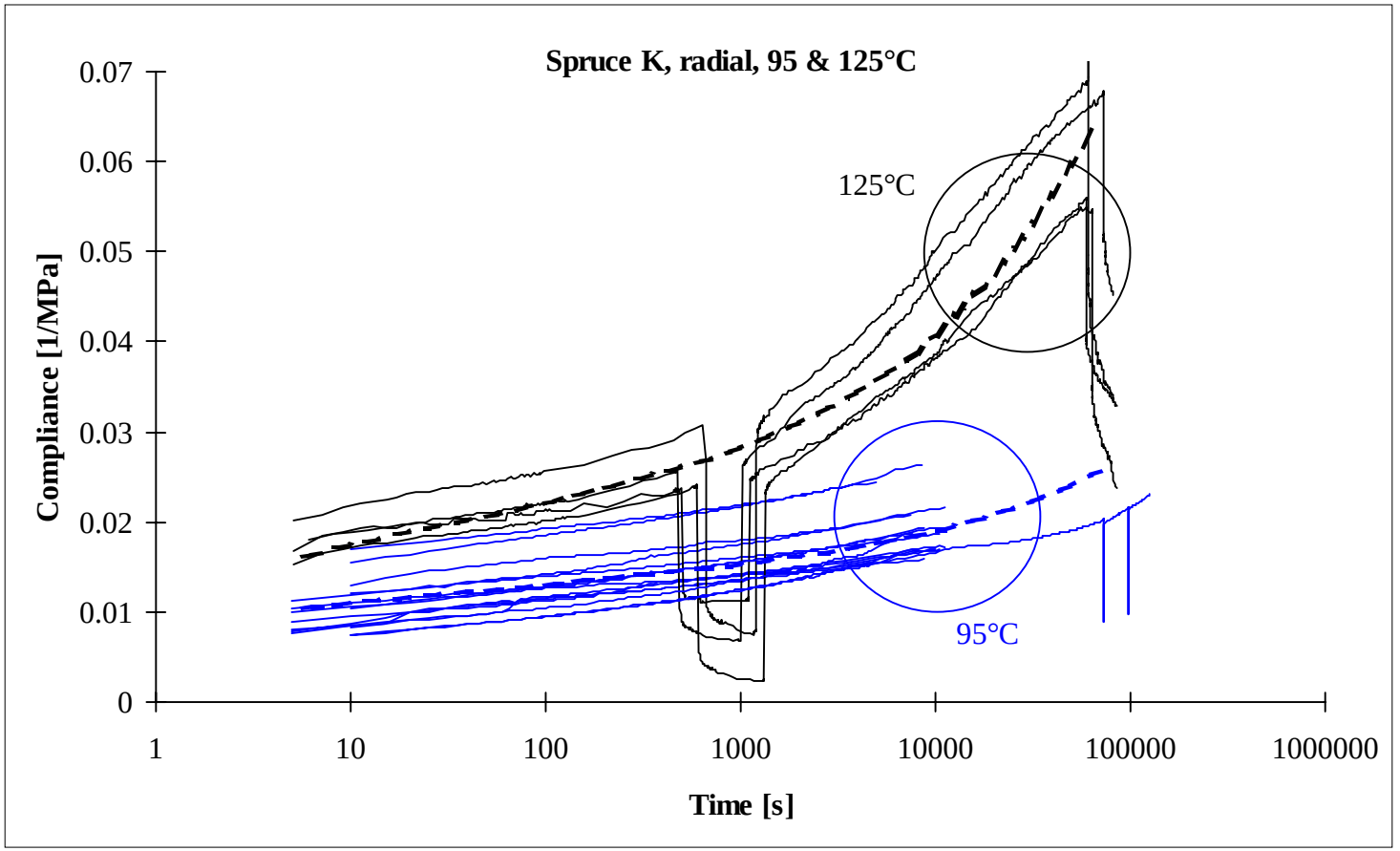

Fig. 24. Compliance in wet condition creep tests drawn against log_{10}-time for radial Spruce K specimens at temperatures 95 and 125°C, stress 0.096–0.496 MPa. In most tests the load was removed for few hours before the end of the experiment to investigate recovery. In some cases there was a short recovery period even earlier during the experiment.

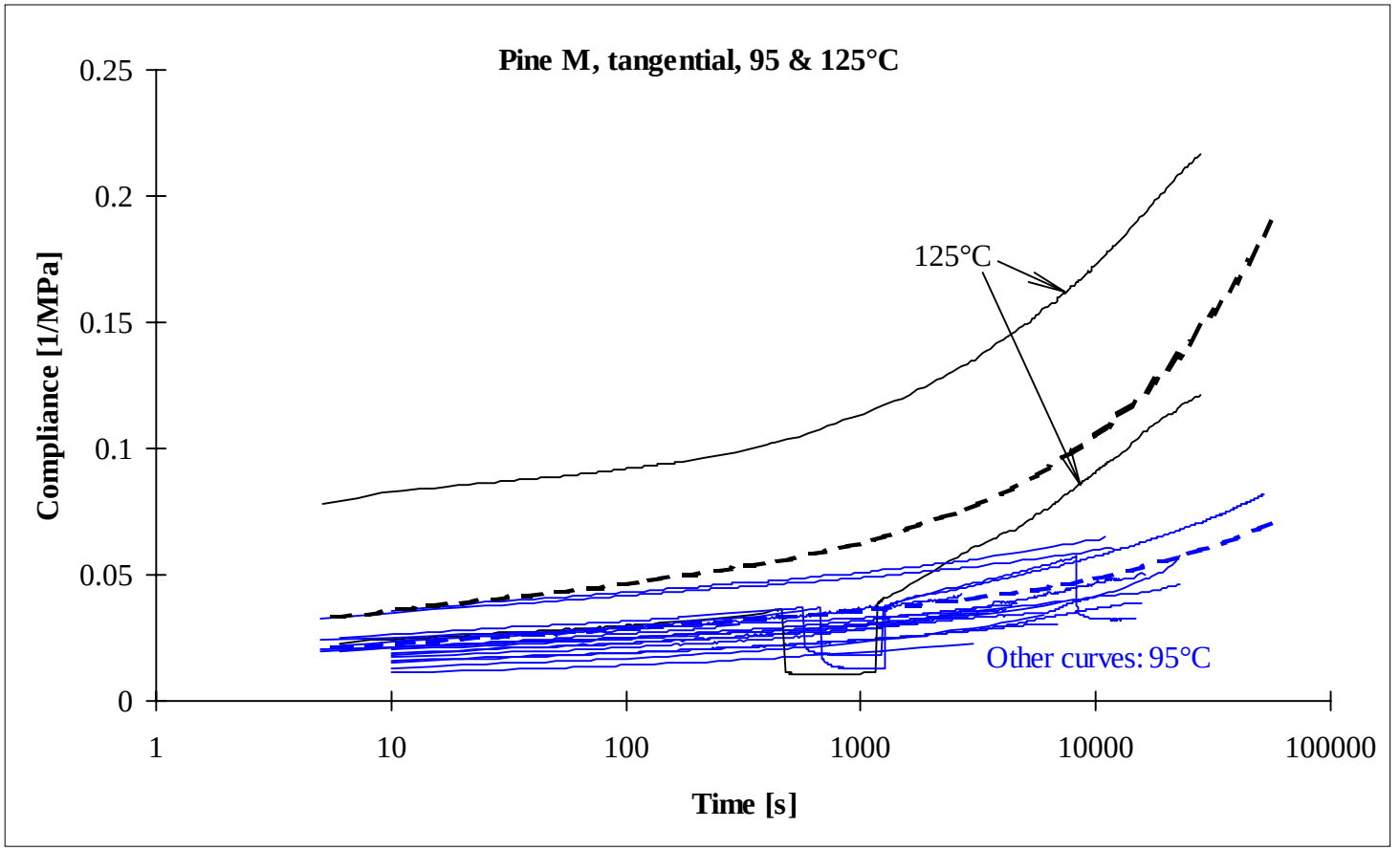

Fig. 25. Compliance in wet condition creep tests drawn against log_{10}-time for tangential Pine M specimens at temperatures 95 and 125°C, stress 0.021–0.3 MPa. In most tests the load was removed for few hours before the end of the experiment to investigate recovery. In some cases there was a short recovery period even earlier during the experiment.

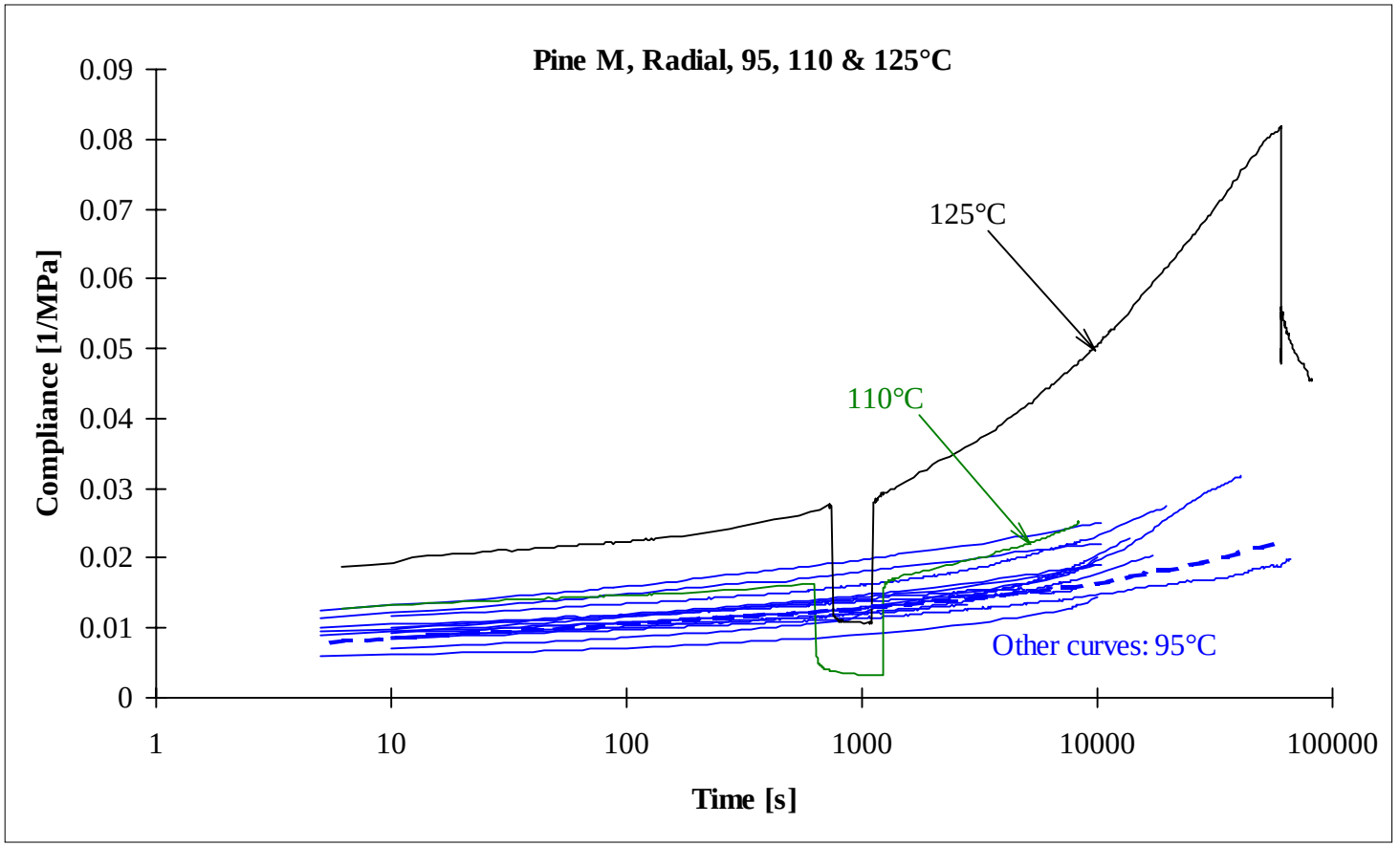

Fig. 26. Compliance in wet condition creep tests drawn against log_{10}-time for radial Pine M specimens at temperatures 95, 110 and 125°C, stress 0.096–0.496 MPa. In most tests the load was removed for few hours before the end of the experiment to investigate recovery. In some cases there was a short recovery period even earlier during the experiment.

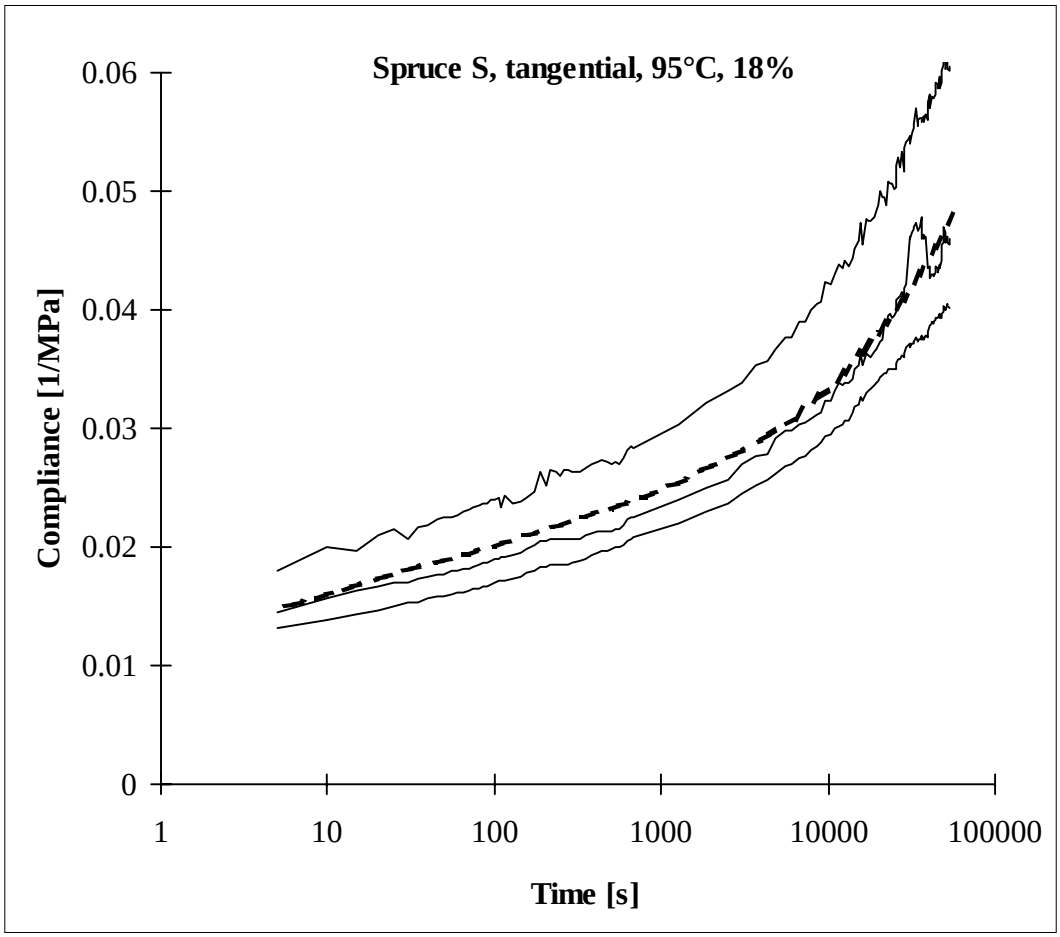

Fig. 27. Compliance in constant condition creep tests at approximately 18% moisture content and 95°C drawn against $\log_{10}$-time for tangential Spruce S specimens, stress 0.046–0.196 MPa.

To compare the constant condition results with other researchers' results and to test the applicability of the time–temperature–moisture-content superposition principle, the fitted creep curves were plotted with creep results of Joyet (1992) and Svensson (1996) and short term (MOE) results of Siimes (1967) and of this work. Joyet's test conditions were 30°C with several moisture contents below FSP, and Svensson's 60 and 80°C with two moisture contents below FSP. Both Joyet's and Svensson's results are for pine species, viz. Maritime pine (*Pinus pinaster*) and Scots pine (*Pinus sylvestris*), respectively. Siimes results are at four temperatures and several moisture contents for both Finnish spruce (*Picea abies*) and pine (*Pinus sylvestris*). All test results have been shifted according to the time–temperature–moisture-content superposition principle with (arbitrarily chosen) reference conditions T_{ref} = 100°C and u_{ref} = 0.15. The short term (MOE) results were utilised assuming the short term compliance to correspond to the response at 1 min.

The shifted compliances J_{shifted} have been obtained from the measured compliances J_{measured} according to a combined temperature–moisture-content shift:

$$J_{\text{shifted}}\left(\log_{10} t - a\right) = J_{\text{measured}}\left(\log_{10} t\right) \tag{1}$$

into which time t must be inserted as a dimensionless value (given in consistent units, of course). a is a combined temperature–moisture-content shift factor:

$$a = k_T\left(T - T_{\text{ref}}\right) + k_u\left(u - u_{\text{ref}}\right) \tag{2}$$

Values for the constants k_T and k_u were determined separately for spruce and pine and they are given in Table 1.

Table 1. The values of the parameters k_T and k_u for spruce and pine.

	Spruce	Pine
k_T	0.11 °C^{-1}	0.095 °C^{-1}
k_u	43	43

Figs. 28–35 show the results of the comparisons. All results are fairly well shifted to form continuous chains, but the fits are not very good for the lower ends of the creep curves. Master curves were fitted along the chains and they are shown in Figs. 28–35 also. Anticipating the coming formulation of a creep model, the mathematical form of the Master curves $J_{\text{M}}(t)$ was constructed as a series of Kelvin unit compliances:

$$J_{\text{M}} = J_0 + \sum_{i=1}^{21} J_i\left(1 - \exp\left(-t/\tau_i\right)\right) \tag{3}$$

where J_i's and τ_i's are the constants of the fit. Their values are given for tangential deformation of spruce and pine in Table 2. For radial deformation these constant were determined based on the tangential ones by keeping the values of the τ_i's unchanged and multiplying all the J_i values by a single factor, which was 0.36 for spruce and 0.50 for pine. It should be noted that one cannot use the J_i values to make comparison between the creep susceptibility of spruce and pine, because the k_T values for the two species are different.

Table 2. Parameters for the master curve fit for tangential deformation of spruce (density 450kg/m^3) and pine (density 490kg/m^3) in constant conditions. Reference temperature 100°C and reference moisture content 0.15. It should be noted that one cannot use the J_i values to make comparison between the creep susceptibility of the two species, because their k_T values are different.

i	τ_i [h]	Spruce J_i [1/MPa]	Pine J_i [1/MPa]
0	–	0.002	0.0018
1	10^{-14}	0.00016	0.00008
2	10^{-13}	0.00017	0.0001
3	10^{-12}	0.00018	0.00015
4	10^{-11}	0.0002	0.00018
5	10^{-10}	0.00024	0.00022
6	10^{-9}	0.0003	0.00028
7	10^{-8}	0.0004	0.00035
8	10^{-7}	0.00052	0.00042
9	10^{-6}	0.00065	0.0005
10	10^{-5}	0.00085	0.0006
11	10^{-4}	0.0012	0.0009
12	10^{-3}	0.002	0.0018
13	10^{-2}	0.0035	0.0026
14	10^{-1}	0.0055	0.0045
15	10^{0}	0.008	0.0065
16	10^{1}	0.01	0.009
17	10^{2}	0.013	0.015
18	10^{3}	0.018	0.02
19	10^{4}	0.038	0.07
20	10^{5}	0.06	0.15
21	10^{6}	0.12	0.25

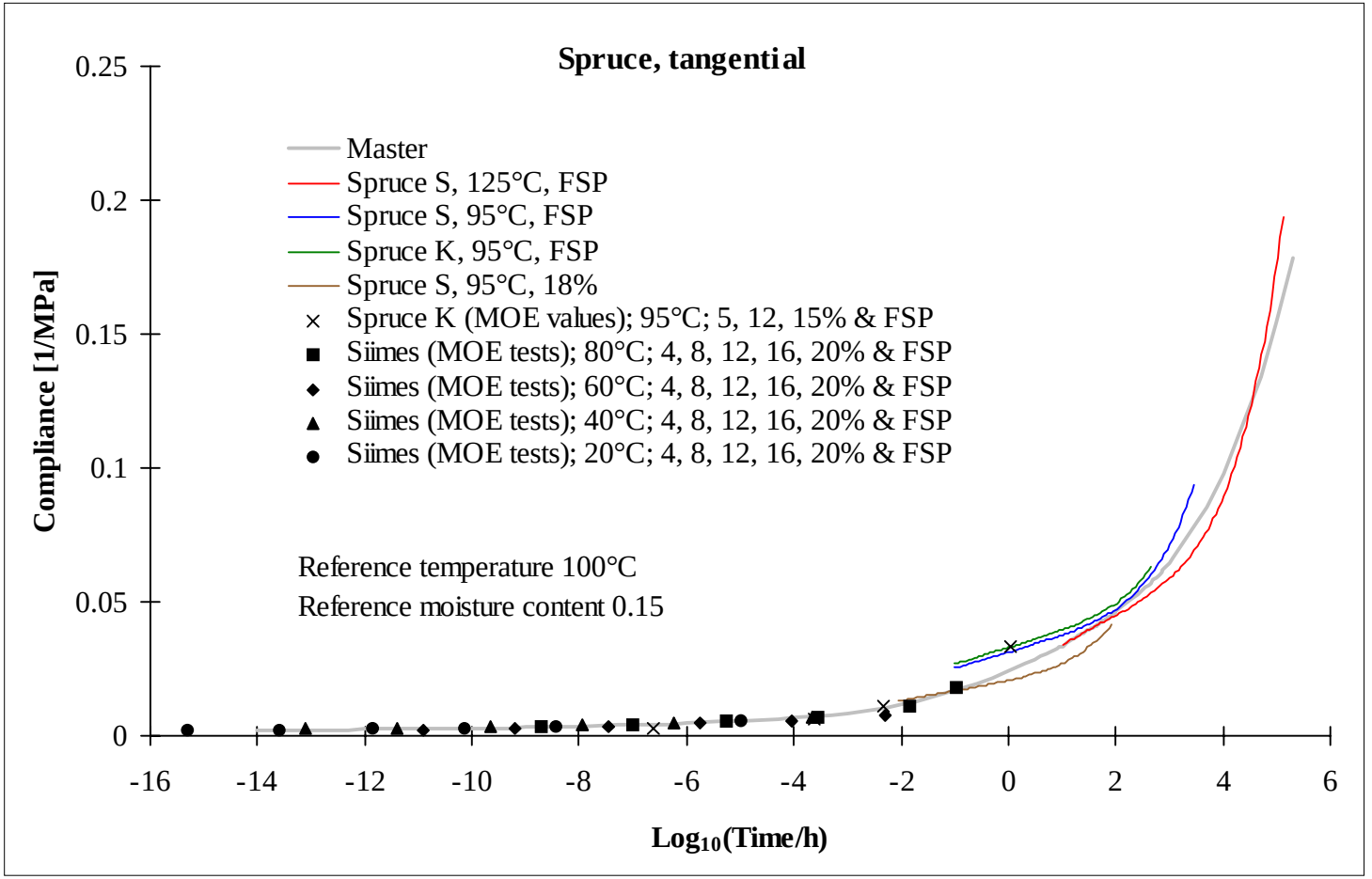

Fig. 28. Comparison of the constant condition test results of tangential spruce to Siimes' (1967) results with a test of the applicability of the time–temperature–moisture-content superposition principle.

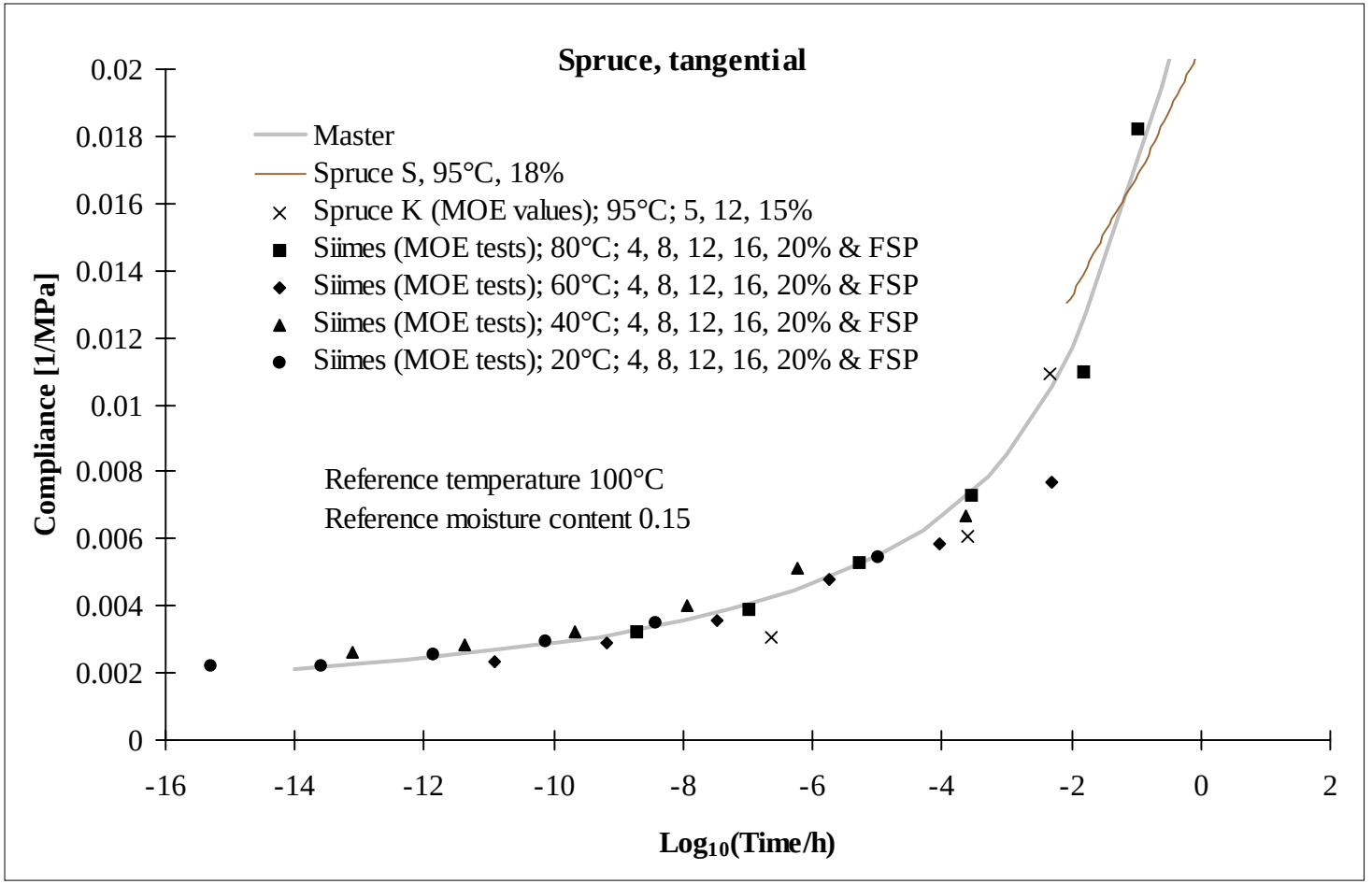

Fig. 29. A detail of the lower end of Fig. 28.

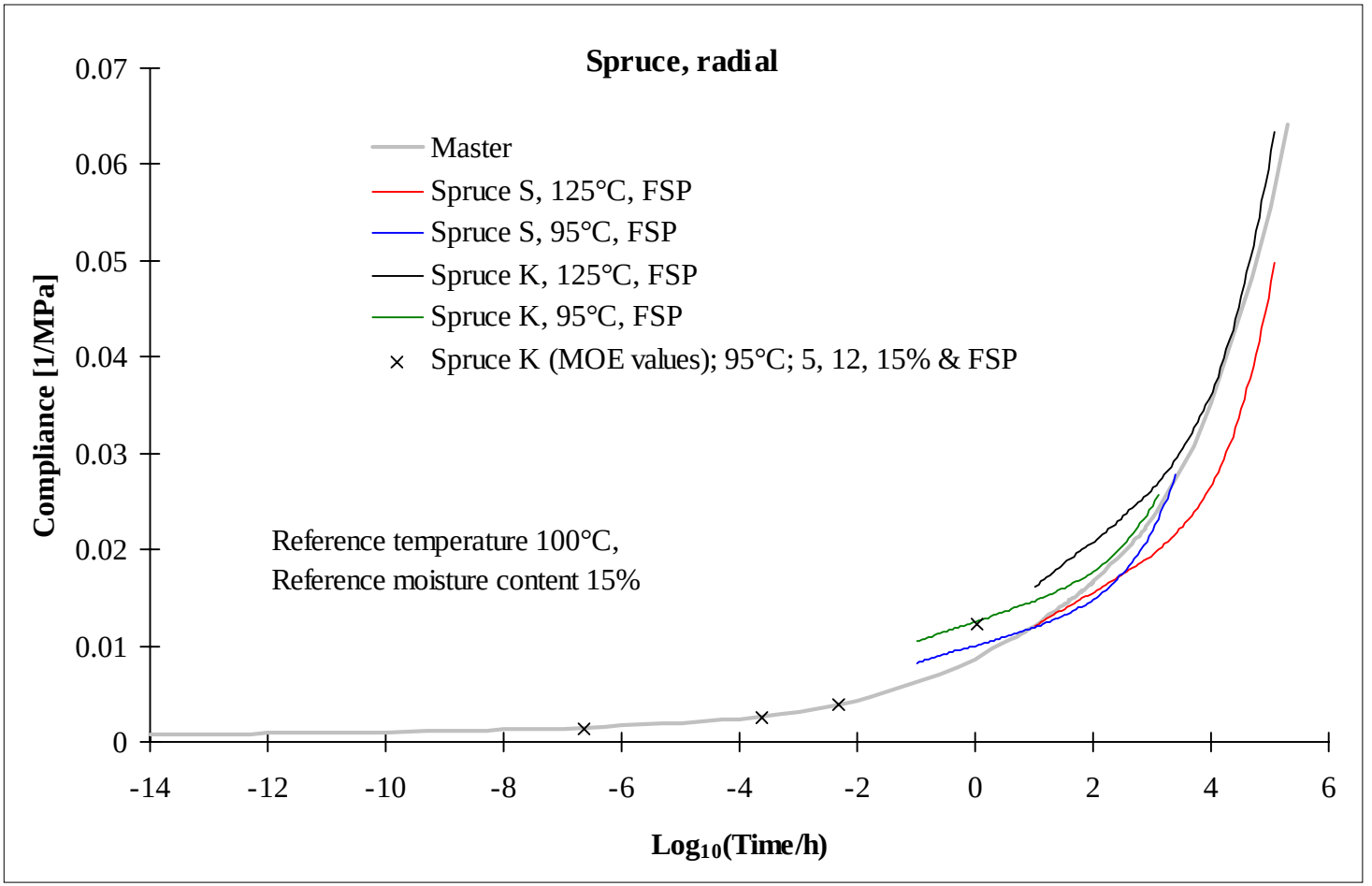

Fig. 30. Comparison of the constant condition test results of radial spruce with a test of the applicability of the time–temperature–moisture-content superposition principle.

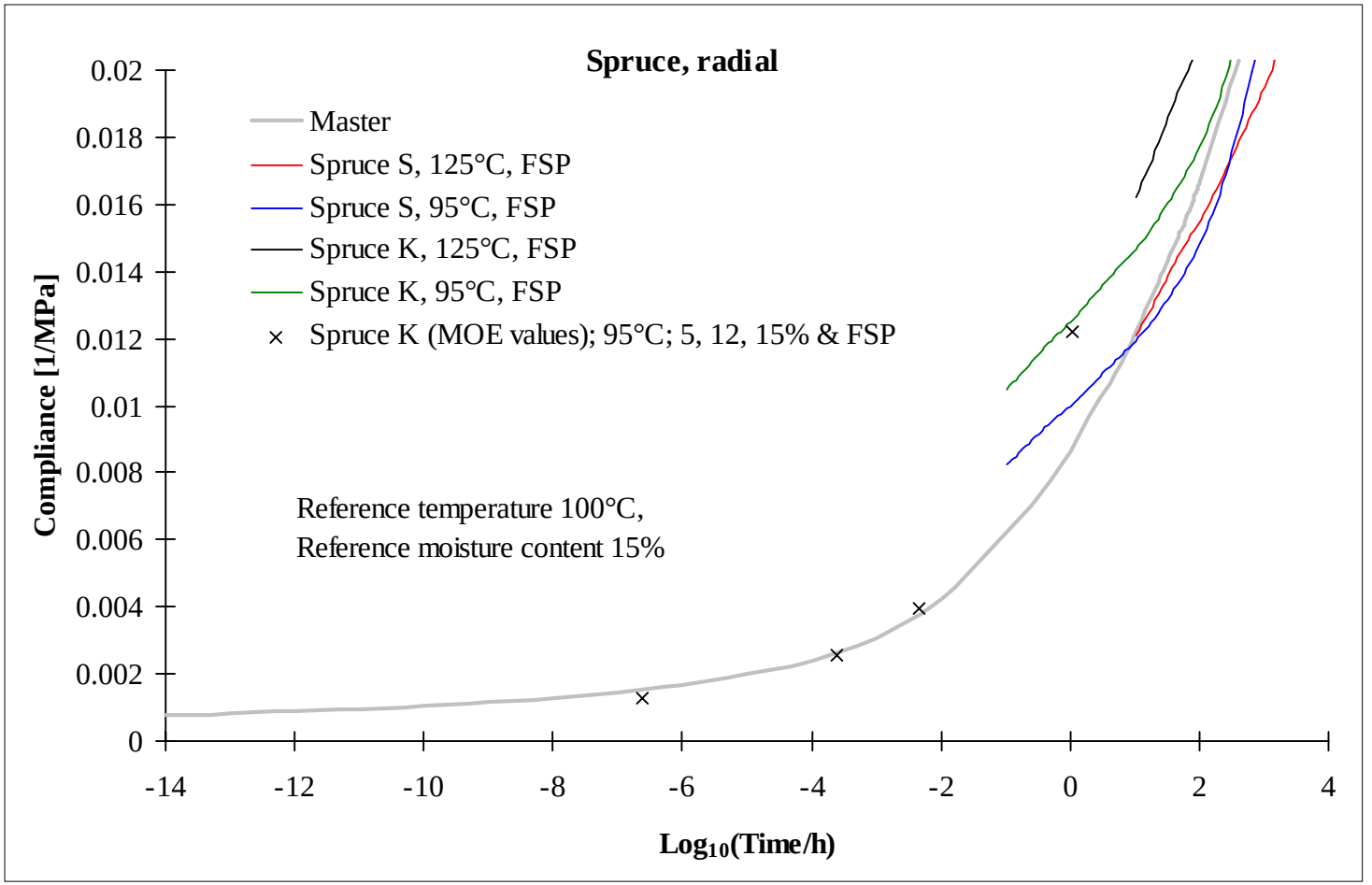

Fig. 31. A detail of the lower end of Fig. 30.

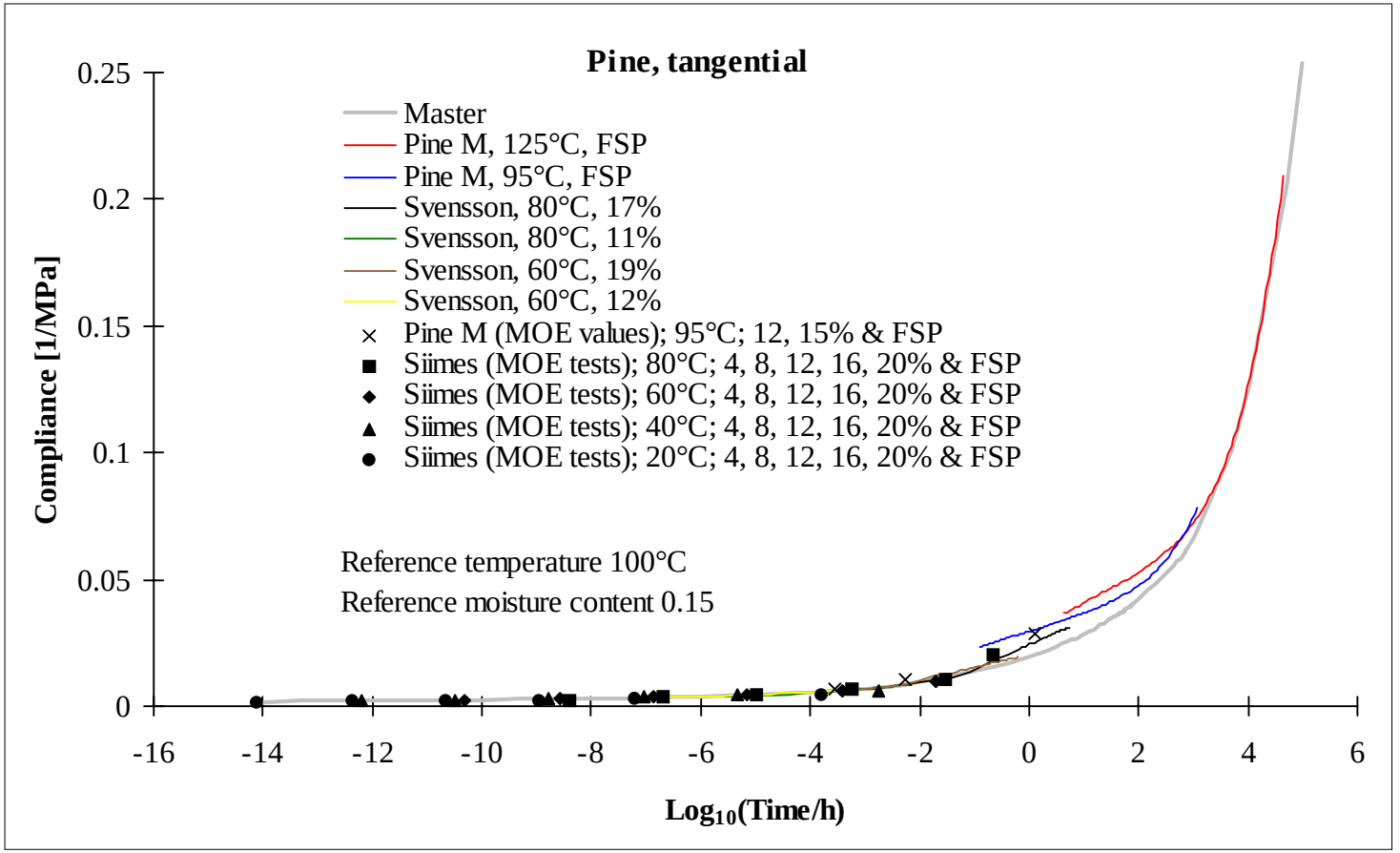

Fig. 32. Comparison of the constant wet condition test results of tangential pine to Svensson's (1996) and Siimes' (1967) results with a test of the applicability of the time–temperature–moisture-content superposition principle.

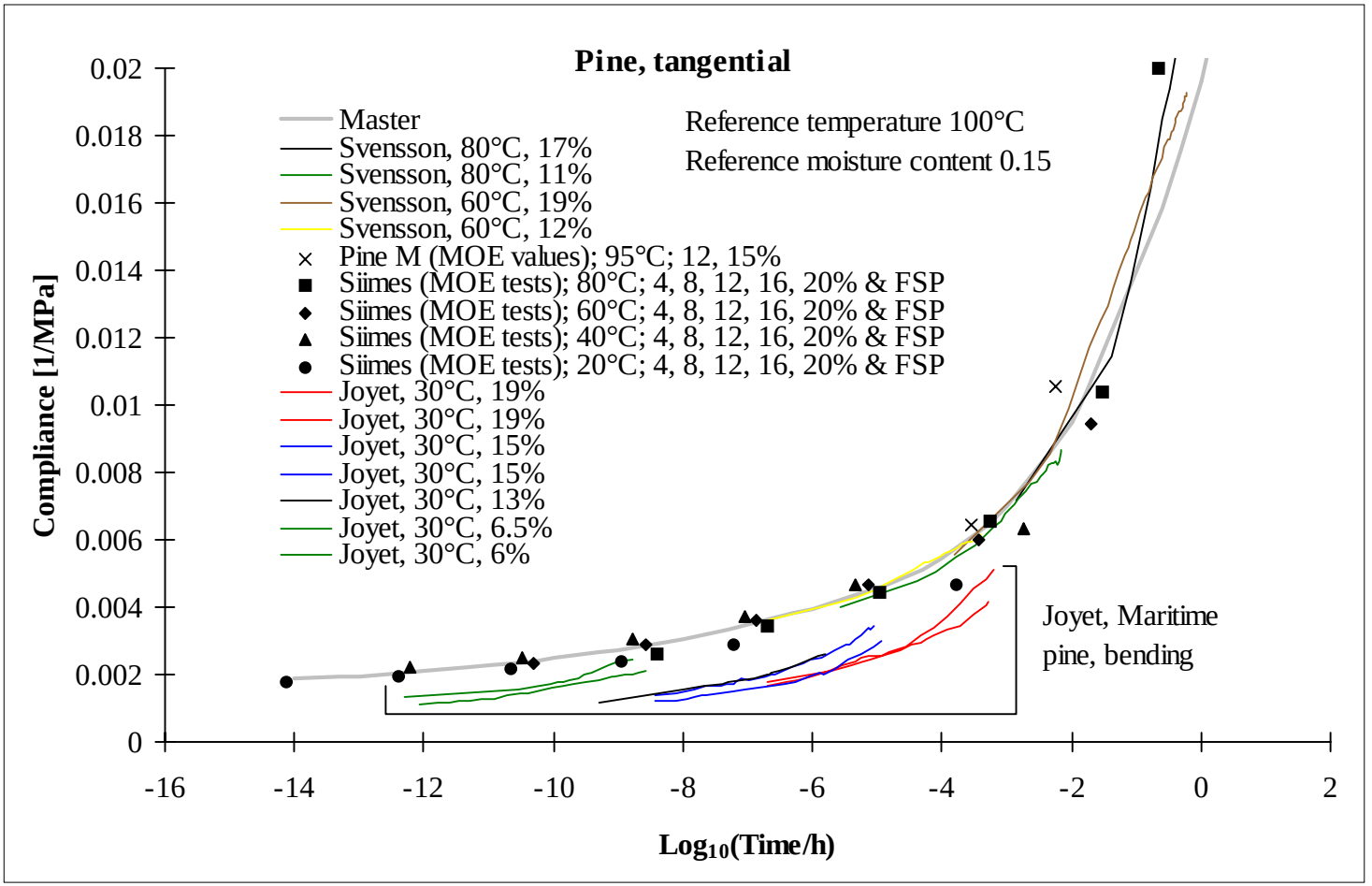

Fig. 33. A detail of the lower end of Fig. 32 with addition of Joyet's (1992) results.

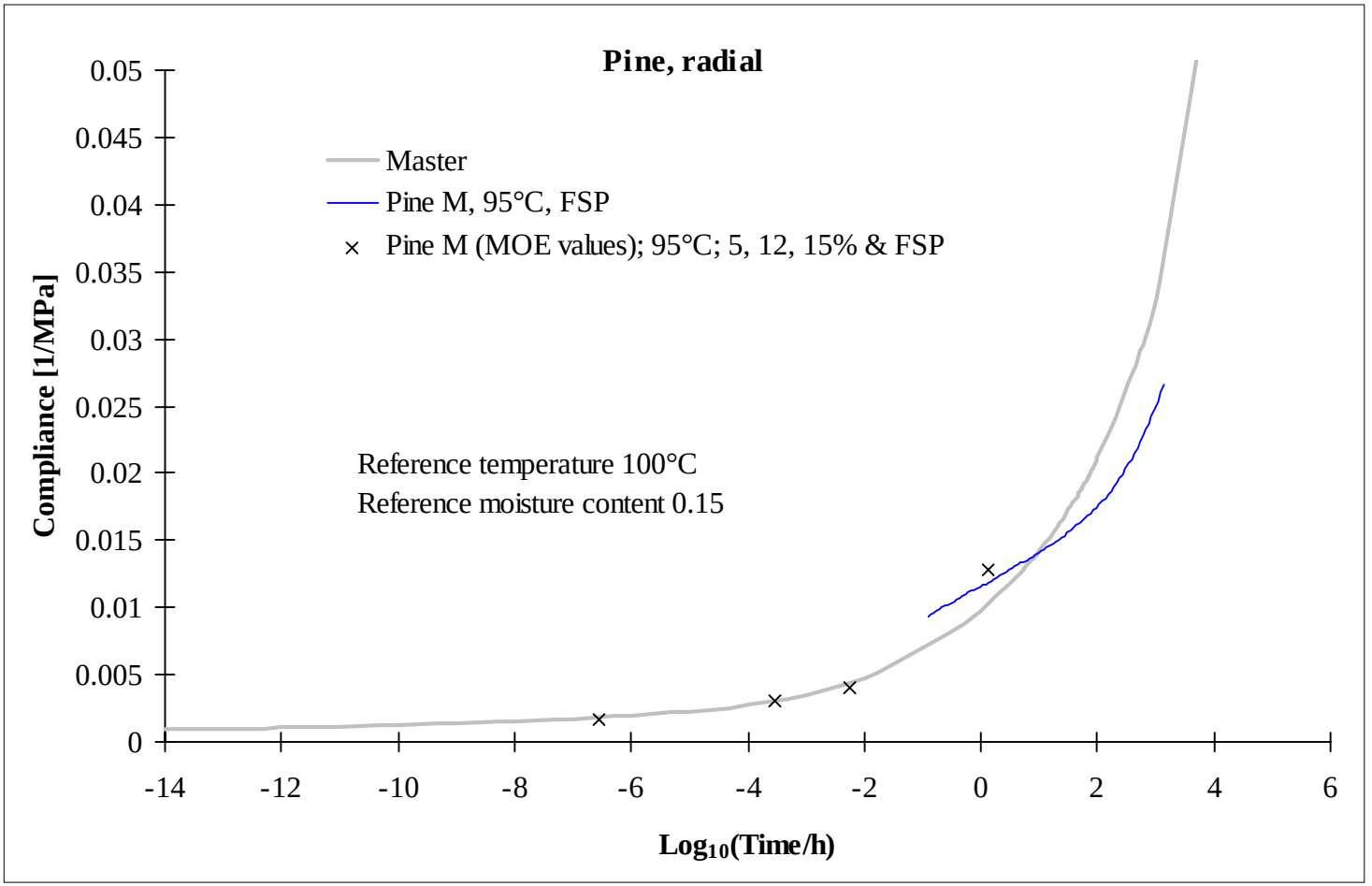

Fig. 34. Comparison of the constant condition test results of radial pine with a test of the applicability of the time–temperature–moisture-content superposition principle.

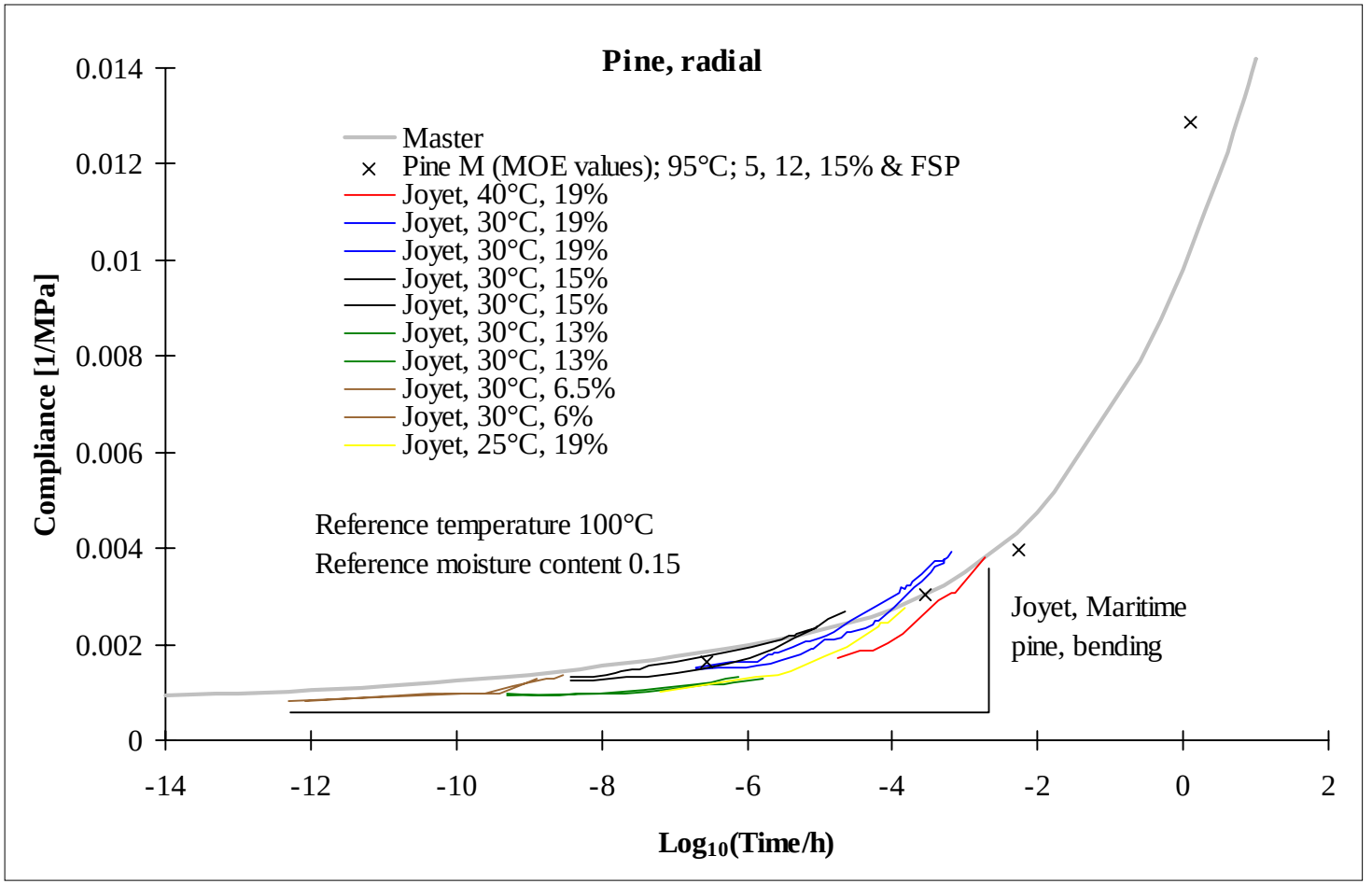

Fig. 35. A detail of the lower end of Fig. 34 with addition of Joyet's (1992) results.

3.6.5 Mechano-sorptive creep

Mårtensson (1994) and Svensson (1994) have introduced the approach of presenting creep curves obtained in drying condition tests as drawn against zero-load shrinkage measured in the same test rather than moisture content or moisture content change. Their approach is advantageous for at least two reasons: because shrinkage is easier to measure than moisture content, and because we do not need to make any assumptions of when the moisture content comes below the fiber saturation point (we can directly observe the beginning of the shrinkage). Furthermore, shrinkage measurement itself corrects possible influence of uneven moisture content distribution within the specimens, because (at least nearly) the same moisture content distribution is present in the zero-load shrinkage specimens as is in the loaded creep specimen. The approach is also supported by more theoretical aspects, if the findings of Hunt (1986) concerning the correlation of the amount of longitudinal mechano-sorptive creep to longitudinal hygroexpansion hold also for the transverse directions. The same concerns the presumption of the phenomenological connection between mechano-sorptive creep and hygroexpansion in general (Hanhijärvi 1995). On the other hand, if and when the amount of shrinkage can be considered linearly proportional to moisture content change below fiber saturation, the two approaches are principally equivalent. Because of these advantages, the results of the creep tests in drying conditions are presented against corresponding zero-load shrinkage strain.

The results of all specimens are given in Appendix C as unprocessed strain measurement vs. time plots and compliance vs. zero-load shrinkage plots. These latter ones are also gathered into Figs. 36–49, as grouped according to the different trunks and the maximum temperature values reached during test. For clarity of Figs. 36–49, the disturbing effect has been corrected which is caused by the ‘phase shift’ between the drying of the creep specimen and its dummy. The correction is done whenever it has been considered to be possible and to make the figures clearer. Whenever the correction has been done the corrected range is plotted with dashed line. (In Appendix C no such corrections have been made.)

Figs. 36–49 contain also estimated curves for combined elastic–viscoelastic compliance and average total compliance. The elastic-viscoelastic compliances have been determined using the Master curve, Eq. (3) for constant load case. The average total compliance curves are *graphical estimations* (not any calculated means) based on all results in the proper direction. For instance, the estimated total compliances for tangential cases have been estimated *based on all tangential test results*, and not on the results in a single figure only. Similarly, estimated total radial compliances are based on all radial results. Furthermore, the average total compliances have been assessed assuming monotonous drying and constant load, which was not the case in most tests. Estimation for the average mechano-sorptive compliance can be obtained as the difference of the two curves.

All cases show clearly that the elastic-viscoelastic compliance curves level so that they are practically horizontal after loading and some viscoelastic creep during early drying. Thus, the slope of the total compliance curve after the early drying is a good estimate of the mechano-sorptive creep development.

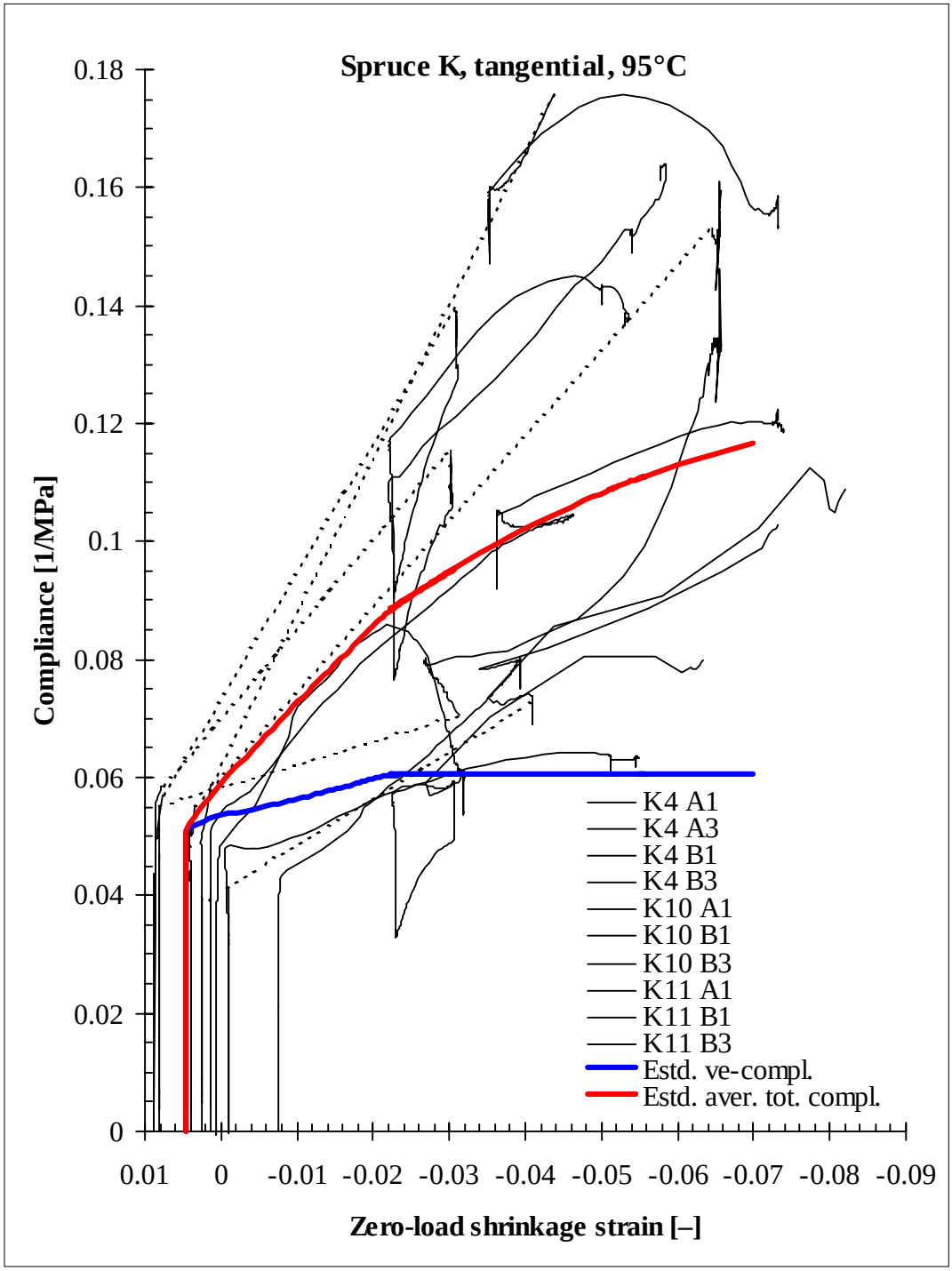

Fig. 36. Compliance vs. zero-load shrinkage strain for tangential Spruce K specimens in the tests at 95°C. The estimated magnitude of the elastic–viscoelastic compliance in the test conditions is also plotted as well as the estimated average total compliance, which is based on all tangential results (not only the ones in this figure).

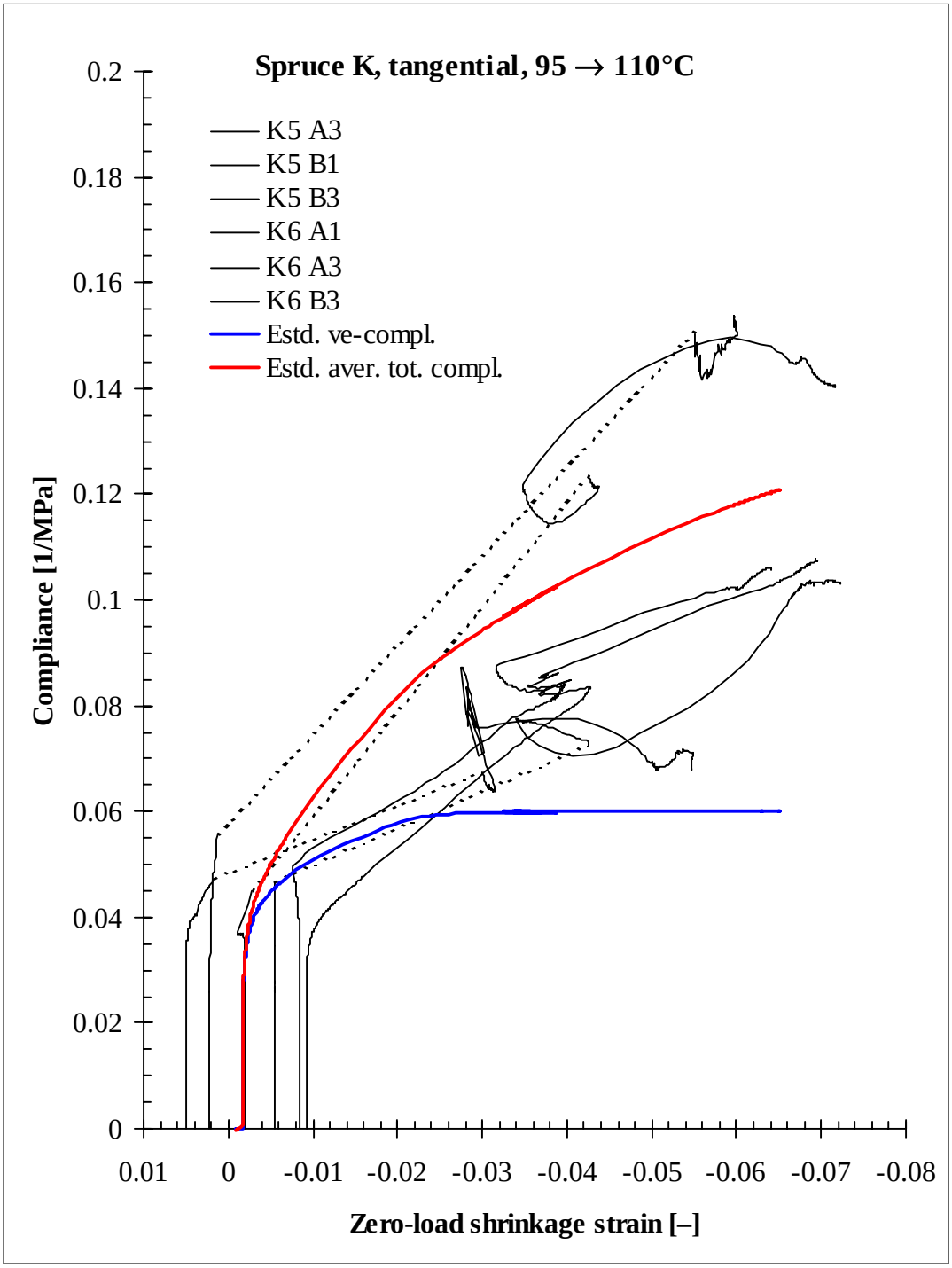

Fig. 37. Compliance vs. zero-load shrinkage strain for tangential Spruce K specimens in the tests with maximum temperature 110°C. The estimated magnitude of the elastic–viscoelastic compliance in the test conditions is also plotted as well as the estimated average total compliance, which is based on all tangential results (not only the ones in this figure).

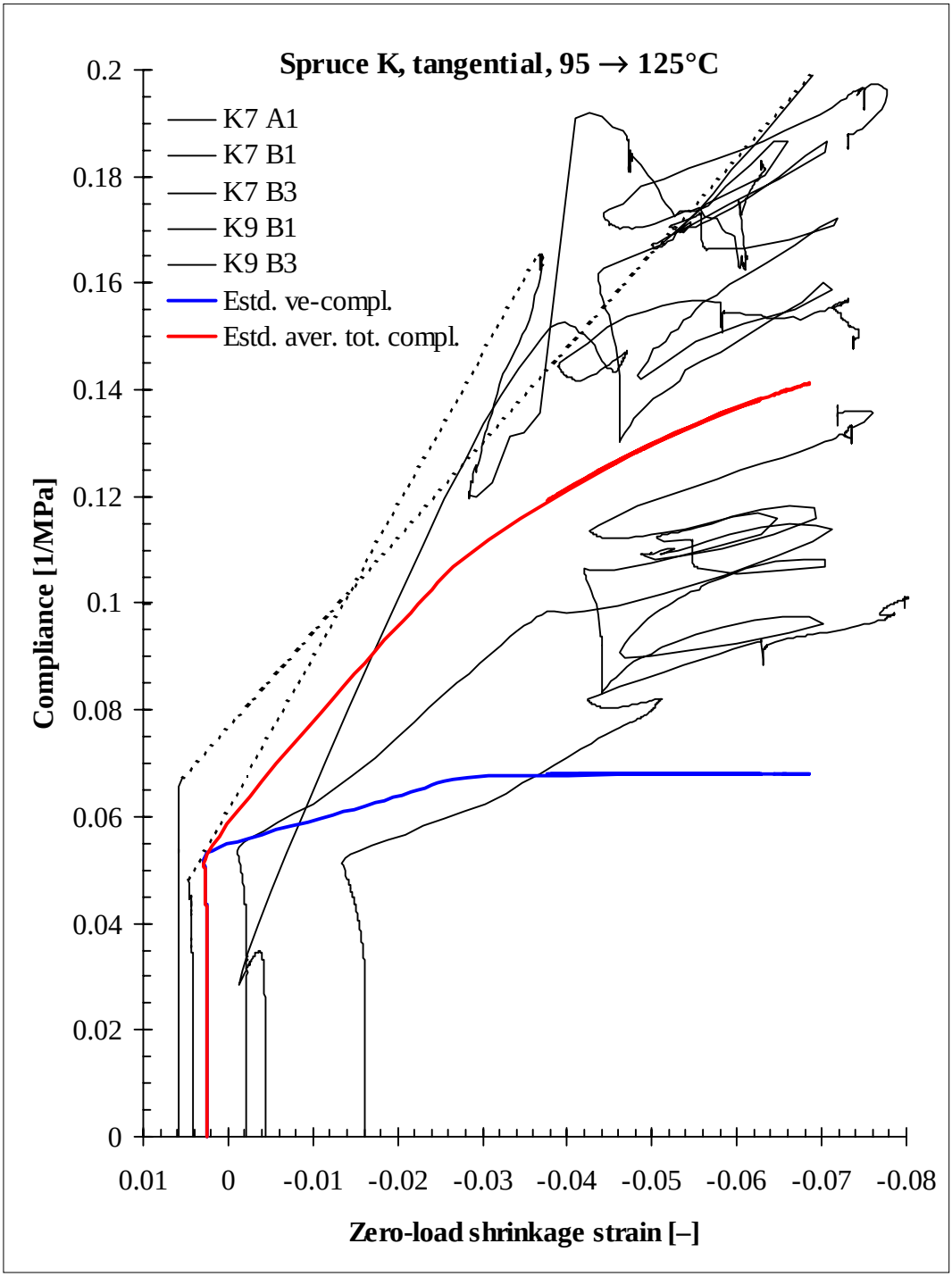

Fig. 38. Compliance vs. zero-load shrinkage strain for tangential Spruce K specimens in the tests with maximum temperature 125°C. The estimated magnitude of the elastic–viscoelastic compliance in the test conditions is also plotted as well as the estimated average total compliance, which is based on all tangential results (not only the ones in this figure).

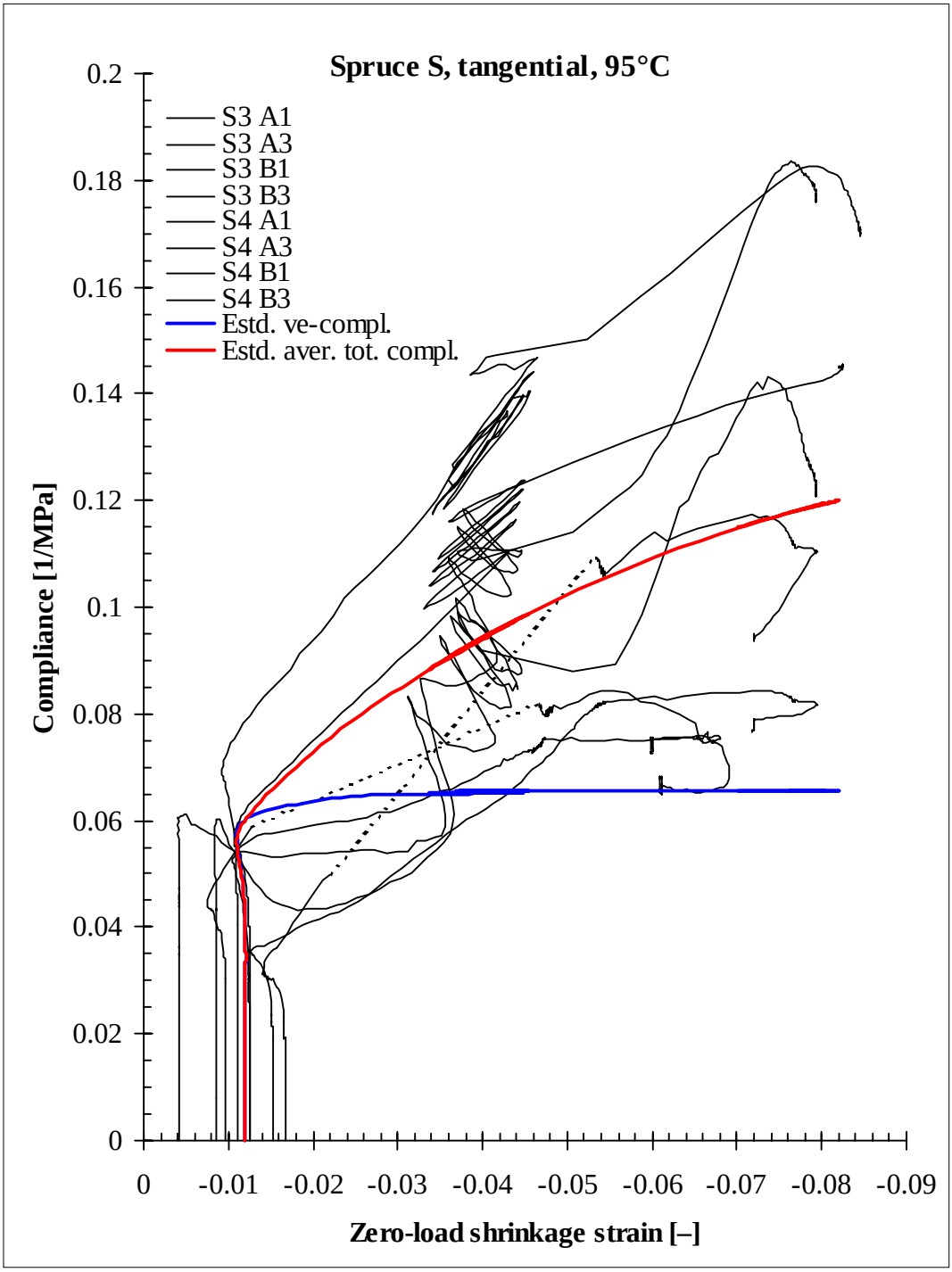

Fig. 39. Compliance vs. zero-load shrinkage strain for tangential Spruce S specimens in the tests at 95°C. The estimated magnitude of the elastic–viscoelastic compliance in the test conditions is also plotted as well as the estimated average total compliance, which is based on all tangential results (not only the ones in this figure).

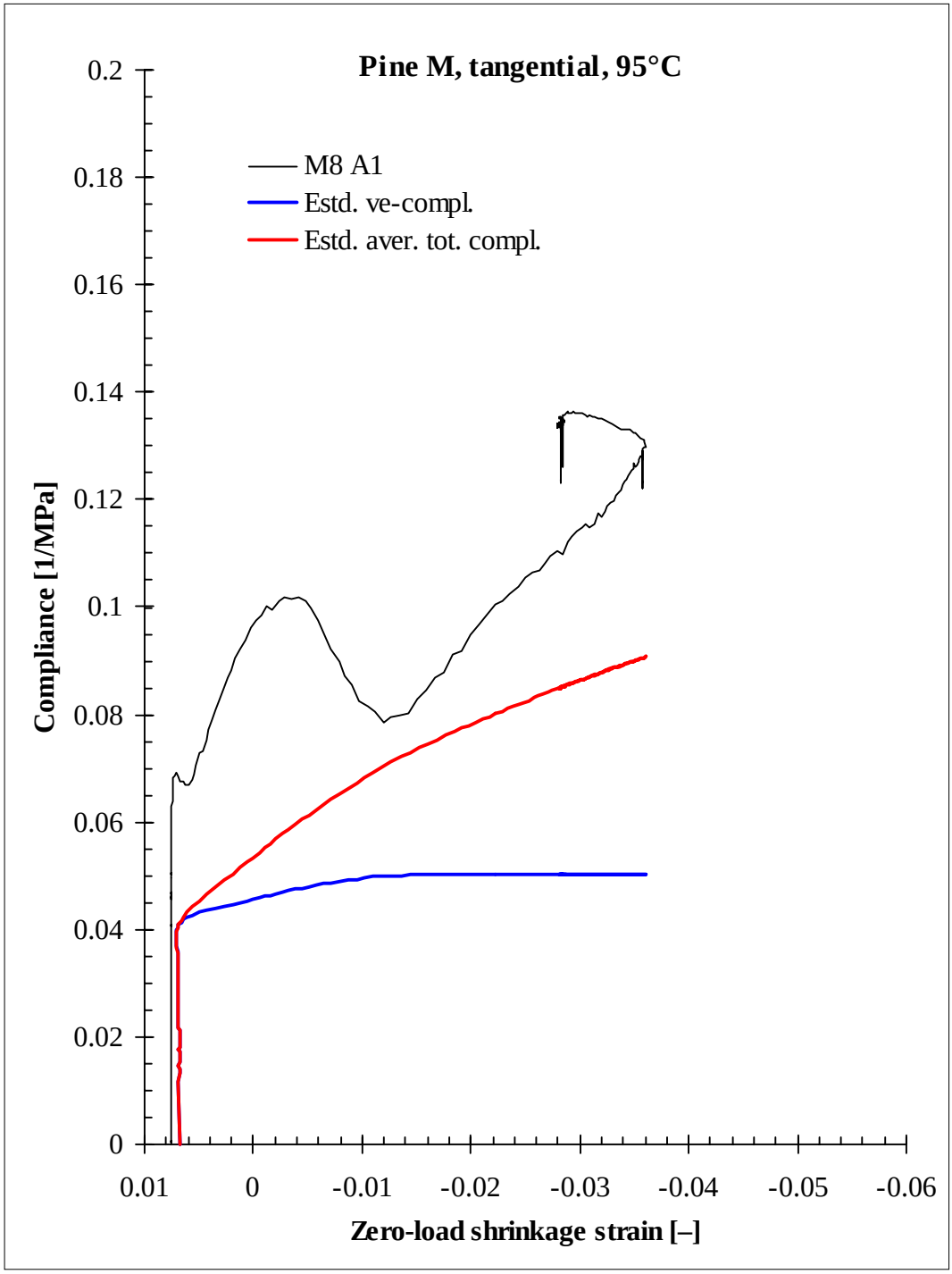

Fig. 40. Compliance vs. zero-load shrinkage strain for tangential Pine M specimens in the tests at 95°C. The estimated magnitude of the elastic–viscoelastic compliance in the test conditions is also plotted as well as the estimated average total compliance, which is based on all tangential results (not only the ones in this figure).

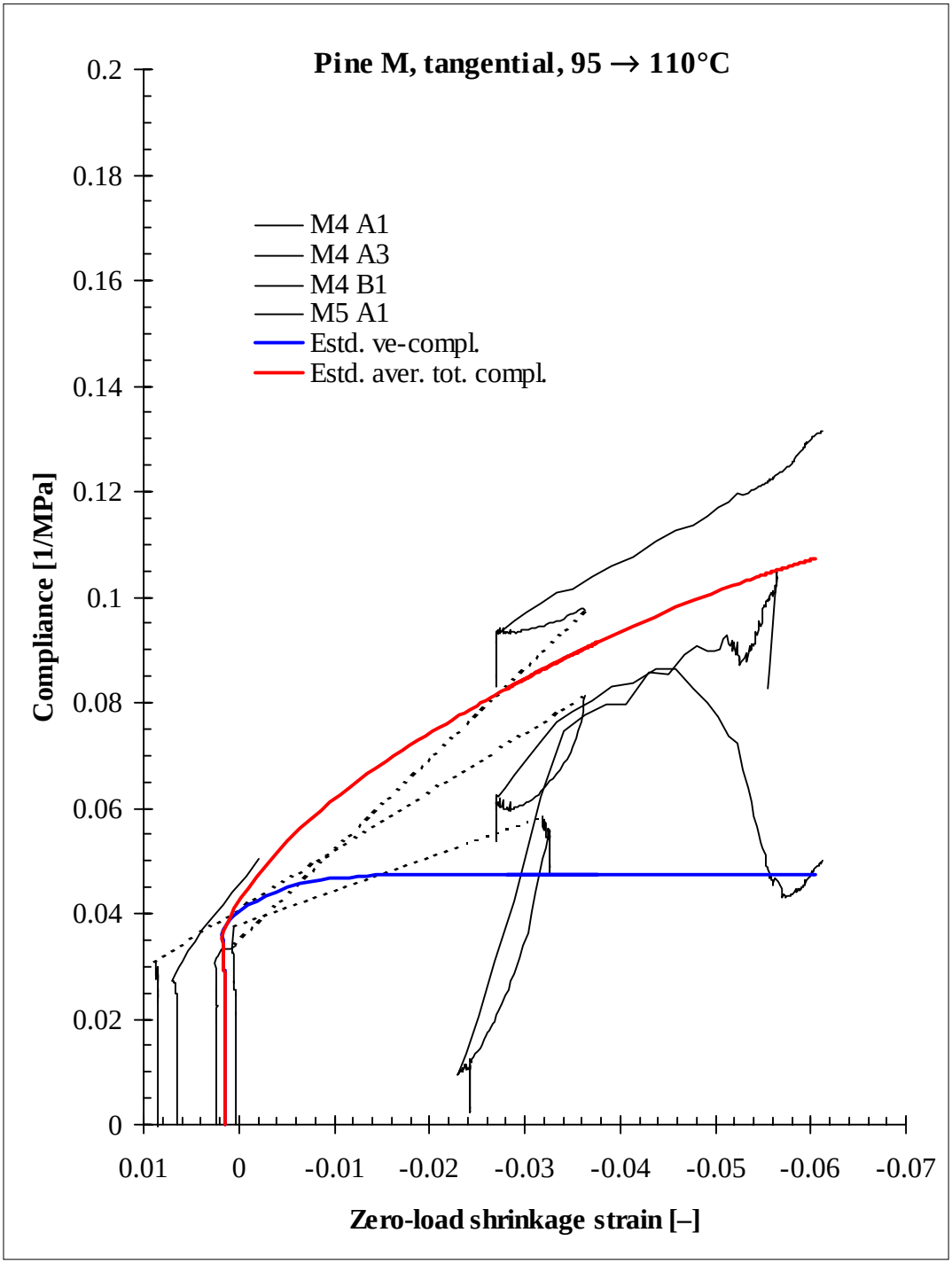

Fig. 41. Compliance vs. zero-load shrinkage strain for tangential Pine M specimens in the tests with maximum temperature 110°C. The estimated magnitude of the elastic–viscoelastic compliance in the test conditions is also plotted as well as the estimated average total compliance, which is based on all tangential results (not only the ones in this figure).

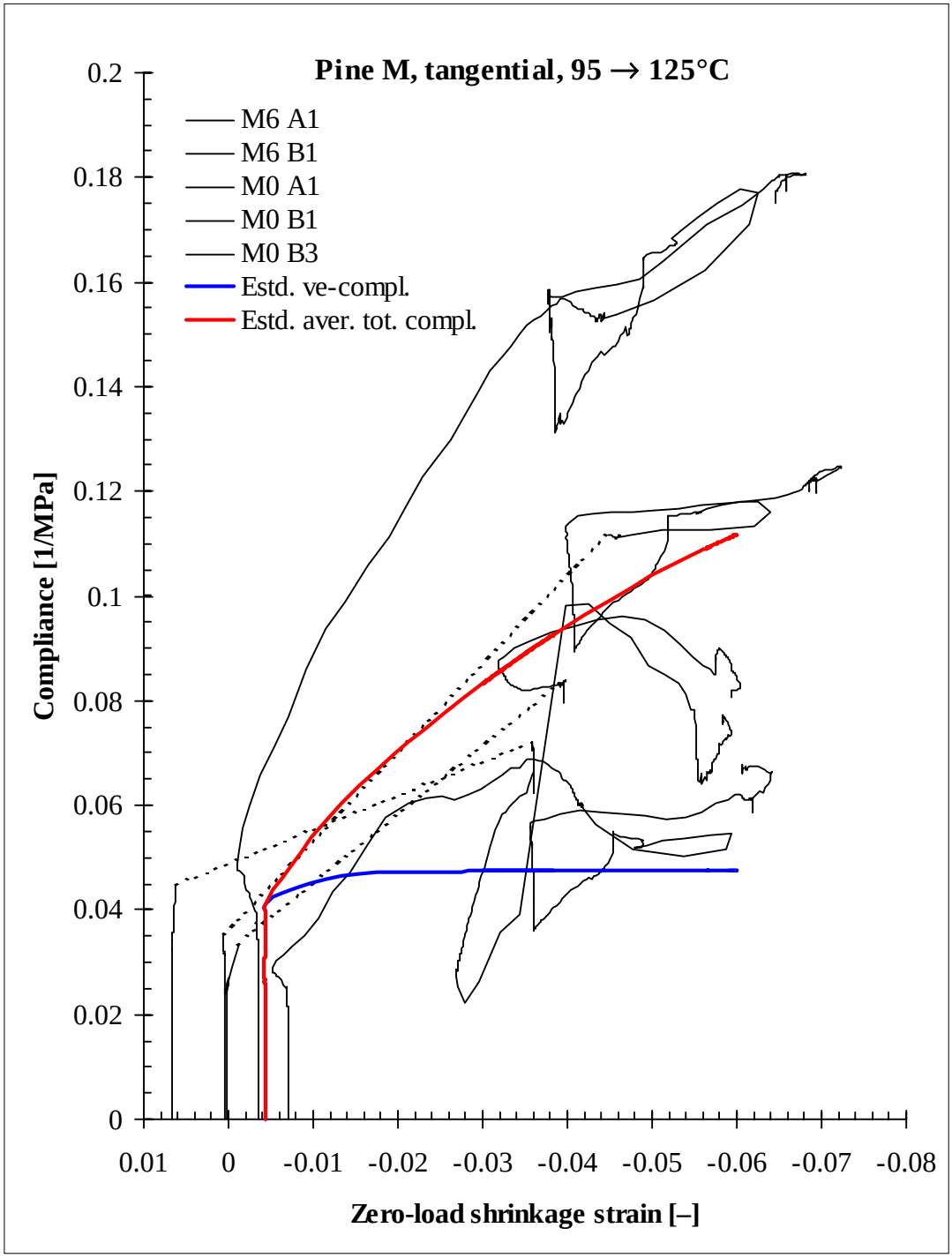

Fig. 42. Compliance vs. zero-load shrinkage strain for tangential Pine M specimens in the tests with maximum temperature 125°C. The estimated magnitude of the elastic–viscoelastic compliance in the test conditions is also plotted as well as the estimated average total compliance, which is based on all tangential results (not only the ones in this figure).

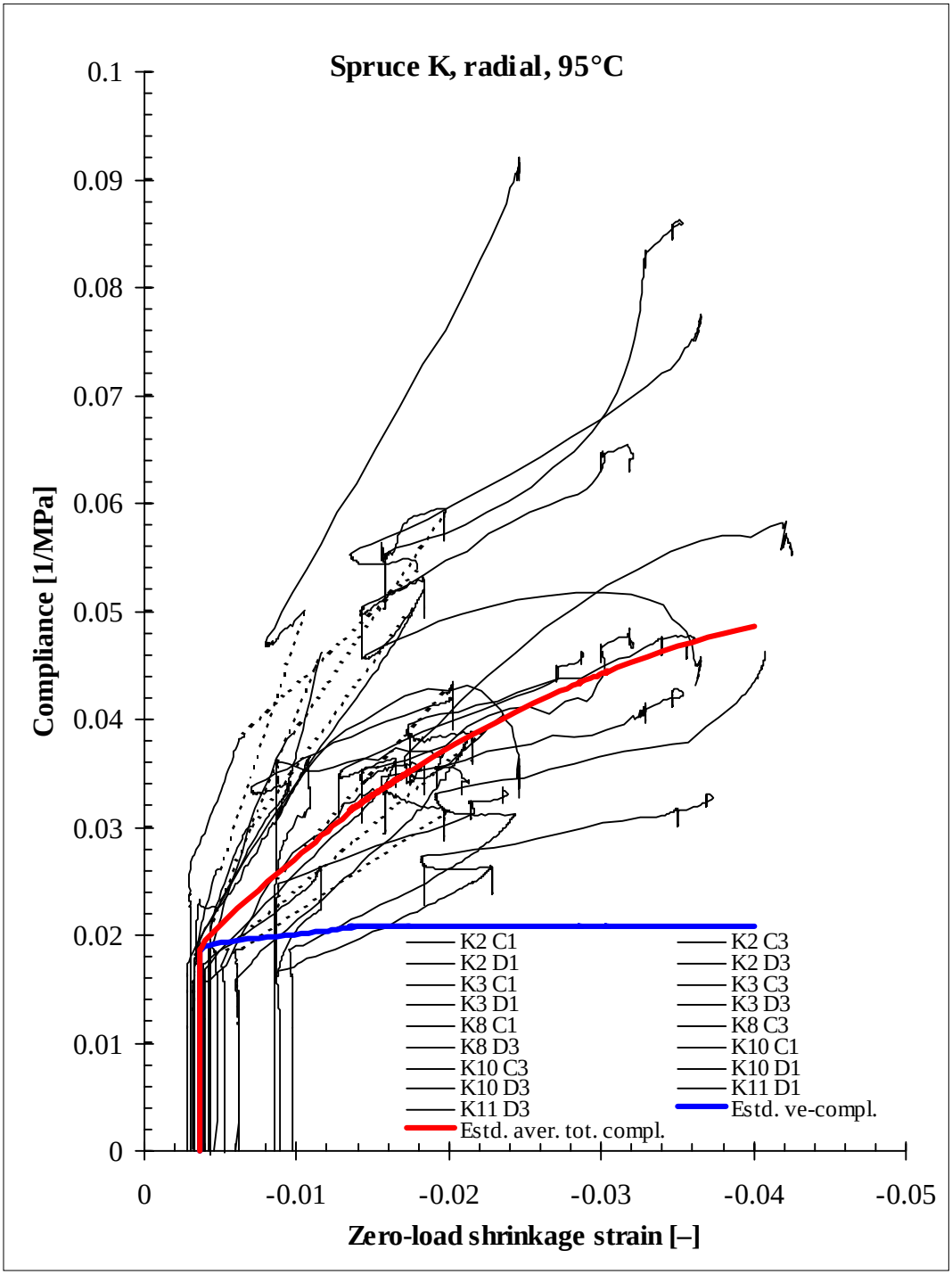

Fig. 43. Compliance vs. zero-load shrinkage strain for radial Spruce K specimens in the tests at 95°C. The estimated magnitude of the elastic–viscoelastic compliance in the test conditions is also plotted as well as the estimated average total compliance, which is based on all radial results (not only the ones in this figure).

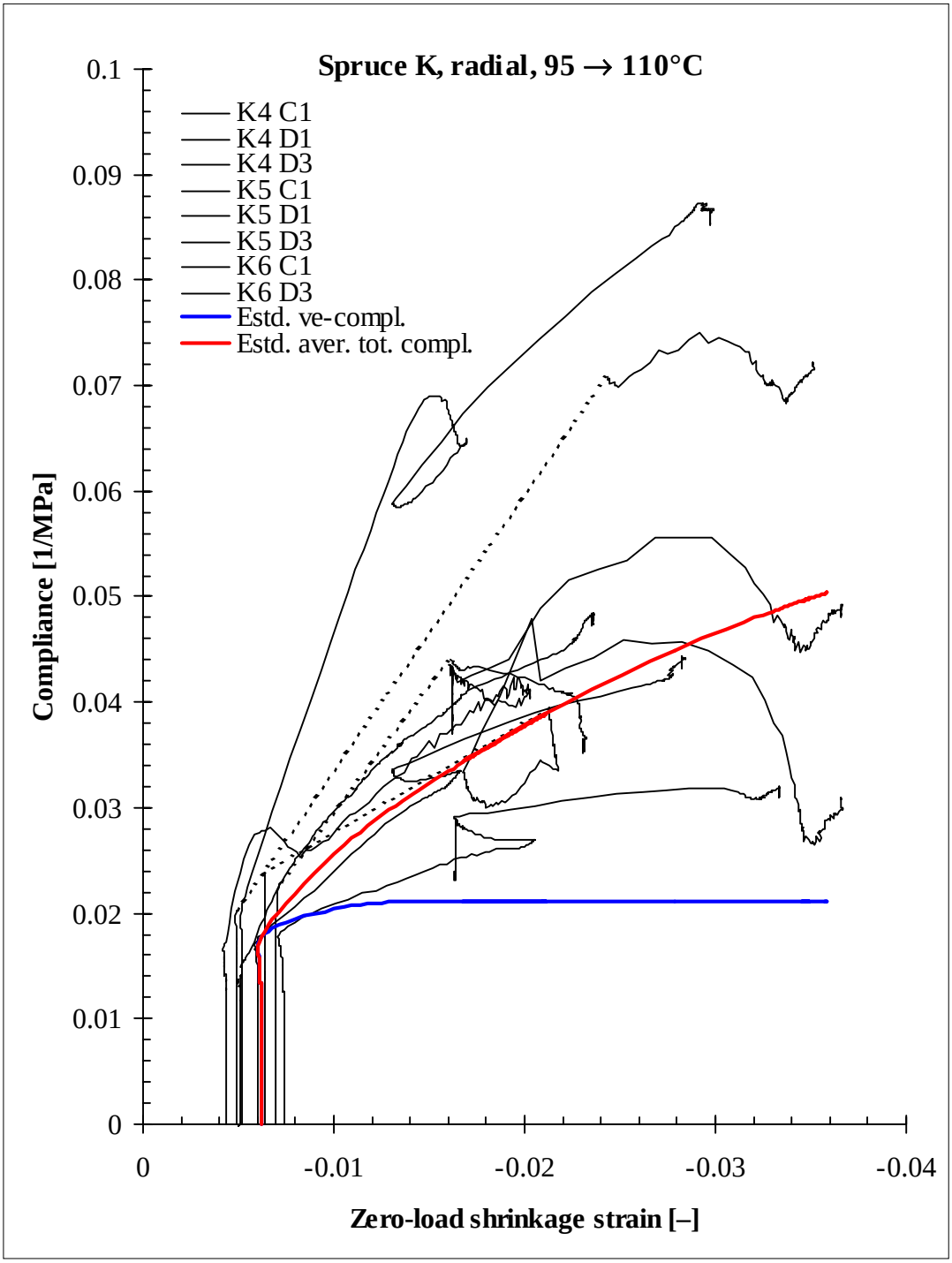

Fig. 44. Compliance vs. zero-load shrinkage strain for radial Spruce K specimens in the tests with maximum temperature 110°C. The estimated magnitude of the elastic–viscoelastic compliance in the test conditions is also plotted as well as the estimated average total compliance, which is based on all radial results (not only the ones in this figure).

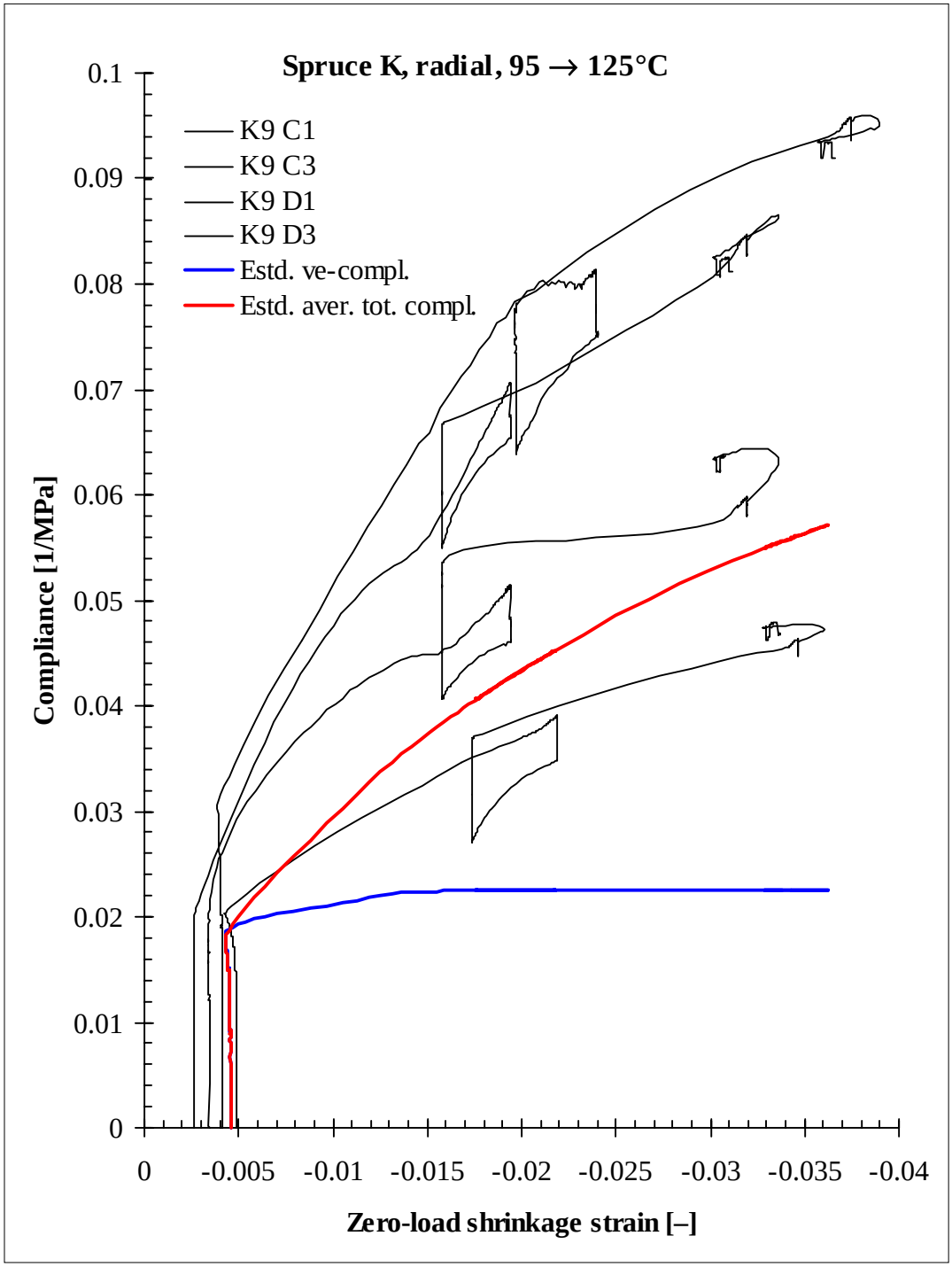

Fig. 45. Compliance vs. zero-load shrinkage strain for radial Spruce K specimens in the tests with maximum temperature 125°C. The estimated magnitude of the elastic–viscoelastic compliance in the test conditions is also plotted as well as the estimated average total compliance, which is based on all radial results (not only the ones in this figure).

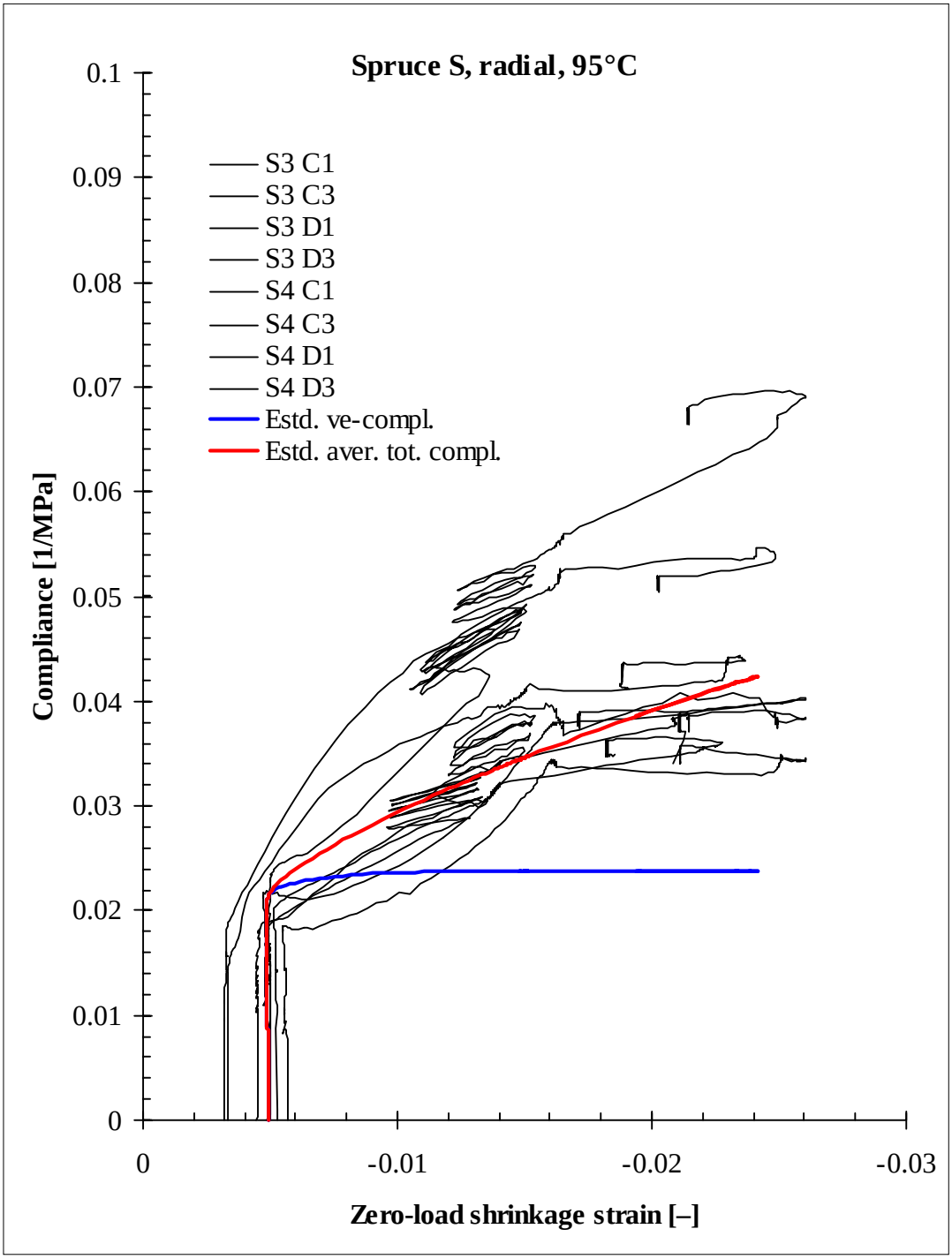

Fig. 46. Compliance vs. zero-load shrinkage strain for radial Spruce S specimens in the tests at 95°C. The estimated magnitude of the elastic–viscoelastic compliance in the test conditions is also plotted as well as the estimated average total compliance, which is based on all radial results (not only the ones in this figure).

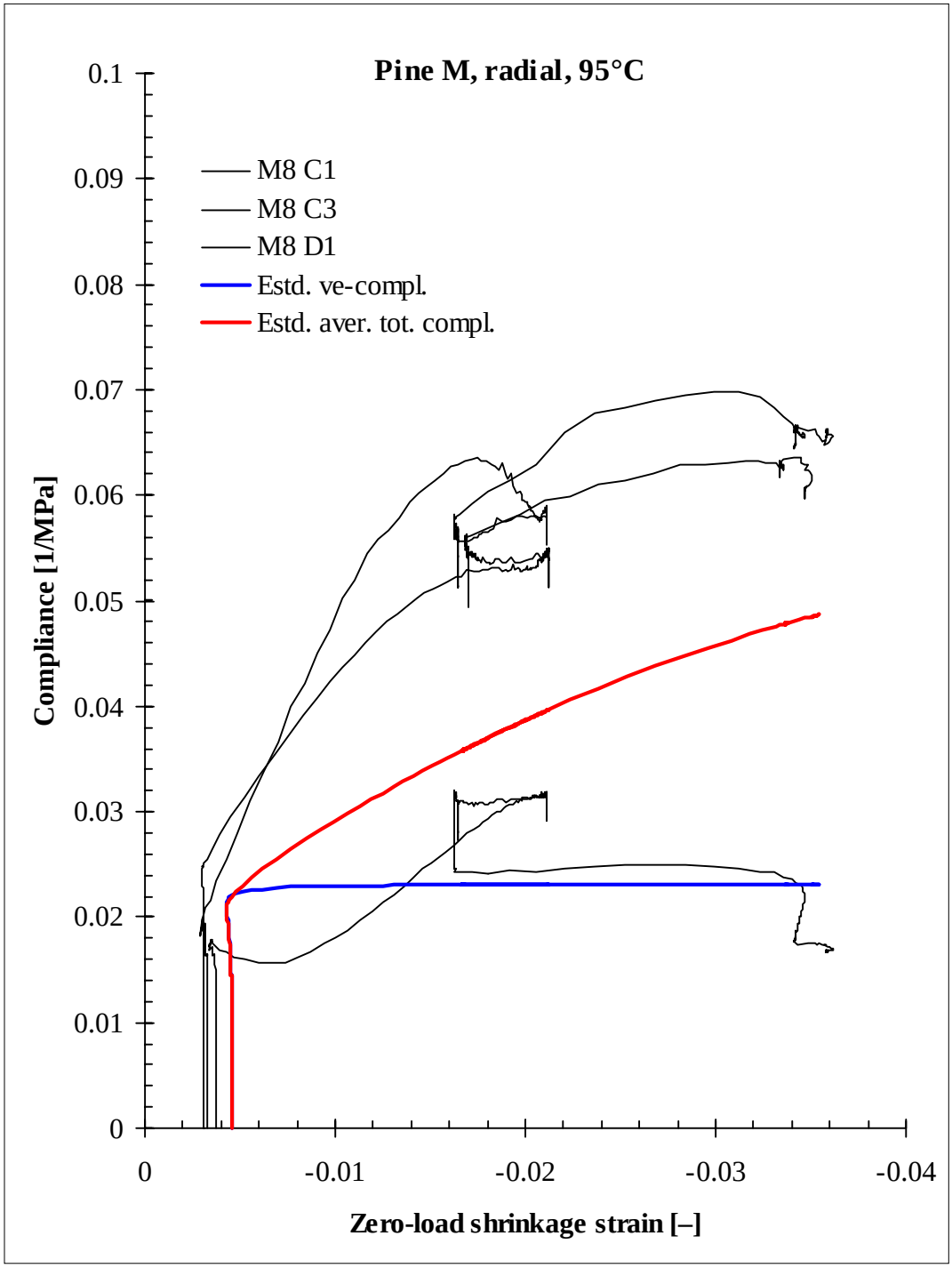

Fig. 47. Compliance vs. zero-load shrinkage strain for radial Pine M specimens in the tests at 95°C. The estimated magnitude of the elastic–viscoelastic compliance in the test conditions is also plotted as well as the estimated average total compliance, which is based on all radial results (not only the ones in this figure).

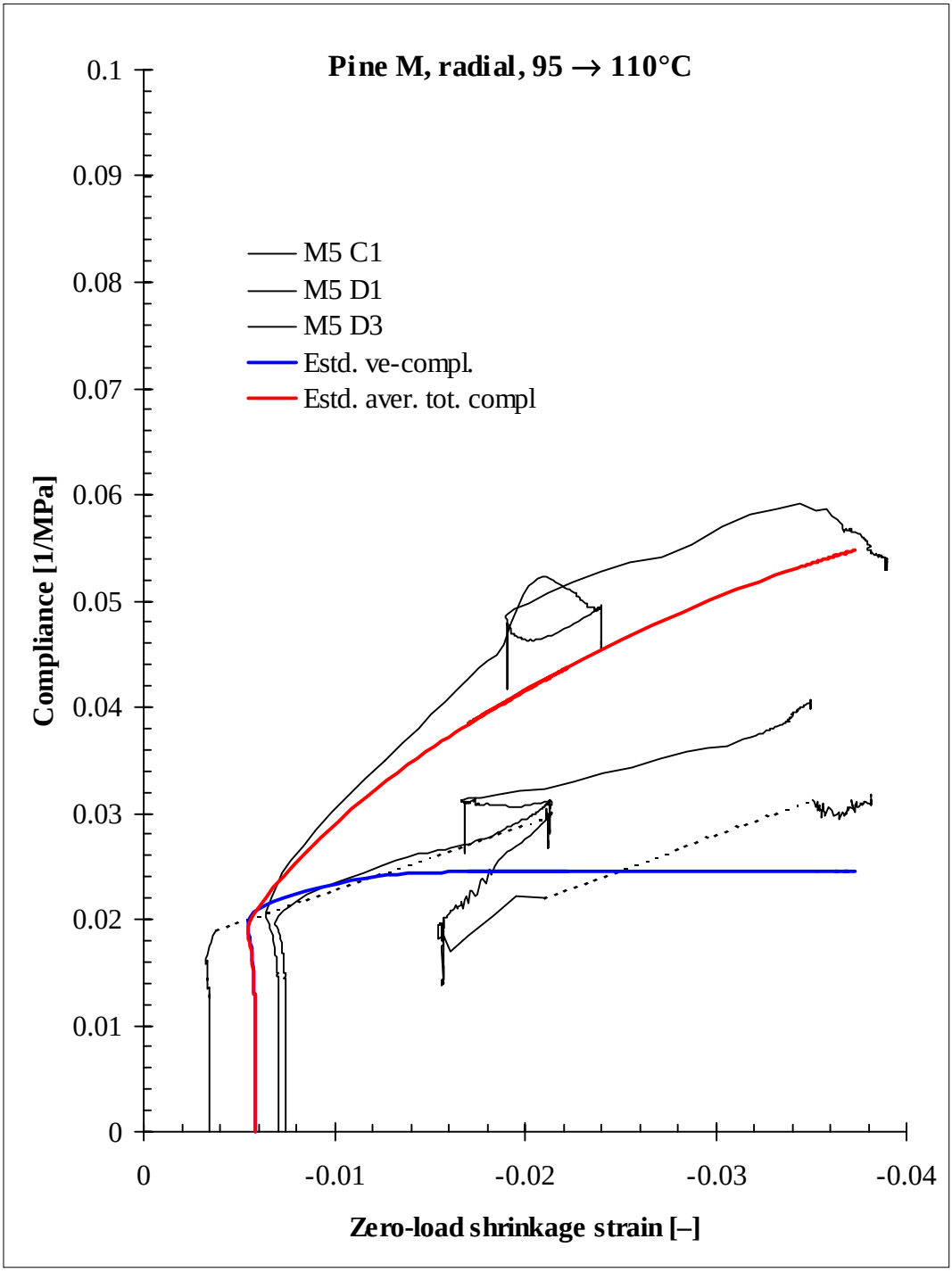

Fig. 48. Compliance vs. zero-load shrinkage strain for radial Pine M specimens in the tests with maximum temperature 110°C. The estimated magnitude of the elastic–viscoelastic compliance in the test conditions is also plotted as well as the estimated average total compliance, which is based on all radial results (not only the ones in this figure).

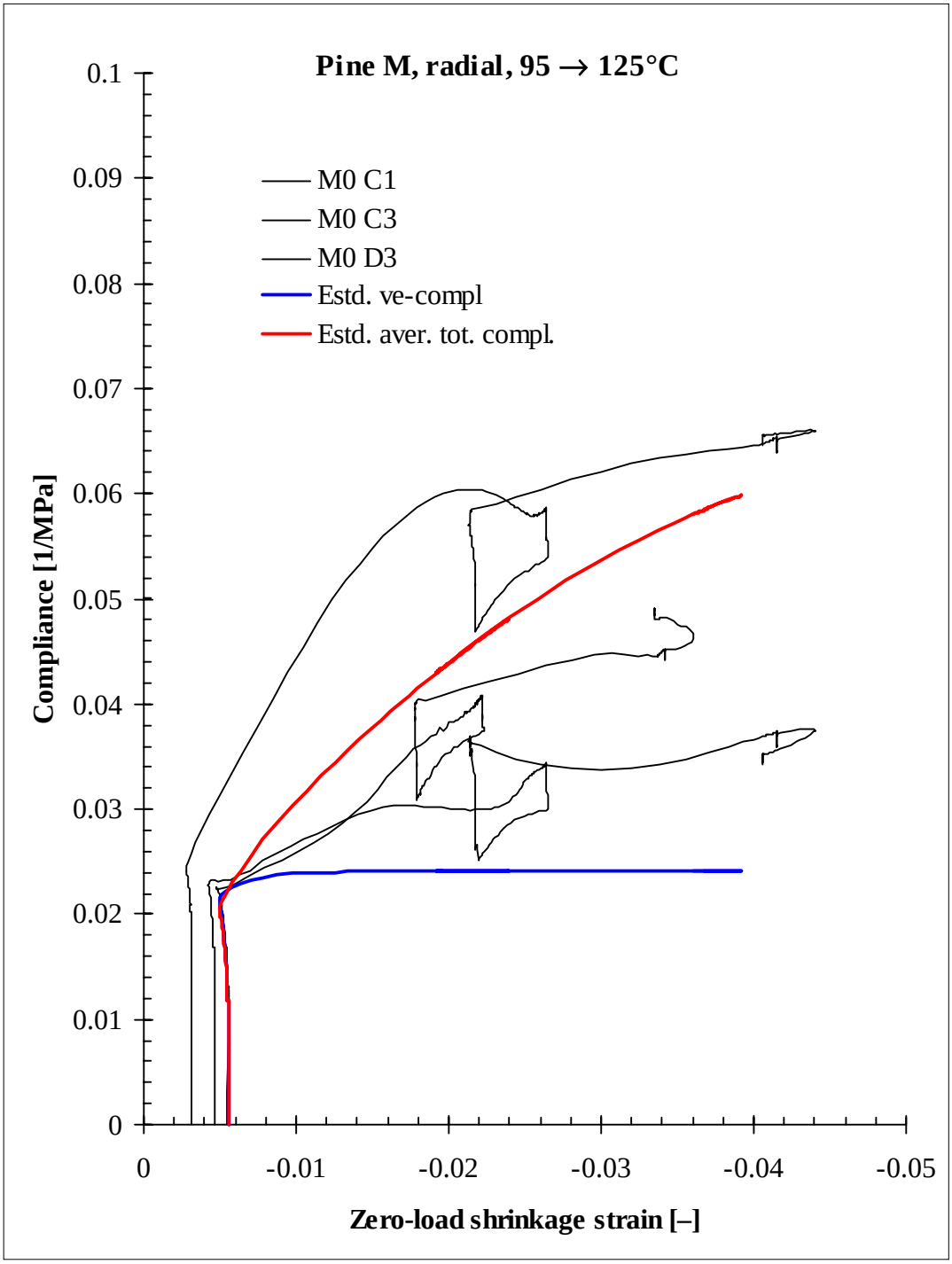

Fig. 49. Compliance vs. zero-load shrinkage strain for radial Pine M specimens in the tests with maximum temperature 125°C. The estimated magnitude of the elastic–viscoelastic compliance in the test conditions is also plotted as well as the estimated average total compliance, which is based on all radial results (not only the ones in this figure).

Magnitude of mechano-sorptive creep

The compliance results in Figs. 36–49 show very large scatter. Apparently, this is mostly due to the analysis procedure, in which the difference of the total strain and the shrinkage strain is taken. This difference is very sensitive to error in determining the zero-load shrinkage. And due to natural variability there is always some difference between the shrinkage of the creep specimen and its dummy, even if they were chosen to match well. Another cause for the large scatter is the fairly low stress level that a significant portion of the specimens was loaded to. Low stress level makes the results more susceptible to error in estimation of the zero-load behaviour. Nevertheless, as the number of tested specimens was quite high the average response can be fairly confidently obtained.

The results did not give reason to determine the mechano-sorptive compliance separately for spruce and pine as their responses seem to be of approximately equal magnitude. However, if the scatter was not as large, the possible difference between the two species might be more detectable.

Also, any possible effect of temperature was not directly detectable from these new results, but this is understandable since in the tests with maximum temperature 110°C and 125°C a large part of the drying took place at a much lower temperature level. The magnitude of the mechano-sorptive creep compliance at 95°C was estimated based on Figs. 36–49 to be:

$$J_{\mathrm{ms,T}} = \left(-1.2\left(\varepsilon_{\mathrm{s}} - \varepsilon_{\mathrm{s,loading}}\right) - 6\left(\varepsilon_{\mathrm{s}} - \varepsilon_{\mathrm{s,loading}}\right)^2 \right) \frac{1}{\mathrm{MPa}} \tag{4}$$

$$J_{\mathrm{ms,R}} = \left(-1.2\left(\varepsilon_{\mathrm{s}} - \varepsilon_{\mathrm{s,loading}}\right) - 12\left(\varepsilon_{\mathrm{s}} - \varepsilon_{\mathrm{s,loading}}\right)^2 \right) \frac{1}{\mathrm{MPa}} \tag{5}$$

where the subscripts T and R refer to tangential and radial directions. ε_s is the zero-load shrinkage strain and $\varepsilon_{s,loading}$ is its value at the time of loading. The compliance magnitudes have been determined for continuous loading and monotonous drying at 95°C.

To get a better picture of the effect of temperature and to quantify the mechano-sorptive creep as function of temperature, the estimated average total compliance in the tangential direction was plotted with other researchers' results. For this, the results from Hisada (1986), Wu and Milota (1995), Svensson (1996) and Kangas (1990) along with the new one are gathered into Fig. 50. Kangas' results were slightly re-processed and an estimated average compliance was determined in the same manner as above. Fig. 50 indicates that temperature has an effect on the amount of mechano-sorptive creep. Based on the slope of the compliance curves (after loading and initial deformation), the dependence of mechano-sorptive creep magnitude was estimated as function of temperature, Fig. 51. The mechano-sorptive creep magnitude as function of temperature was also numerically modelled, by writing the magnitude of the mechano-sorptive creep development as relative to that at 95°C:

$$\frac{J_{\mathrm{ms}}(T)}{J_{\mathrm{ms}}(95°C)} = 1 + 0.014\,°C^{-1}(T - 95°C) + 0.00007\,°C^{-2}(T - 95°C)^2 \quad (6)$$

Although this equation is based on experiments at temperatures 20–95°C, it is assumed that its application range can be extended somewhat above 95°C.

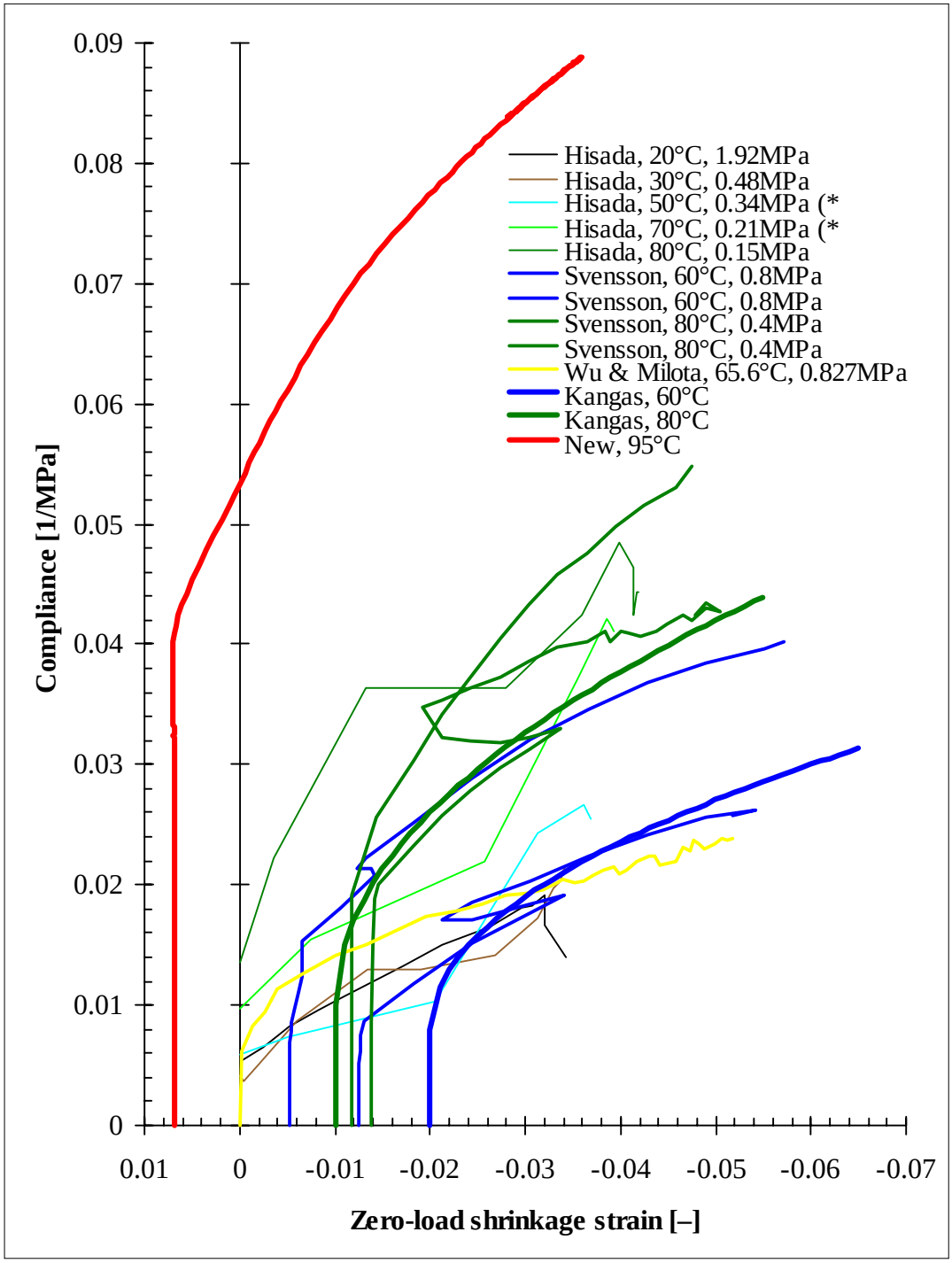

Fig. 50. Effect of temperature on tangential compliance during drying showing results from several researchers. Hisada's (1986) results [*) zero-load shrinkage estimated by the author] are on hinoki (Chamaecyparis obtusa). Wu and Milota's (1995) results are on Douglas fir (Pseudotsuga menziesii). Svensson's (1996) and Kangas' (1990) results are on Scots pine (Pinus sylvestris). Note that the curve of the new results begins at a positive shrinkage strain value due to the hygrothermal effect.

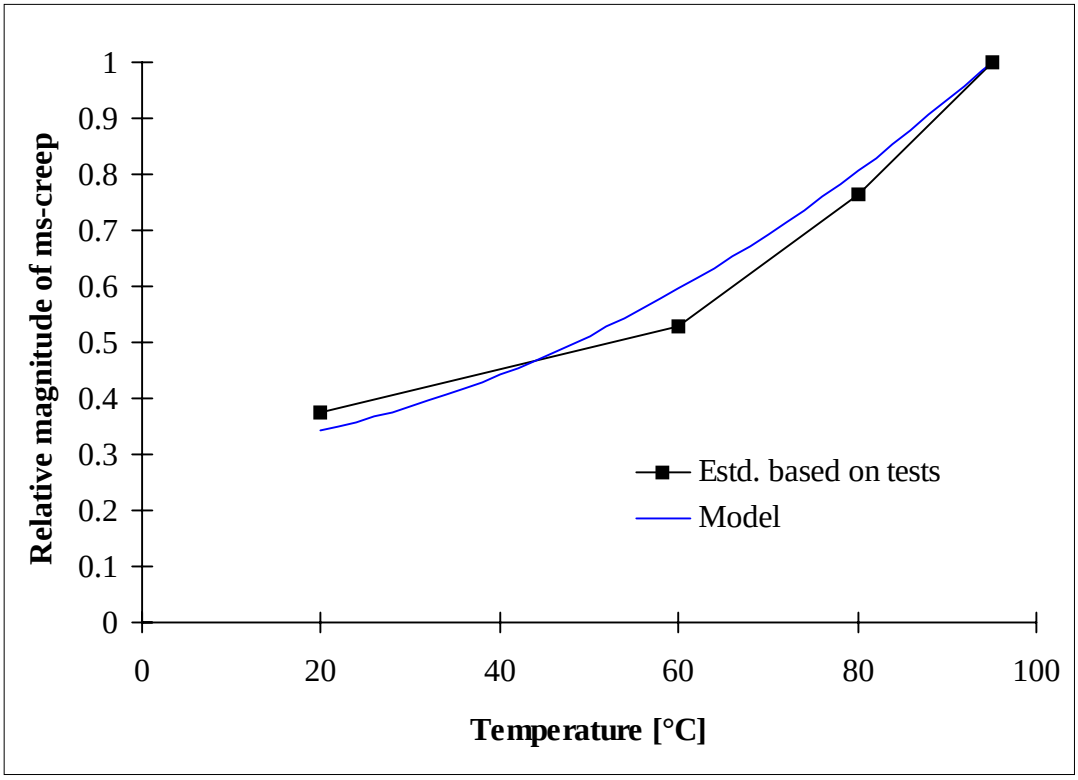

Fig. 51. Estimated magnitude of the mechano-sorptive creep development at different temperatures relative to its magnitude at 95°C. The experimental points are based on estimation of curve slopes in Fig. 50.

Effect of moisture cycling on mechano-sorptive creep

One important aspect in the quantification of the mechano-sorptive effect is the effect of repeated moisture cycles. This feature was investigated in the late part of the experimental programme by performing experiments that consisted either of a single monotonous drying or of several drying-moistening cycles (Appendix C, T95K19–T95K23). Fig. 52 shows an example of the resulting compliance curve of both drying schedule types. The curves are chosen so that they resemble each other as much as possible except the presence or lack of the moisture cycles. The curves indicate that there is some more creep development due to the moisture cycles but the effect is not very strong.

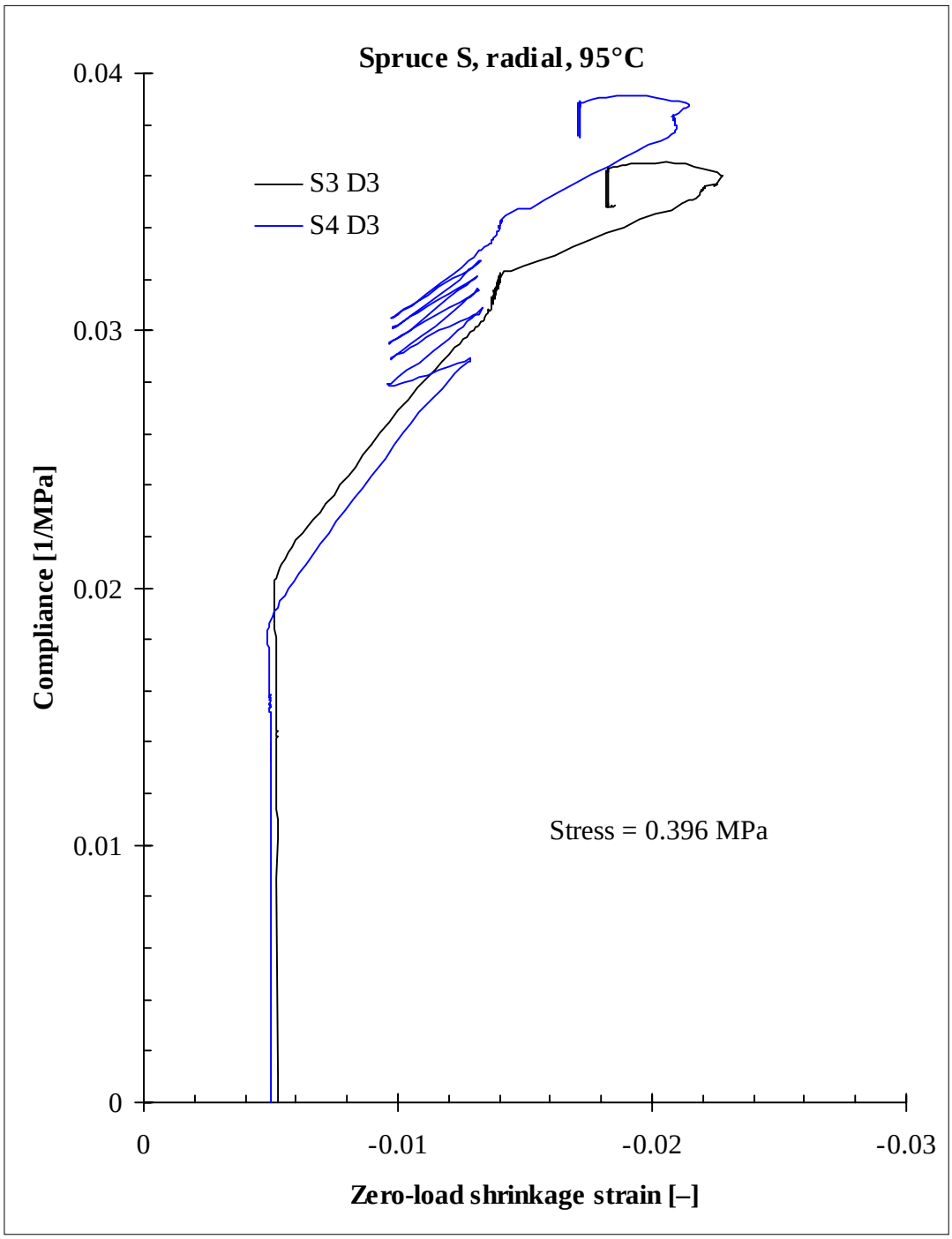

Fig. 52. Effect of moisture cycling on mechano-sorptive creep development. Comparison between two specimens that underwent a monotonous drying or a drying with moisture cycles.

Recoverability of mechano-sorptive creep

Another interesting aspect of the mechano-sorptive creep in conjunction with drying is the recoverability. In Kangas' (1990) experiments it was found that mechano-sorptive creep is largely recoverable during re-wetting. In the present project, recovery was investigated in a test in which the load was removed at about halfway of the drying. The results are shown in Appendix C, T95K19. In Fig. 53, the compliance of two specimens is compared; the first one of them had the load on through the whole experiment, whereas the second one had the load removed at halfway. Except the load history, the specimens have been chosen to show a very similar response. It can be seen that the recovery is very little if much anything during drying. This is a somewhat surprising result, because very often it has been assumed that mechano-sorptive creep is recoverable by any moisture change regardless of its direction.

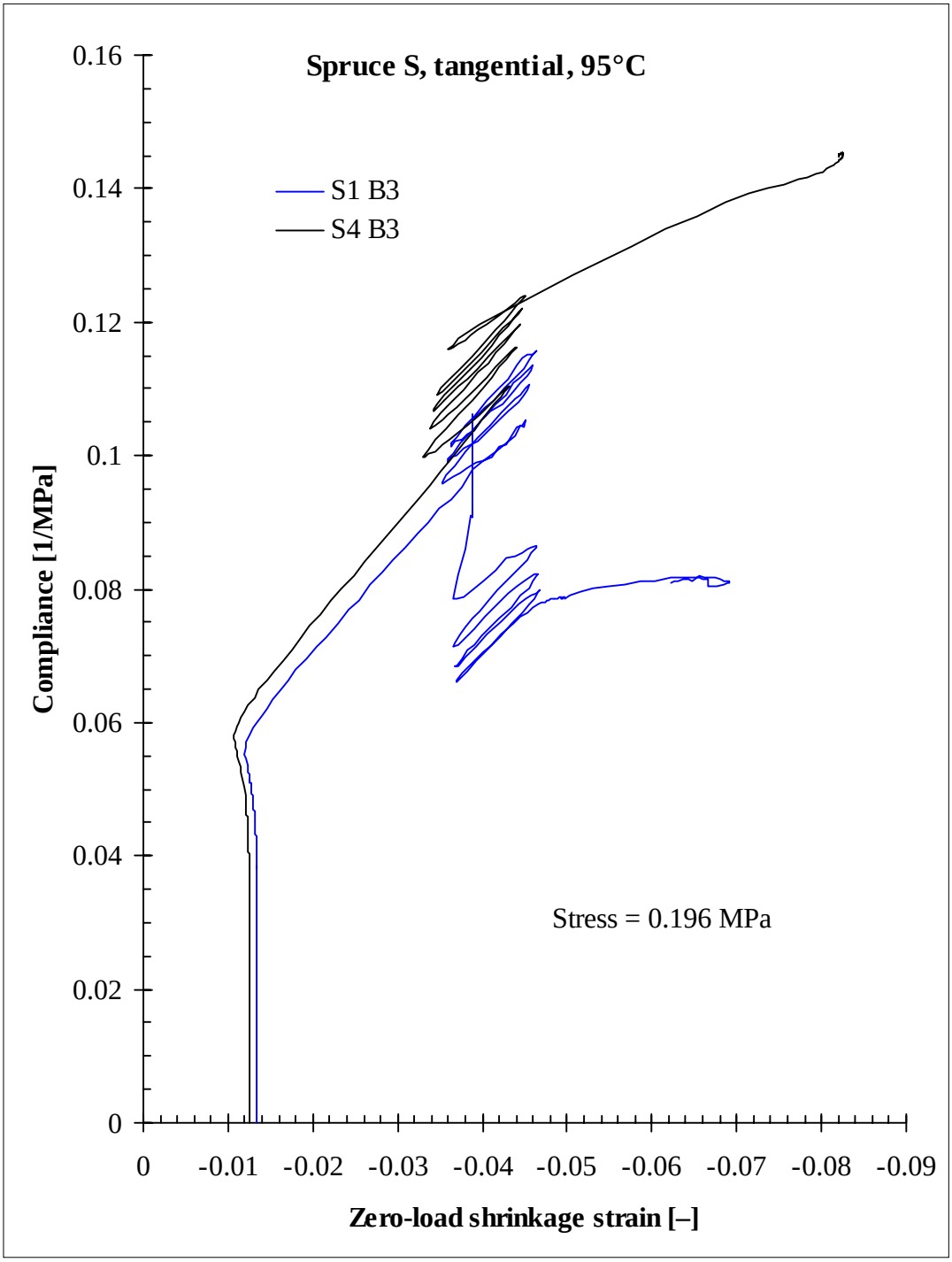

Fig. 53. Test of recoverability of mechano-sorptive creep if load is removed at about halfway of drying. The two specimens have been chosen to resemble each other as much as possible in the response except that the other one had the load on through the whole experiment and the other one had it removed at about halfway.

3.6.6 Strength

As an extra extension to the constant wet condition creep tests a very limited strength test series was carried out. The test set-up and conditions were the same as for the creep tests, i.e. hot steam/water bath at temperatures 95 and 125°C. The specimens were of Spruce S only. The specimens were slightly modified for the strength tests by cutting a round waisting along the two edges of the specimen middle parts, so that the smallest cross-section area at the middle of the specimens was 20 mm × 21.5 mm. The strength tests were carried out in just the same way as the constant wet condition creep tests, only that, at loading, the load increase was continued until failure.

The results of the strength test of individual specimens are gathered in Table 3. Not all specimens failed "properly" at the middle part, but in quite a few specimens the fracture surface passes at least partly along the glued joint. All radial specimens failed at least somewhat "improperly". This is no surprise, since the specimens used were just modified creep specimens and not designed for strength tests. Nevertheless, a preliminary idea of the strength can be obtained from the results for the tangential direction but the results for the radial direction are doubtful. The tangential results show a fairly consistent continuation of the strength test results of Siimes (1967) on spruce (*Picea abies*) as shown in Fig. 54. Koran's (1979) results on Black spruce (*Picea mariana*) have also been included.

Table 3. Strength test results. The results should be considered as preliminary, because so many specimens failed at the glued joint; this holds especially for the radial results.

Speci-men	Specimen direction	Tempe-rature [°C]	Max. force [kN]	Failure remark (†	Strength [MPa]	Average all	Average non-joint (‡
S0A4	Tangential	95	0.348		0.810		
S1A5	Tangential	95	0.388		0.902		
S3A7	Tangential	95	0.283	**	0.658		
S3B7	Tangential	95	0.321	*	0.747		
S4B5	Tangential	95	0.317	**	0.737		
	Tangential	95				0.771	0.856
S1C3	Radial	95	0.599	*	1.393		
S1D1	Radial	95	0.682	**	1.587		
S1D3	Radial	95	0.529	**	1.230		
S4C4	Radial	95	0.496	**	1.153		
	Radial	95				1.341	–
S1A6	Tangential	125	0.268		0.624		
S3A8	Tangential	125	0.205	**	0.477		
S3B8	Tangential	125	0.215		0.500		
S4A4	Tangential	125	0.214	**	0.497		
S4B6	Tangential	125	0.205		0.476		
S5A6	Tangential	125	0.245	**	0.569		
	Tangential	125				0.524	0.534
S1C4	Radial	125	0.488		1.135		
S1D2	Radial	125	0.598		1.390		
S3C4	Radial	125	0.549	**	1.277		
S5C4	Radial	125	0.295	**	0.686		
	Radial	125				1.122	1.263

†) **– Failure occurred at the joint
* – Failure occurred partly at the joint
‡) Average of failures that occurred outside the joint.

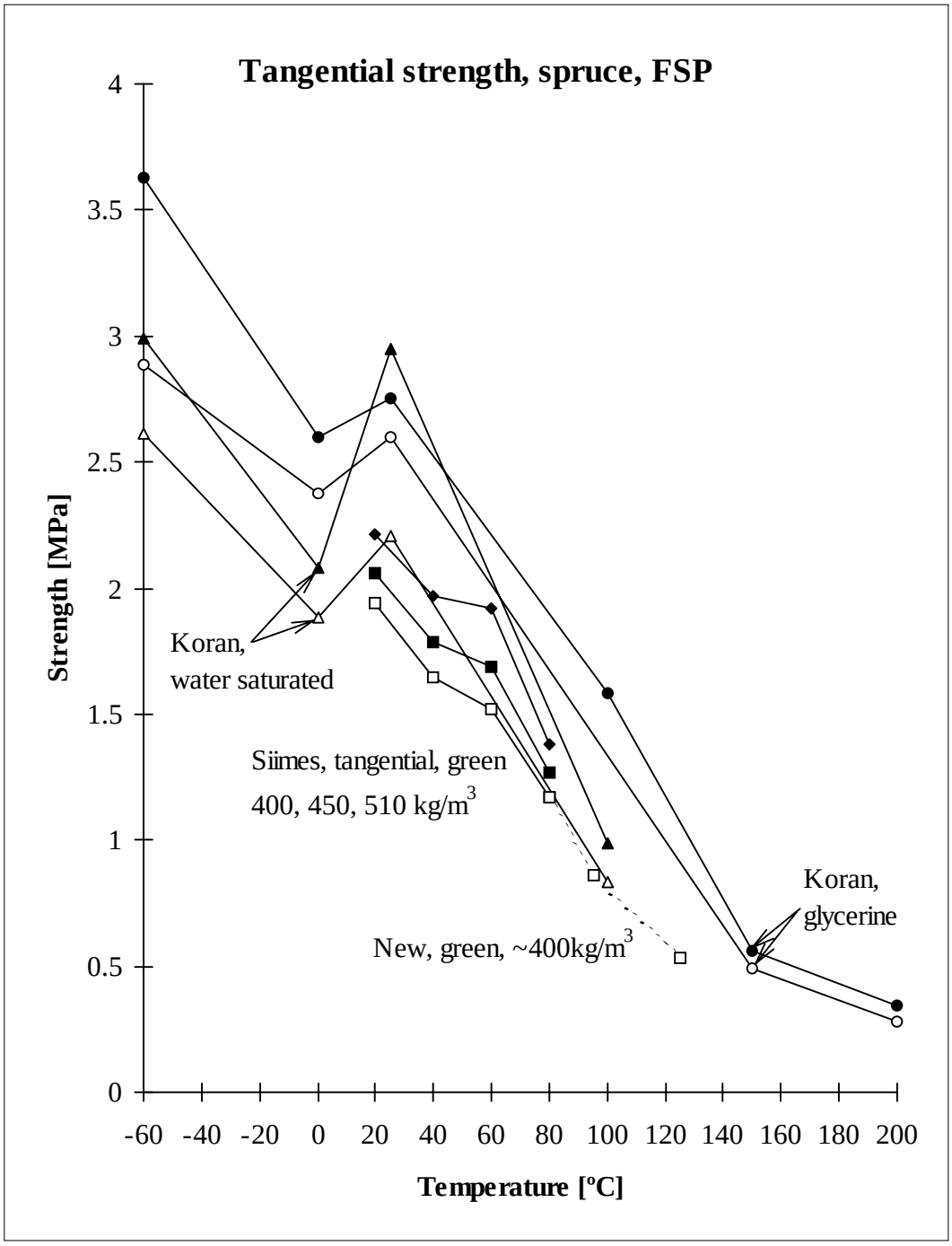

Fig. 54. Tangential strength of spruce wood in saturated condition as function of temperature. Even if the sample size is very small, the new results (Picea abies) show a reasonably consistent continuation of the results of Siimes (1967, Picea abies). Koran's (1979) results on Black spruce (Picea mariana) are also shown for reference.

4 MODELLING

The final goal of the work was to be able to model the stress and strain development during drying using numerical simulation. Therefore, for use in simulation programs, a constitutive model of the mechanical behaviour of wood in the high temperature drying conditions was constructed, which would conform as closely as possible with the obtained experimental results.

Based on test results and on demands set by simulation performance, the following presumptions were taken as the basis of modelling:

- the model should be kept simple and linear for fast simulation capability,
- shrinkage is linear with moisture content below fiber saturation,
- no categorisation is made between elastic and viscoelastic strains, but these two are considered jointly under viscoelastic label,
- time–temperature–moisture-content equivalence principle is used in modelling viscoelastic creep,
- mechano-sorptive creep is assumed to be closely related to shrinkage,
- a fairly large fraction of the mechano-sorptive creep is irrecoverable, unless the direction of the stress is reversed.
- cycling moisture content (repeated drying and wetting periods) does not induce much additional creep compared to monotonous drying.

It should be noted that the assumptions concerning the character of the mechano-sorptive creep were adopted especially keeping in mind the high temperature conditions (90–125°C). The model was created separately for tangential deformation and radial deformation and any coupling effects between them were not considered in this work.

The model is based on the commonly used idea that the strain is separable into parts which, when summed together yield the total strain:

$$\varepsilon = \varepsilon_s + \varepsilon_{ht} + \varepsilon_{ve} + \varepsilon_{ms} \tag{7}$$

where ε is the total strain, ε_s is the hygroexpansion (shrinkage) strain, ε_{ht} is the hygrothermal strain, ε_{ve} is the combined elastic-viscoelastic strain and ε_{ms} is the mechano-sorptive strain.

Assumption of the separability of the different strain terms, Eq. (7), or holding to linear modelling, are not necessarily correct from the theoretical point of view (Hanhijärvi 1995), but were adopted here because of the simplicity they bring to the modelling. In the following an evolution law is developed for all strain terms to actualise the model.

4.1 SHRINKAGE AND HYGROTHERMAL STRAIN

In order to facilitate the expressions needed for describing shrinkage and creep in function of moisture content, an "effective moisture content" $\hat{u}$ is defined as

$$\hat{u} = \min(u, u_{FS}) \tag{8}$$

where u is the moisture content of wood calculated on the dry weight basis [$u = (m\text{-}m_0)/m_0$, m = mass, m_0 = mass at absolute dry condition]. u_{FS} denotes the value of u at fiber saturation point (it is considered as a function of temperature).

The assumption of linear shrinkage with moisture content change is expressed as function of the effective moisture content:

$$d\varepsilon_s = \alpha \, d\hat{u} \tag{9}$$

where ε_s is the hygroexpansion strain and α the hygroexpansion coefficient, which obtains differents value for radial and tangential cases and which may be a function of specific gravity and temperature. In the perpendicular-to-grain directions the linear shrinkage assumption is well supported by experiment results except maybe the very beginning of shrinkage around FSP.

The hygrothermal deformation was modelled assuming that it is proportional to the temperature rise, but it begins only when temperature exceeds 60°C and ceases to develop after temperature has reached 120°C. Also, it takes place *only when* the temperatures between 60°C and 120 °C *are reached for the first time* during the drying and is irrecoverable. With these assumptions:

$$\begin{aligned} &d\varepsilon_{HT} = \beta \, dT, \quad \text{when } T \geq T_{MAX} \text{ and } 60^\circ\text{C} \leq T \leq 120^\circ\text{C} \\ &d\varepsilon_{HT} = 0, \qquad \text{otherwise} \end{aligned} \tag{10}$$

where ε_{ht} is the hygrothermal strain, T the temperature and β the hygrothermal coefficient, which is of course different in the radial and tangential directions. T_{MAX} is the maximum temperature which the considered material particle has reached during the drying. Another assumption was that hygrothermal deformation occurs in full measure only if the moisture content is at fiber saturation or above. No hygrothermal deformation is developed if the moisture content is less than fiber saturation point minus 10%. These assumptions can be modelled by making β moisture content dependent:

$$\beta = \beta_{FS} \max\left(\frac{(\hat{u} - u_{FS} + 0.1)}{0.1}, 0\right) \tag{11}$$

where β_{FS} is the value of β at FSP. Based on the experiment results, the values 0.00023 $°C^{-1}$ and –0.000086 $°C^{-1}$ can be obtained for β_{FS} in the tangential and radial directions, respectively.

It should be noted that the above modelling of the hygrothermal strain assumes that is occurs immediately with temperature rise. This is not in full agreement with the test results introduced earlier since especially in case of tangential specimens the hygrothermal strain development seems to continue even after the end of heating. However, since the hygrothermal deformation is a rather unexplored topic, no dependence on time was applied to it.

4.2 ELASTIC STRAIN AND VISCOELASTIC CREEP

The separation of the elastic and viscoelastic strain from experiment results is indefinite. By *theoretical definition*, the elastic strain is that part of the strain, which is completely recoverable and occurs immediately at loading. Its recovery occurs also immediately at unloading. On the other hand, viscoelastic strain is also recoverable, but occurs as delayed, only after loading. The recovery of viscoelastic deformation also takes place as a delayed phenomenon. However, in real experiments, the separation of these two is impossible because viscoelastic phenomena occur very fast — even in high frequency excitation, time-dependent phenomena have been recorded (Launay 1987, referred to in Huet 1988) and no load can be applied in 'zero time'. Normally, in interpretation of test results, the problem is avoided by some *practical* way, assuming an instant after loading, at which the strain is defined as 'elastic', e.g. one minute after loading. From the practical point of view this approach is very useful. From the *modelling* point of view it contains the problem that the thus defined 'elastic' deformation always includes some viscoelastic, time-dependent part. If this definition of 'elastic' deformation as the deformation at a certain instant after loading is applied in different conditions, the fraction of the strain that is not truly elastic but time-dependent, viscoelastic may vary considerably.

This problem is troublesome in conjunction with the use of the principle of time-temperature equivalence in the modelling of viscoelastic creep. This principle suggests, in short, that the effect of temperature on the viscoelastic creep amount can be modelled by defining a 'material time', which is the real time multiplied with a temperature dependent coefficient. At the reference temperature this coefficient equals 1 and the material time is the real time; at temperatures higher than that the coefficient obtains a value over 1 and material time 'passes' faster than real time. At lower temperatures than the reference temperature, on the other hand, the coefficient is less than 1 and the material time 'passes' slower than real time. The time-temperature equivalence principle states that the viscoelastic creep at different temperatures is taken into account by merely replacing the real time with the material time in the viscoelastic creep model applicable at the reference temperature. Now, if the immediate elastic deformation is

defined in different conditions as the deformation value at, say, 1 min after loading and as it inevitably contains some viscoelastic deformation, the use of the time-temperature equivalence principle becomes obscure. Thus, in conjunction with the time-temperature equivalence principle, the elastic strain should be determined as consistent to the definition of viscoelastic creep.

Due to this obscurity in the separation of elastic deformation from the viscoelastic creep, the following approach was chosen in this work: it was resolved that all immediate elastic and time-dependent viscoelastic deformation can be dealt under the concept of viscoelastic strain. This assumption was used in conjunction with adopting the time–temperature–moisture-content equivalence.

The modelling was done by a series of rheological units of the Kelvin type, i.e. the generalised Kelvin material, as was earlier anticipated in the analysis of results. 22 units are used which obey the following equations:

$$\begin{aligned} \varepsilon_0^{\mathrm{ve}} &= J_0^{\mathrm{ve}}\sigma \\ d\varepsilon_i^{\mathrm{ve}} &= \frac{J_i^{\mathrm{ve}}\sigma - \varepsilon_i^{\mathrm{ve}}}{\tau_i^{\mathrm{ve}}} d\xi, \quad i = 1, 2 \ldots 21 \end{aligned} \tag{12}$$

where σ is the stress, $\varepsilon^{\mathrm{ve}}{}_{,i}$'s are the strains of the units, $J^{\mathrm{ve}}{}_{,i}$'s are their limit compliances and $\tau^{\mathrm{ve}}{}_{,i}$'s their retardation times. $d\xi$ is the material time differential. The equation governing the unit 0 resembles the normal definition of elastic behaviour, but it should not be considered as elastic behaviour, but rather to be understood as a Kelvin unit, whose retardation time is so small that, in any condition, it reaches the limit compliance in a time which is shorter than the shortest time period that can come into consideration. The values of the $J^{\mathrm{ve}}{}_{,i}$'s and $\tau^{\mathrm{ve}}{}_{,i}$'s have already been given in Table 2.

The material time differential is, according to the time–temperature–moisture-content superposition principle:

$$d\xi = a(T,u)dt \tag{13}$$

where dt is the time differential. a is the shift factor, whose value is defined in Eq. (2).

4.3 MECHANO-SORPTIVE CREEP

The previous modelling of mechano-sorptive creep in conjunction with drying has been based on analogy to Maxwell or Kelvin type viscoelastic models (a review of models of mechano-sorptive creep can be found in ref. Hanhijärvi 1995), so that for use in modelling the mechano-sorptive creep the time differential dt has been replaced by the absolute value of the moisture content change $|du|$. These mechano-sorptive models repeat the properties of their viscoelastic predecessors, when the effect of time is

assumed to be replaced by the cumulative amount of moisture content change in any direction, drying or wetting or alternating drying–wetting cycles. Under constant load, the "mechano-sorptive Maxwell model" produces linear creep development as function of cumulative moisture change with no recovery, even if load is removed and moisture change continues. "The mechano-sorptive Kelvin model" produces slowing creep rate as cumulative moisture content change increases and exhibits complete recovery, if load is removed and moisture change continues enough. Both models show a linear response with respect to stress.

Neither one of these models nor a combination of them was found to be satisfactory for modelling the behaviour found in the experiments. The experiments showed that large proportion of the developed mechano-sorptive creep does not recover, even if the load is removed and drying continues. However, based on earlier results at lower temperature levels (Kangas 1990), it was concluded that mechano-sorptive creep developed in predominantly drying condition is recoverable at least to some extent during wetting after removal of load. Furthermore, moisture cycling does not increase creep in proportion to the amount of cumulative moisture change. It was concluded that the elementary mechano-sorptive Maxwell and Kelvin models or their combination is too simple to produce a satisfactory result in a wide range of conditions. Also, the type of modelling, in which different values are assigned for the mechano-sorptive creep development depending whether de- or adsorption occurs, was rejected, because it may cause problems in case the state of stress alternates with same rhythm as the direction of the moisture content change. For longitudinal creep, a non-linear model has been suggested by the author (Hanhijärvi 1995), that can describe the apparent irrecoverability, even if it shows slowing creep rate as function of cumulative moisture change. However, the applicability of a non-linear model to drying simulation was not attempted, because it requires an iterative solution algorithm and thus would be computationally too slow for fast enough simulation.

Instead, a new model was developed which maintains computational simplicity and incorporates the experimentally discovered recovery and other properties. The development was based on the mechano-sorptive Kelvin-type model and to the idea that irrecoverable creep develops in proportion to the total creep. The development was built on expressing mechano-sorptive creep development on shrinkage development, or precisely speaking the absolute value of the shrinkage strain differential $|d\varepsilon_s|$ as has been done by Mårtensson and Svensson (1996). This is for convenience of the consistency with the analysis of experiment results. Exactly same model could be obtained also in the more traditional way by expressing the mechano-sorptive creep development in terms of the absolute value of effective moisture content change $|d\hat{u}|$, because of the linear relationship between these two, Eq. (9).

The apparent recovery in adsorption was modelled by introducing a dependence of compliance on shrinkage – or equivalently it could be described as dependence on moisture content.

The expression of mechano-sorptive strain rate in the new model resembles that of the Kelvin type model, but now a new variable "irrecoverable mechano-sorptive strain" ε_{ir} is introduced:

$$d\varepsilon_{ms} = \frac{J_{ms}\sigma - (\varepsilon_{ms} - \varepsilon_{ir})}{\tau_{ms}} |d\varepsilon_s| \tag{14}$$

J_{ms} and τ_{ms} correspond to the usual two parameters of the Kelvin model. The evolution of ε_{ir} is defined in a four-branched equation:

$$\begin{aligned}
&\text{if } d\varepsilon_{ms}\,\sigma \le 0: \\
&\quad d\varepsilon_{ir} = 0 \\
&\text{if } d\varepsilon_{ms}\,\sigma > 0 \text{ and } \varepsilon_{min} \le \varepsilon_{ms} + d\varepsilon_{ms} \le \varepsilon_{max}: \\
&\quad d\varepsilon_{ir} = 0 \\
&\text{if } d\varepsilon_{ms}\,\sigma > 0 \text{ and } \varepsilon_{ms} + d\varepsilon_{ms} > \varepsilon_{max}: \\
&\quad d\varepsilon_{ir} = a_{ir} |\varepsilon_{ms} + d\varepsilon_{ms} - \varepsilon_{max}| \operatorname{sgn}(J_{ir}\sigma - \varepsilon_{ir}) \min\left\{ b_{ir}, \left| \frac{J_{ir}\sigma - \varepsilon_{ir}}{\sigma} \right| \right\} \\
&\text{if } d\varepsilon_{ms}\,\sigma > 0 \text{ and } \varepsilon_{ms} + d\varepsilon_{ms} < \varepsilon_{min}: \\
&\quad d\varepsilon_{ir} = a_{ir} |\varepsilon_{ms} + d\varepsilon_{ms} - \varepsilon_{min}| \operatorname{sgn}(J_{ir}\sigma - \varepsilon_{ir}) \min\left\{ b_{ir}, \left| \frac{J_{ir}\sigma - \varepsilon_{ir}}{\sigma} \right| \right\}
\end{aligned} \tag{15}$$

where the quantities ε_{min} and ε_{max} are defined:

$$\begin{aligned}
&\text{if } \varepsilon_{ms} \ge \varepsilon_{ir}: \\
&\quad \varepsilon_{max} = \max\left\{ \lim_{\tau \to t^-} \varepsilon_{max}(\tau), \varepsilon_{ms} \right\} \\
&\text{if } \varepsilon_{ms} < \varepsilon_{ir}: \\
&\quad \varepsilon_{max} = \varepsilon_{ir}
\end{aligned} \tag{16}$$

and

$$\begin{aligned}
&\text{if } \varepsilon_{ms} \le \varepsilon_{ir}: \\
&\quad \varepsilon_{min} = \min\left\{ \lim_{\tau \to t^-} \varepsilon_{min}(\tau), \varepsilon_{ms} \right\} \\
&\text{if } \varepsilon_{ms} > \varepsilon_{ir}: \\
&\quad \varepsilon_{min} = \varepsilon_{ir}
\end{aligned} \tag{17}$$

a_{ir} and b_{ir} as well as J_{ir} are additional model parameters.

For the Eqs. (14) – (17) to be well-defined, an initial condition must be defined for the variables ε_{ms}, ε_{ir}, ε_{min} and ε_{max}. The natural initial condition for simulation of drying is that before the beginning of consideration (e.g. before felling) all of them obtain the value zero:

$$\varepsilon_{ms} = \varepsilon_{ir} = \varepsilon_{max} = \varepsilon_{min} = 0 \quad \text{when } t \le t_0 \tag{18}$$

where t_0 is the time at the beginning of consideration.

To take into account the recovery during adsorption J_{ms} and J_{ir} are made dependent on the amount of shrinkage (or equivalently, this could be expressed by making them dependent on moisture content).

The definition of ε_{ir}, ε_{max} and ε_{min} may seem awkward at first sight, so some comments on the purpose of these variables may be necessary. The "irrecoverable mechano-sorptive strain" ε_{ir} is the part of the mechano-sorptive strain that is not recoverable unless the direction of the acting stress changes. It modifies the "internal equilibrium state" of the Kelvin model in Eq. (14). The evolution of ε_{ir} is defined in the four-branched Eq. (15):

- **the first branch** governs the case of recovery of ε_{ms}, when the stress is zero or $d\varepsilon_{ms}$ occurs in different direction than the stress acts: $d\varepsilon_{ir} = 0$.
- **the second branch** governs the case after temporary recovery, when $\varepsilon_{ms} + d\varepsilon_{ms}$ is still in an area where no irrecoverable strain occurs: $d\varepsilon_{ir} = 0$.
- **the third branch** governs the case of increasing ε_{ms} under tensile stress: $d\varepsilon_{ir}$ is non-zero; the first factors (a_{ir} and the absolute value expression) on the right side make it proportional to $d\varepsilon_{ms}$; the sgn-function gives it the correct sign; and the last factor is used to regulate its growth in a similar manner as in the Kelvin model (J_{ir} defines the limit compliance of ε_{ir}; b_{ir} is used for limiting the change rate of ε_{ir}).
- **the fourth branch** governs the case of compression and decreasing ε_{ms} and is symmetrical to the third branch.

ε_{max} and ε_{min} are variables, which are used to define the limit values for ε_{ms}, outside which it must move in order to produce irrecoverable creep ε_{ir}. ε_{max} and ε_{min} are needed for proper treatment of reversing stress, e.g. change from tension to compression. Their evolution laws, Eqs. (16) and (17), are such that ε_{max} and ε_{min} follow either one of the values of ε_{ms} or ε_{ir} or remain at a previous maximum or minimum value of ε_{ms}. Their evolution is schematically illustrated in Fig. 55.

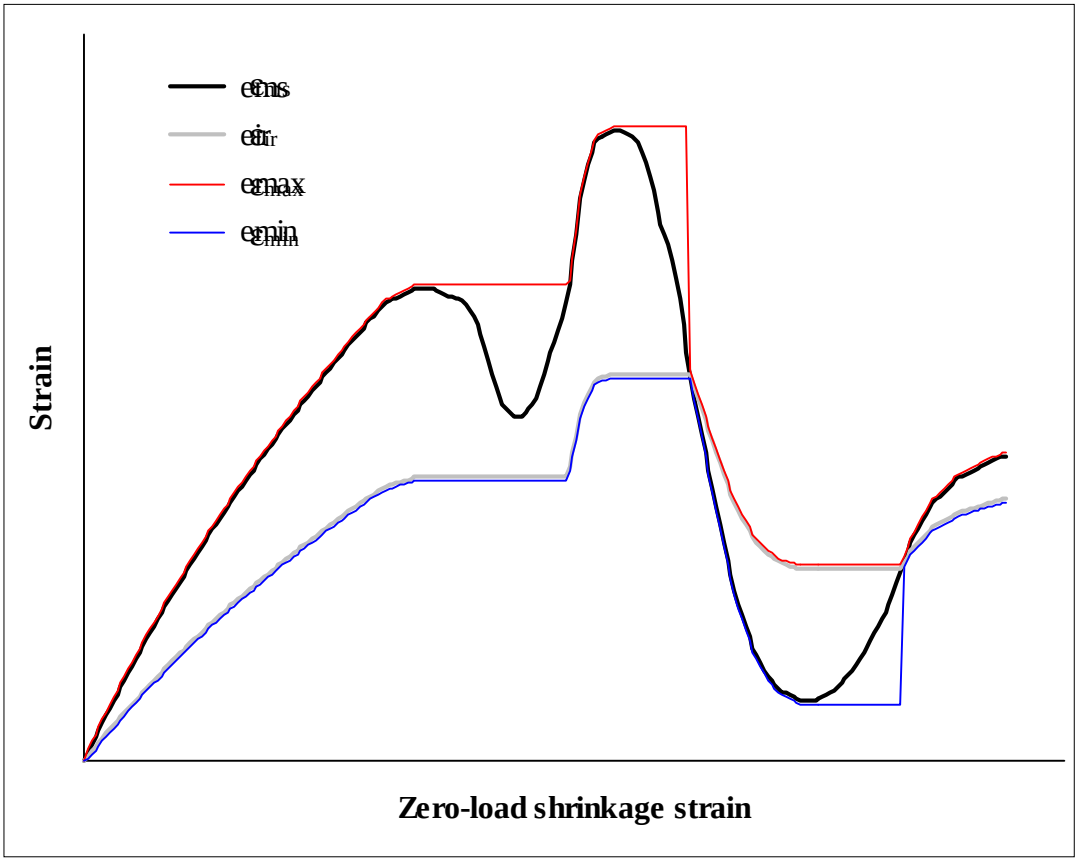

Fig. 55. Schematic illustration of the evolution of ε_{max} and ε_{min} as function of ε_{ms} and ε_{ir}.

It should be noted that ε_{ir}, ε_{max} and ε_{min} are internal variables, which describe the state of the material due to previous loading and straining history, but which are not directly related to any measurable or immeasurable quantity within the material. Their definition is made in a rather crude way, which is due to the striving for a simple model.

The suitability of the model can be improved if several units governed by Eqs. (14) – (17) are put in series; the total mechano-sorptive strain is then the sum of the units. In this work three units were used, the total mechano-sorptive strain is then obtained:

$$\varepsilon_{ms} = \sum_{i=1}^{3} \varepsilon_i^{ms} \tag{19}$$

where $\varepsilon^{ms}_{,i}$'s are the strain values of the three individual units. Each unit is governed by a separate set of equations similar to Eqs. (14) – (17) but obtain separate parameters, which can be noted by $J^{ms}_{,i}$, $\tau^{ms}_{,i}$, $J^{ir}_{,i}$, $a^{ir}_{,i}$ and $b^{ir}_{,i}$, i = 1…3. The internal variables are also independent for each unit and can be noted by $\varepsilon^{ir}_{,i}$, $\varepsilon^{max}_{,i}$ and $\varepsilon^{min}_{,i}$, i = 1…3.

In Table 4, a set of model parameter values is given, which were determined based on the obtained experimental results. This set is intended

for the temperature 95°C and the effect of temperature can be incorporated with the help of Eq. (6) (i.e. the values of the $J^{ms}{}_{,i}$'s and $J^{ir}{}_{,i}$'s are made temperature dependent as Eq. (6) shows).

Table 4. Model parameter values for the mechano-sorptive creep model.

Direc-tion	i	$J^{ms}{}_{,i}$ [MPa^{-1}]	$\tau^{ms}{}_{,i}$ [–]	$J^{ir}{}_{,i}$ [MPa^{-1}]	$a^{ir}{}_{,i}$ [MPa]	$b^{ir}{}_{,i}$ [MPa^{-1}]
Tang.	1	$0.003\text{-}0.03\varepsilon_s$	0.005	$0.003\text{-}0.09\varepsilon_s$	150	1
	2	$0.008\text{-}0.04\varepsilon_s$	0.015	$0.008\text{-}0.12\varepsilon_s$	150	1
	3	$0.014\text{-}0.05\varepsilon_s$	0.045	$0.014\text{-}0.15\varepsilon_s$	150	1
Radial	1	$0.0015\text{-}0.03\varepsilon_s$	0.0025	$0.0015\text{-}0.09\varepsilon_s$	150	1
	2	$0.005\text{-}0.04\varepsilon_s$	0.0075	$0.005\text{-}0.12\varepsilon_s$	150	1
	3	$0.008\text{-}0.05\varepsilon_s$	0.0225	$0.008\text{-}0.15\varepsilon_s$	150	1

4.4 FEATURES AND PERFORMANCE

The most important features for a constitutive model for use in drying simulation are the prediction accuracy, of course, the wide application range and simplicity for fast calculation.

Except mechano-sorptive strain model, the model parameters were given values directly from the experiment results, so the model response automatically fits the results. The mechano-sorptive creep model parameters were also adjusted to fit the experiment results. The performance of the mechano-sorptive creep model with these parameters is demonstrated in different situations in Fig. 56. It can be seen that the model is capable of following the observed compliance magnitude very well. It also follows the results well in other features, viz. the effect of moisture cycling and recovery.

The application range of the model is intended to be quite large (~ 20–125°C, ~ 4%–FSP, length of application time depends on conditions). It is mainly determined by the range and duration of the experiments to which its parameter values have been fitted, which can also be used for the estimation of its applicability to a certain application. It should be noted that the model development has been made in conjunction with the high temperature drying conditions and more attention has been paid to the model accuracy in these conditions; the low temperature prediction may not be so accurate.

The model can be characterised as a simple one except maybe the fact that 22 serial units are used in the modelling of the viscoelastic creep. They are needed in order to cover reasonably well the wide range of moisture contents and temperatures. Fortunately, from the computational point of view, the high number of units requires only somewhat more computer memory and a little more computation time, but no time-consuming iteration is needed. Furthermore, for particular applications, the model can be easily simplified by reducing the number of serial units. If moist and hot conditions are considered only, the number of units can be reduced by

adding the values of the $J^{ve},_i$'s in the lower end to $J^{ve},_0$. Or, if dry and cool conditions are considered, the higher end units can simply be dropped out. Of course, the length of loading time also affects how many units will be needed.

The application of the model into numerical calculation is straightforward, if the explicit, Euler-forward, procedure is followed. Neither should any impenetrable obstacles occur when implicit methods are used, although the author has not tried the use of any implicit methods in conjunction with the mechano-sorptive model.

Altogether, the developed model meets the requirements set by the applicability to simulation.

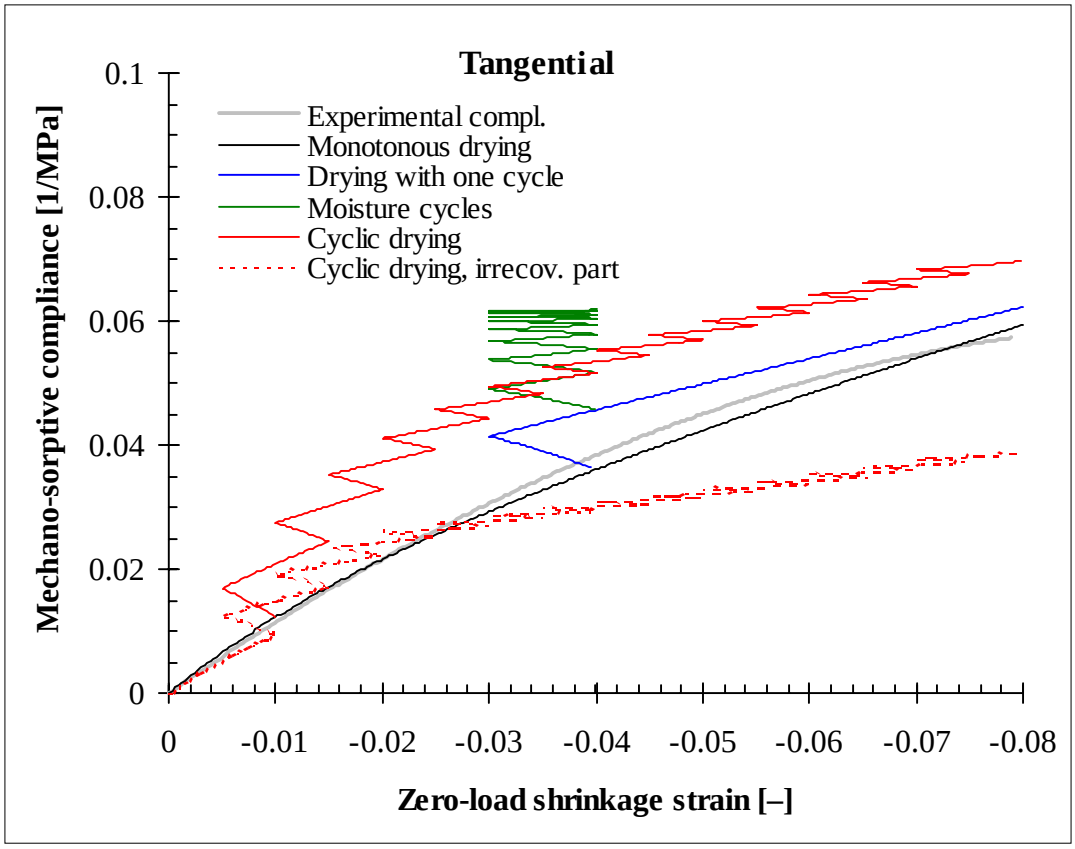

Fig. 56. Performance of the mechano-sorptive creep model in different situations. All cases have been calculated at constant stress 1 MPa and using the Euler forward algorithm with maximum zero-load shrinkage strain step value 0.0003.

5 CONCLUSIONS

High temperature drying is a promising technique for faster and higher quality drying process than drying at the conventional kiln temperatures. The potential of the use of higher temperatures is well credible based on the results of this work, which show clearly the greater deformation capacity (compliance) of wood in this temperature range (90–125°C) than at the conventional drying temperatures (60–80°C). This is seen for instance as the decrease of the modulus of elasticity with increasing temperature, Figs. 19 and 20. Greater deformation capacity means that drying stresses can be kept lower. On the other hand, the strength of wood drops with increasing temperature, but the effect of increased compliance is apparently greater allowing faster drying at higher temperatures.

The substantial development of the high temperature drying technique requires the optimisation of schedules, which must be done for all different types of sawn timber raw material and different conditions. If the drying process can be computationally simulated, this process becomes considerably easier. So far, the simulation has not been possible due to lack of knowledge about the material properties in the high temperature range. The experimental results and modelling achievements provide an adequate base for the simulation with regard to mechanical properties. Of course, for a functioning simulation the moisture transfer properties must also be mastered.

The experiments carried out in this work cover a wide section about the knowledge of mechanical properties needed for the simulation of drying stresses. The weakest part at this point is the quantification of the susceptibility to checking – strength and its dependence on the duration of the acting stresses, which is an important future research need. Also, the difference between compression and tension creep behaviour is an important aspect into which this work has not been able to pay any attention. It is to be hoped that lively research activity can be continued in the future for better understanding of the phenomena during the drying process.

REFERENCES

Byvshykh, M. D. 1959. Influence of temperature and moisture content of wood on its elastic properties. Derev. Prom., vol. 8, no. 2, pp. 13–15. (In Russian.)

Gerhards, C. 1982. Effect of moisture content and temperature on the mechanical properties of wood: an analysis of immediate effects. Wood and Fiber, vol. 14, no. 1, pp. 4-36.

Goulet, M. 1960. Dependence of transverse tensile strength of oak, beech and spruce on moisture content and temperature within the range of 0° to 100°C. Holz als Roh- und Werkstoff, vol. 18, no. 9, pp. 325–331. (In German.)

Hanhijärvi, A. 1995. Modelling of creep deformation mechanisms in wood. Espoo: Technical Research Centre of Finland (VTT). 143 p. + app. 3 p. (VTT Publications 231.) ISBN 951-38-4769-1

Hisada, T. 1986. Creep and set behaviour of wood related to kiln drying. Bull. For. & For. Prod. Res. Inst., vol. 7, no. 335, pp. 31–130. (In Japanese.)

Huet, C. 1988. Modelizing the kinetics of the thermo-hygro-viscoelastic behaviour of wood in constant climatic conditions. In: Itani, R. Y. (Ed.) Proceedings of the 1988 International Conference on Timber Engineering, Seattle 19–22 Sep. 1988. Madison, Wisconsin: Forest Products Research Society. Pp. 395–401. ISBN 0-935018-41-7

Hukka A. 1996. A simulation program for optimisation of medium temperature drying on an industrial scale. 5th International IUFRO Wood Drying Conference, Quebec City, Canada, 13–17 August 1996.

Hunt, D. G. 1986. The mechano-sorptive creep susceptibility of two softwoods and its relation to some other materials properties. Journal of Materials Science, vol. 21, pp. 2088–2096.

Iida, I. 1986. The thermal softening of green wood evaluated by its Young's modulus in bending. Mokuzai Gakkaishi, vol. 32, pp. 472–477.

Joyet, P. 1992. Comportement differe du materiau bois dans le plan transverse sous des conditions hydriques evolutives. L'Université Bordeaux I. (Doctoral dissertation no. 812.) 132 p. + app. 31 p. (In French.)

Kangas, J. 1990. Sahatavaran kuivauksen laadun parantaminen. Virumiskokeiden raportti 1990. (Improvement of the quality of timber drying. Report of creep experiments 1990). Unpublished report. VTT Laboratory of Structural Engineering. 35 p. + app. 16 p.

Kangas, J. & Ranta-Maunus, A. 1989. Havupuun viruminen syitä vastaan kohtisuorissa suunnissa. (The creep of softwood in directions perpendicular to the grain.) Espoo: Technical Research Centre of Finland. 60 p. + app. 15 p. (Technical Research Centre of Finland, Research Notes 969.) ISBN 951-38-3418-2

Koran, Z. 1979. Tensile properties of spruce under different conditions. Wood and Fiber, vol. 11, pp. 38–49

Kubler, H. 1973. Role of moisture in hygrothermal recovery of wood. Wood Science, vol. 5, no. 3, pp. 198–204.

Launay, J. 1987. Mesure des constantes élastiques d'un épicéa par goniométrie ultrasonore. Rapport ESEM pour le CTBA, Contrat de programme M.R.E.S.

Mårtensson, A. 1994. Stress development in drying timber, a theoretical description. In: Haslett, A. N. and Laytner, F. Proceedings of the 4th IUFRO Wood Drying Conference, Rotorua, New Zealand, 9–13 Aug. 1994. New Zealand Forest Research Institute. Pp. 173–180. ISBN 0-477-01730-4

Mårtensson, A. & Svensson, S. 1995. Stress–strain relationship of drying wood. In: Svensson, S. Hygro-mechanical behaviour of drying wood. Lund: Lund Institute of Technology, Department of Structural Engineering. (Report TVBK-1010.) ISSN 0349-4969 (Article to be published also in Journal of Materials in Civil Engineering.)

Okuyama, T., Suzuki, S. & Terazawa S. 1977. Effect of temperature on orthotropic properties of wood. I. On the transverse anisotropy in bending. Mokuzai Gakkaishi, vol. 23, pp. 609–616. (In Japanese.)

Ranta-Maunus, A. 1992. Determination of drying stresses in wood when shrinkage is prevented: Test method and modelling. In: Vanek, M. (Ed.) Proceedings of the 3rd IUFRO Conference on Wood Drying, Vienna, Austria, 18–21 Aug. 1992. International Union of Forestry Research Organisations (IUFRO). Pp. 139–144. ISBN 3-900962-08-1

Ranta-Maunus, A. 1993. Rheological behaviour of wood in directions perpendicular to the grain. Materials and Structures, vol. 26, pp. 362–369.

Ranta-Maunus, A., Forsén, H., Hanhijärvi, A., Hukka, A. & Partanen, J. 1995. Sahatavaran kuivauksen simulointi (Simulation of sawn timber drying). Espoo: VTT (Technical Research Centre of Finland). 62 p. + app. 50 p. (VTT Julkaisuja 805.) ISBN 951-38-4514-1 (In Finnish.)

Salmén, L. 1984. Viscoelastic properties of in situ lignin under water-saturated conditions. Journal of Materials Science, vol. 19, pp. 3090–3096.

Salmén, N. L. & Fellers, C. 1982. The fundamentals of energy consumption during viscoelastic and plastic deformation of wood. Transactions of the Technical Section, A Journal of Pulp and Paper Science, vol. 8, no. 4, pp. TR93–99.

Sawabe, O. 1974. Studies on the thermal softening of wood. III. Effects of the temperature on the bending creep of dry Hinoki wood. Mokuzai Gakkaishi, vol. 20, no. 11, pp. 517–522.

Siimes, F. E. 1967. The effect of specific gravity, moisture content, temperature and heating time on the tension and compression strength and elasticity properties perpendicular to the grain of Finnish pine spruce and birch wood and the significance of these factors on the checking of timber at kiln drying. Helsinki: The State Institute for Technical Research, Finland. (Publication 84.)

Svensson, S. 1994. Elementary tensile tests in a controlled climate. In: Haslett, A. N. and Laytner, F. Proceedings of the 4th IUFRO Wood Drying Conference, Rotorua, New Zealand, 9–13 Aug. 1994. New Zealand Forest Research Institute. Pp. 195–202. ISBN 0-477-01730-4

Svensson, S. 1995. Strain and shrinkage force in wood under kiln drying conditions I. Measuring strain and shrinkage under controlled climate conditions. Equipment and preliminary results. Holzforschung, vol. 49, no. 4, pp. 363–368.

Svensson, S. 1996. Strain and shrinkage force in wood under kiln drying conditions II. Strain, shrinkage and stress measurements under controlled climate conditions. Holzforschung, vol. 50, no. 5, pp. 463–469.

Viitaniemi, P. & Pennanen, J. 1993. Softening of wood with moisture and heat. In: Birkinshaw, C., Morlier, P. & Seoane, I. (Eds.) Proceedings of the COST508 Wood Mechanics Workshop on Wood Plasticity and Damage, Limerick, Ireland. Commission of the European Communities. Pp. 155–162.

Wu, Q. & Milota, M. R. 1995. Rheological behavior of Douglas-fir perpendicular to the grain at elevated temperatures. Wood and Fiber Science, vol. 27, no. 3, pp. 285–295.

Appendices of this publication are not included in the PDF version. Please order the printed version to get the complete publication (http://www.inf.vtt.fi/pdf/publications/1998/)